Rockefeller University
Digital Commons @ RU

Student Theses and Dissertations

2011

Rapid Functional Dissection of Genetic Networks Via RNAi In Mouse Embryos

Geulah Livshits

Follow this and additional works at: http://digitalcommons.rockefeller.edu/student_theses_and_dissertations

Part of the Life Sciences Commons

Recommended Citation

Livshits, Geulah, "Rapid Functional Dissection of Genetic Networks Via RNAi In Mouse Embryos" (2011). *Student Theses and Dissertations.* Paper 135.

This Thesis is brought to you for free and open access by Digital Commons @ RU. It has been accepted for inclusion in Student Theses and Dissertations by an authorized administrator of Digital Commons @ RU. For more information, please contact mcsweej@mail.rockefeller.edu.

RAPID FUNCTIONAL DISSECTION OF GENETIC NETWORKS VIA RNAI IN MOUSE EMBRYOS

A Thesis Presented to the Faculty of

The Rockefeller University

in Partial Fulfillment of the Requirements for

the degree of Doctor of Philosophy

by

Geulah Livshits

June 2011

© Copyright by Geulah Livshits 2011

RAPID FUNCTIONAL DISSECTION OF GENETIC NETWORKS VIA RNAI IN MOUSE EMBRYOS

Geulah Livshits, Ph.D.

The Rockefeller University 2011

The development and maintenance of epithelial tissues is regulated by a complex array of signal cues from adjacent cells, the extracellular milieu and intracellular signaling cascades. In the mammalian epidermis, these cues instruct the specification and invagination of hair follicles as well as the stratification and turnover of the interfollicular epidermis. These processes rely on a coordinate balance of tissue growth, differentiation and regulation of cell-cell adhesion to maintain the integrity of the epithelium. Understanding the interplay between the various pathways controlling tissue development requires model systems that recapitulate the events that occur *in vivo*. Genetic studies in *Drosophila* and other lower eukaryotes have uncovered many of the genes and pathways involved. However, genetic studies in mammals, where the relation to human development and disease is more direct are often hampered by the length of time required to generate mutations in the gene of interest. The ability to probe genetic interactions is even more limited in this system as the generation of double or triple mutants is even more inefficient. To circumvent these limitations, I have developed and optimized a lentivirus-based strategy to achieve rapid manipulation of the mammalian epidermis *in vivo*. Using ultrasound-guided *in utero* injections of fluorescently-traceable lentivirus particles carrying shRNA or Cre-recombinase into mouse embryos, I demonstrated a highly efficient, non-invasive, selective transduction of surface

epithelium. Epidermal progenitors stably incorporated and propagated the desired genetic alterations. Importantly, I achieved epidermal-specific infection using small generic promoters from existing shRNA libraries, thus enabling rapid assessment of gene function and complex genetic interactions in skin morphogenesis and disease *in vivo.* Using this technology, I have developed a new quantitative method to ascertain whether a gene confers a growth advantage or disadvantage by measuring relative growth of mutant clones in a mosaic tissue. Taking the adherens junction protein α-catenin as a paradigm, this approach was used to uncover new insights into its role as a widely expressed tumor suppressor and regulator of epithelial integrity. Using simultaneous gene depletion I uncovered physiological interactions between α-catenin and the Ras-MAPK and Trp53 pathways in regulating skin proliferation and apoptosis, respectively. Surprisingly, the apoptotic cells were primarily localized in the suprabasal cells. I found that cells lacking α-catenin showed elevated focal adhesion signaling, and using the lentiviral knockdown approach, I found that co-depletion of focal adhesion signaling components reduced the protection from apoptosis afforded to the basal layer cells in the absence of α-catenin. These studies illustrate the strategy, its broad applicability for investigations of tissue morphogenesis, lineage specification and cancers, and yield new insights into the complex mechanisms of growth regulation in tissues.

To my parents, who have always encouraged and supported my love of science.

ACKNOWLEDGEMENTS

I would first like to extend my deepest gratitude to Elaine Fuchs, who has been a truly supportive and encouraging mentor throughout my PhD career. She has inspired me to think critically, work hard and to not be afraid to take risks in my science.

I would also like to thank the members of the Fuchs lab, past and present, who have enriched my graduate experience not only in terms of scientific advice, but also in making the lab an exciting and fun place to work, even on late nights and weekends. In particular, I would like to thank Slobodan Beronja, my co-author on the *in utero* lentiviral injection project. The development of this system has been our joint effort from the start, and I could not have asked for a better partner on the project. He is a creative thinker, a hard worker, and also a generally entertaining person to be around. I have learned quite a bit from him during our many, many hours of mouse surgeries and marathon FACS sessions, and I am truly grateful for the experience.

I am also grateful to the other members of the laboratory whose expertise contributed to my projects. Scott Williams put a great deal of effort into optimizing viral constructs and protocols for the system, to make it accessible for the rest of the lab. Amalia Pasolli provided me with beautiful electron microscopy images. I would also like to thank Markus Schober for providing guidance and advice for the focal adhesion signaling and cell survival studies. My work was made possible by previous studies conducted in the lab by Valeri Vasioukhin and Agnes Kobielak, and I would like to thank them for their advances.

I am indebted to our excellent mouse technicians, Nicole Stokes, Lisa Polak and Dan Oristian, who have helped manage all my various mouse lines and also took it upon themselves to learn and perfect the *in utero* infection protocol, so that it could be used by the rest of the lab for their own projects. Maria Nikolova, Ellen Wong, June Racelis and Sophia Chai have worked tirelessly to make sure that our tissue culture facilities run smoothly and that the lab is well stocked. I would also like to thank Brice Keyes, who has been an excellent baymate and who has put up with all my clutter without complaint.

Outside of the lab, I would like to thank a number of people whose support has allowed me to keep my sanity: my parents, who have provided me with continuous and unequivocal support for the last 27 years; my friends, and especially my roommate Clare Walton, who have made the last several years famtastic; Brad Rosenberg, who has also provided unwavering support, encouraged me to push myself, and who has allowed our social life to be dictated by mouse matings and viral collection timepoints.

I would like to thank the graduate program at Rockefeller University, and the staff at the dean's office for their advice and assistance throughout my graduate career. Finally, I would like to thank the members of my thesis committee, Leslie Vosshall and Sandy Simon, and my external examiner Pamela Cowin for their guidance and support.

TABLE OF CONTENTS

Acknowledgements ..... **(iv)**

List of Illustrations ..... **(viii)**

List of Figures ..... **(ix)**

CHAPTER 1: INTRODUCTION **1**

Architecture of Mammalian Epidermis **2**

The Interfollicular Epidermis *3*

The Hair Follicle *7*

Cell-Cell Adhesion in Tissue Morphogenesis and Homeostasis **11**

Composition of Adherens Junctions *12*

Regulation of the Actin Cytoskeleton by Adherens Junction Proteins *14*

Adherens Junction Function In Vivo *19*

Cross-talk Between Adherens Junctions and Other Signaling Pathways **24**

Cell-Matrix Adhesions and Control of Migration *24*

Growth-Factor and Survival Signaling *29*

Adherens Junctions and Cancer *31*

The Tissue Morphogenesis and Cancer Toolbox **34**

Lower Eukaryotes: Simpler Genetics *34*

Cell Culture *36*

Mammalian Genetics *37*

Specific Aims **38**

CHAPTER 2: DEVELOPMENT OF AN *IN UTERO* EPIDERMAL INFECTION SYSTEM **42**

Results **43**

Ex vivo manipulation of skin explants *43*

Transduction of surface epithelium with lentiviral vectors *45*

Development of a quantitative cellular growth assay *61*

Discussion **63**

Materials and Methods **67**

Lentiviral vector constructs *67*

Large-scale lentivirus production and concentration *67*

Mice and in utero ultrasound-guided microinjection. *68*

Immunostaining and β-galactosidase detection. *70*

Explant culture for tissue morphogenesis *72*

Flow cytometry *72*

Statistics. *73*

CHAPTER 3: USE OF THE LENTIVIRAL EPIDERMAL DELIVERY SYSTEM TO DISSECT A GENETIC NETWORK **74**

Results **76**

Efficient gene knockdown using lentiviral RNAi in vivo *79*

Using RNAi in vivo to dissect a genetic network *87*

Discussion **95**

Materials and Methods **99**

Lentiviral vectors *99*

Mice *100*
Skin culture. *100*
mRNA and protein quantification. *101*
Immunostaining and β-galactosidase detection. *101*
Flow cytometry *102*
Statistics *102*

CHAPTER 4: FURTHER INSIGHTS INTO THE ROLE OF α-CATENIN IN EPIDERMAL MORPHOGENESIS **104**
Results **105**
Characterization of epithelial disorganization in the absence of α-catenin *105*
Changes in integrin signaling in the absence of α-catenin *109*
Effect of altered integrin signaling in the absence of α-catenin *118*
Discussion **128**
Materials and Methods **133**
Lentiviral vectors *133*
Mice *134*
Tissue culture *135*
mRNA and protein quantification *135*
Immunofluorescence *136*
Videomicroscopy *137*
Statistics *138*

CHAPTER 5: SUMMARY AND PERSPECTIVES **139**
Applications and further development of the in utero epidermal targeting technology *140*
α-catenin in survival and cancer pathways *144*

REFERENCES **152**

LIST OF ILLUSTRATIONS

1.1 Schematic of mammalian skin organization..... 4
1.2 Cellular Architecture of the interfollicular epidermis..... 6
1.3 Hair follicle morphogenesis and the hair cycle..... 9
1.4 Schematic of adherens junction signaling..... 15
1.5 Schematic of focal adhesions signaling centers..... 25

LIST OF FIGURES

2.1 Embryonic skin explants continue to develop in culture and can be manipulated through chemical inhibitors..... 44
2.2 Transmission electron microscopy of periderm development during embryogenesis..... 46
2.3 Basal epidermal cells selectively take up microspheres until E11.5 when they become fully covered by protective peridermal cell..... 47
2.4 Ultrasound-guided embryonic injections successfully target the amniotic cavity..... 49
2.5 Intra-amniotic injection of lentivirus can achieve epidermal transduction and gene expression..... 50
2.6 Intra-amniotic injection of lentivirus at E9.5 results in non-invasive, high-efficiency, stable and epidermally restricted transduction..... 52
2.7 Epidermal infection depends on viral titer and is permissive for delivery of multiple viral constructs..... 54
2.8 Lentiviral-Cre mediated excision precedes that achieved by K14-Cre by 2-3 days..... 55
2.9 Epidermal infection permits delivery of multiple viral constructs simultaneously..... 56
2.10 Lentiviral transduction of the epidermis shows no spurious effects on apoptosis, proliferation and tissue differentiation..... 58
2.11 Lentiviral transduction of the developing epidermis does not trigger an overt immune response..... 59
2.12 Lower levels of lentiviral infection in other ectoderm-derived tissues..... 60
2.13 Rapid assay for measuring an epidermal growth advantage or disadvantage conferred by a gene mutation..... 62

3.1 Lentiviral Cre infection and CGI analysis reveals an unexpected growth disadvantage following 1-catenin loss despite hyperproliferation..... 77
3.2 Efficient epidermal-specific lentivirus RNAi-mediated knockdown of *Ctnna1* in vivo..... 80
3.3 *Ctnna1* knockdown recapitulates gross LV-Cre and K14-Cre *Ctnna1* knockout phenotypes..... 82
3.4 Lentiviral RNAi-mediated knockdown of Ctnna1 faithfully recapitulates morphological phenotypic abnormalities displayed by K14-Cre conditional and LV-Cre induced knockout counterparts..... 84
3.5 Lentiviral knockdown of *Ctnna1* is accompanied by changes in cell fate and gene expression..... 86
3.6 Lentiviral RNAi-mediated *Ctnna1* knockdown recapitulates *Ctnna1* knockout perturbations in actin organization and intercellular adhesion.. 88
3.7 Hyperproliferation of *Ctnna*1 mutant cells is dependent upon RAS-MAPK signaling *in vivo*..... 90
3.8 Loss of α1-catenin does not result in cell senescence, but does result in apoptosis and activation of p53 signaling..... 92
3.9 Concomitant depletion of Trp53 rescues apoptosis and CGI in *Ctnna1*-null tissue..... 94

4.1 *Ctnna1* cKO tissue shows morphological, adhesive and cytoskeletal alterations by E15.5..... 107
4.2 *Ctnna1* ablation results in disruption of epithelial networks *in vivo*..... 108
4.3 *Ctnna1* ablation rapidly induces breaks between the basal and spinous layers, which are associated with apoptotic cells..... 110
4.4 Suprabasal bias for apoptosis in *Ctnna1* KO tissues relative to wild-type. 111
4.5 Slight but consistent activation of integrin signaling in the absence of *Ctnna1*..... 113
4.6 IGF-R localization shifts from focal adhesions to adherens junctions upon calcium switch in control but not *Ctnna1* cells. 114
4.7 EGFR localization shifts to adherens junctions upon calcium switch in control but not *Ctnna1* cells..... 116
4.8 Calcium switch enhances the disparity in IGFR activation between control and *Ctnna1* null cells..... 117
4.9 IGFR and EGFR localize near adherens junctions in control but not *Ctnna1* KO tissues in vivo..... 119
4.10 Increased membrane protrusion dynamics and Pak activation in Ctnna1 KO tissue relative to controls..... 121
4.11 Ctnna1 KO cells are sensitized to inhibition of Pak signaling..... 123
4.12 Morphological and cytoskeletal changes in keratinocytes upon depletion of Pak1, Pak2 or Fak..... 125
4.13 Concomitant depletion of focal adhesion signaling factors alters migration and apoptosis in the absence of α-catenin..... 127

CHAPTER 1: INTRODUCTION

The human body develops from a single-celled embryo into an assemblage of up to one hundred trillion cells (Sears, 2005). These cells must be arranged into a network of functionally distinct tissues and organs that can cooperate to promote the survival and reproduction of the individual. In order to facilitate their coordinate regulation, cells utilize numerous transmembrane proteins to anchor themselves to each other and to components of the extracellular space, forming simple sheets or epithelia. The morphogenesis of complex three-dimensional organ structures from uniform epithelial sheets is a recurrent theme throughout mammalian development, and understanding how this occurs is a fundamental problem at the interface between cell, molecular and developmental biology. This process generally requires the integration of signaling pathways that turn on transcriptional programs specifying cell fate, with coordinated changes in cell-cell adhesion, cell-matrix interaction, and cytoskeletal remodeling that give rise to morphologically distinct cell types (Hogan, 1999).

After morphogenesis, precise regulation of cellular interaction continues to be critical for the maintenance of proper tissue architecture and integrity during homeostasis throughout the lifetime of the organism. Dynamic coordination of adhesion and signaling between neighboring cells also enables a tissue to repair itself after injury. Additionally, improper regulation of cell adhesion signaling can lead to a variety of developmental defects (Stepniak et al., 2009), to delayed wound healing, or to an increased susceptibility to tumor formation (Desgrosellier and Cheresh, 2010; Perez-Moreno and Fuchs, 2006).

Over the past century, our understanding of epithelial development and homeostasis has greatly expanded. Advances in the adaptation of various model organisms have enabled the precise characterization of the cellular processes involved in tissue development across multiple species. The advent of new genetic tools has allowed us to begin to identify the molecules involved. Improvements in imaging technology have allowed us to better understand the dynamic nature of the processes involved in development. As our understanding progresses, we continue to develop new tools and systems to further our knowledge of epithelial biology.

Architecture of Mammalian Epidermis

The epidermis and its appendages act as a barrier at the body's surface to protect the internal organs from myriad environmental assaults such as microbes and ultraviolet irradiation, while preventing fluid loss and regulating body temperature. It performs these functions while undergoing continual self-renewal to replace old cells and respond to injury, and thus, a tightly regulated balance between proliferation and differentiation is essential for maintenance of tissue homeostasis (Fuchs, 2007). The accessibility, well-characterized architecture and spatially segregated cell types comprising the mammalian epidermis make it an excellent system to study the cellular mechanisms regulating tissue growth in development.

The mammalian epidermis is a stratified squamous epithelium that lies atop a basement membrane (BM) rich in extracellular matrix (ECM) components and growth factors, which separates it from the underlying dermal mesenchyme (Blanpain and Fuchs, 2006). During embryogenesis, the epidermis and its

appendages, including hair follicles, sebaceous glands, eccrine glands as well as mammary glands arise from a single sheet of multipotent non-neural ectoderm that overlies the surface of the embryo after neural tube closure (Illustration 1.1). A transient cell layer called periderm, composed of tightly connected squamous cells, covers the developing epidermis until stratification and differentiation have been completed. In the mouse, whose embryonic development closely resembles that of humans and has thus been an excellent model for the study of epidermal morphogenesis, neural tube closure is complete by embryonic day 9 (E9), while periderm formation occurs between E9-E12 in a patterned manner across different parts of the embryo. (Copp et al., 2003; M'Boneko and Merker, 1988).

The Interfollicular Epidermis

In the interfollicular epidermis, proliferation is restricted to the innermost cell layer, referred to as the basal layer (BL). Cells of the basal layer adhere to the basement membrane and are responsible for giving rise to the non-dividing suprabasal layers that are continually sloughed from the surface. Basal cells are characterized by their high expression of keratins K14 and K5, which form 10-nm heteropolymeric intermediate filaments. These filaments anchor to hemidesmosomes at the base of the cell and to desmosomes at intercellular junctions to provide mechanical strength across the epithelial sheet (Fuchs and Cleveland, 1998). Mutations in K14 or K5 disrupt proper assembly of the filament network and transgenic expression of a mutant K14 protein in the epidermis of mice resulted in aberrations in keratin network assembly and skin blistering (Vassar et al., 1991). This work predicted the genetic basis for the human skin

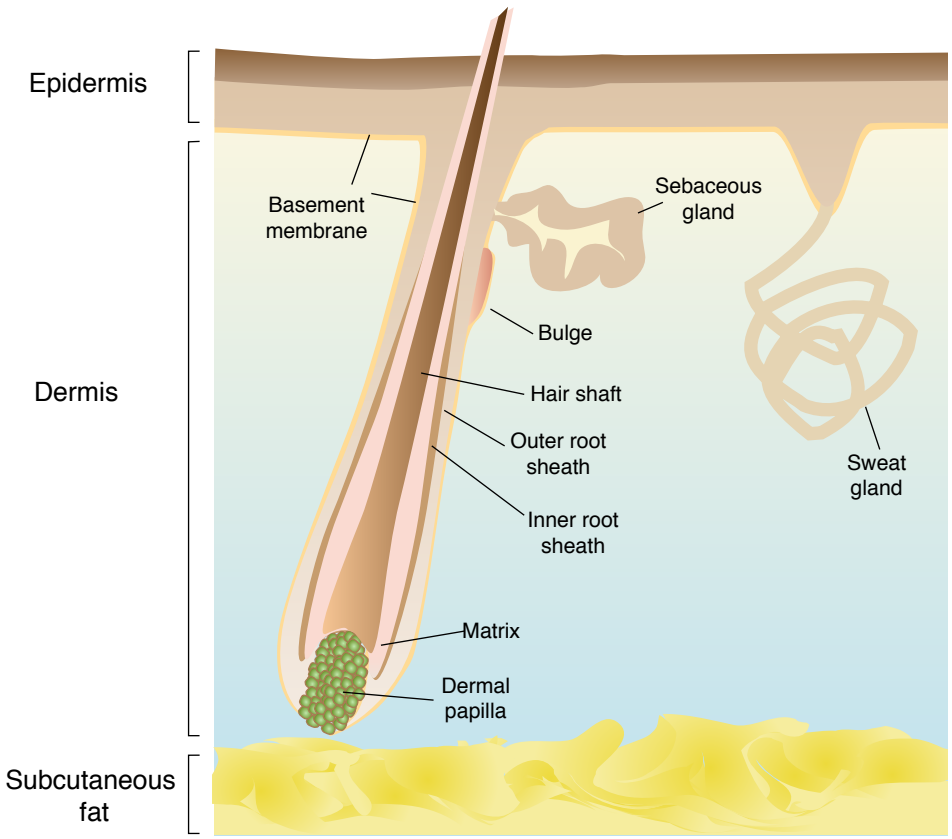

Illustration 1.1 Schematic of mammalian skin organization. Mammalian skin is composed of numerous cell types and distinct structures that enable it to serve as a barrier at the body's surface. The stratified interfollicular epidermis is maintained by a proliferative basal layer and terminally differentiating suprabasal cells. It lies atop the dermal layer, which assists the epidermis in insulating the body from heat loss. Hair follicles, sebaceous glands and sweat glands originate in the epidermis and grow down into the dermal layer. The outer root sheath of hair follicles is contiguous with the basal layer and provides a channel for the developing hair follicle to reach the skin surface. The sebaceous gland grows out from the top region of the hair follicle and produces lipids that lubricate the hair channel. Sweat glands also grow down into the dermis and aid in the temperature regulation function of the skin. Adapted from Fuchs and Raghavan, 2002.

disorder epidermolysis bullosa simplex (EBS), where patients present with a similar skin blistering phenotype (Bonifas et al., 1991; Coulombe et al., 1991; Lane et al., 1992). The basal cells in these patients are extremely fragile and easily rupture upon physical trauma, resulting in intraepithelial blisters.

Upon their exit from the basal layer, the epidermal cells, or keratinocytes, cease to proliferate and commit to a program of terminal differentiation that progresses through three stages: the spinous and granular layers, and the stratum corneum. The commitment to differentiation and spinous cell fate is reflected by a switch to expression of the keratins K1 and K10 (Fuchs and Green, 1980). Other keratins, such as K6 can also be expressed suprabasally, but only under conditions of wounding or hyperproliferation (Mansbridge and Knapp, 1987). The transition between basal and spinous layers is regulated by Notch signaling through its canonical partner RBP-J, to repress basal genes and promote spinous cell fate (Blanpain et al., 2006). In addition to transcriptional changes, the basal-spinous transition is also accompanied by a dramatic change in cell shape, as cuboidal cells of the basal layer adopt a more flattened, squamous morphology upon reaching the spinous layer (Illustration 1.2).

As spinous cells progress outwards into the granular layer, they form keratohyalin granules, where keratin is bundled into macrofibrillar cables aided by the protein filaggrin, as well as lipid-filled lamellar-bodies (LB) that eventually fuse with the plasma membrane. These cells also synthesize glutamine- and lysine-rich cornified envelope (CE) proteins, which are deposited under the plasma membrane (Segre, 2003). The cells subsequently flatten and degrade their intracellular organelles, including nuclei, and extrude the lipid

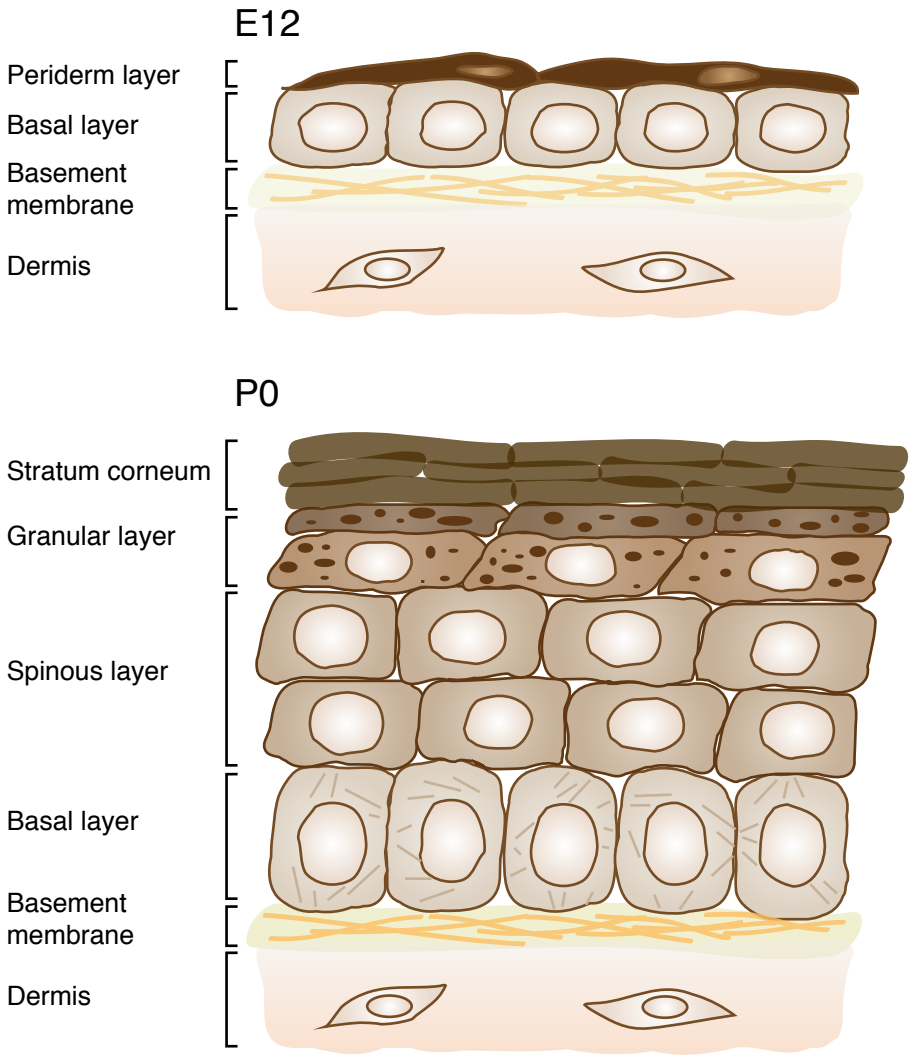

Illustration 1.2 Cellular architecture of the interfollicular epidermis (IFE). The interfollicular epidermis arises from a single layered sheet of ectoderm that is anchored to a basement membrane. During development it is protected by the transient periderm layer, which is shed after stratification is complete. The fully developed epidermis contains a proliferative basal layer that continuously replenishes the differentiating suprabasal layers. The differentiation process consists of a series of transcriptional and cytoskeletal changes that results in the formation of the stratum corneum, a highly cross-linked lipid-rich barrier that renders the skin water impermeable and resistant to external assaults and pathogens.

bilayers onto the deposited CE proteins (Swartzendruber et al., 1989). A calcium influx then activates transglutaminase to crosslink the CE proteins, to generate a lipid-rich barrier at the skin's surface (Peterson et al., 1983).

This barrier continues to be replenished by the continuous differentiation cycle initiated by the proliferating basal cells throughout the lifetime of the organism. Basal cells are capable of dividing both symmetrically and asymmetrically to form and maintain the stratified epidermal structure (Lechler and Fuchs, 2007; Poulson and Lechler, 2010). During the single layer stage, most cell divisions occur parallel to the plane of the basement membrane, with both daughter cells retaining basement membrane contact. In contrast, upon initiation of stratification at E14.5, the majority (70%) of cell divisions occur perpendicular to the basement membrane, yielding one basal and one suprabasal cell; this ratio is maintained until completion of stratification at E18.5 (Lechler and Fuchs, 2005). This process is regulated by a set of conserved asymmetric cell division (ACD) machinery components that preferentially localize to the apical cortex of perpendicularly dividing cells and recruit spindle microtubules. Depletion of these proteins in the developing epidermis results in a thinner skin and impaired epidermal differentiation corresponding with their bias towards symmetric division and a reduction in Notch signaling (Williams et al., 2011).

The Hair Follicle

Concurrently with the initiation of stratification, reciprocal signaling interactions between the epidermis and the underlying dermal mesenchyme initiate the specification of hair follicle cell fate. Fibroblast growth factors (FGFs) and bone morphogenic protein (BMP) inhibitors from the dermis induce the

formation of "hair placodes," or clusters of basal cells with an elongated morphology in the epithelial sheet (Schmidt-Ullrich and Paus, 2005). These placodes will give rise to hair follicles, while BMPs, elevated in the placode inhibit hair follicle cell fate in the surrounding interfollicular epidermal cells, resulting in a hexagonal pattern of follicle induction in the skin. In the mouse, hair follicle morphogenesis occurs in waves, from E14.5 to E18.5, giving rise to the distinct types of hairs (guard, awl, auchenne, and zig-zag) that make up the hair coat (Schmidt-Ullrich and Paus, 2005). With each new wave, the next hair placodes arise in the center of the hexagon, consistent with a gradient of BMP inhibition (Byrne et al., 1994).

Several genetic studies have shown that Wnt/β-catenin signaling is critical for both the specification of hair follicle cell fate as well as the maintenance of the follicular lineage (Gat et al., 1998; Noramly et al., 1999; van Genderen et al., 1994; Zhou et al., 1995). Conditional ablation of β-catenin or ectopic expression of the Wnt inhibitor Dickkhopf1 in the epidermis both inhibit placode formation (Andl et al., 2002; Huelsken et al., 2001). Conversely, mice expressing a stabilized form of β-catenin in the skin exhibit *de novo* hair follicle formation (Gat et al., 1998). Signaling through stabilized β-catenin as well as sonic hedgehog (Shh) signaling in the placode promote changes in proliferation and cell shape that lead to the invagination of a bud structure into the dermis (Illustration 1.3) (Chiang et al., 1999; St-Jacques et al., 1998). At the same time, adjacent dermal cells receiving these signals condense to form the dermal papilla (DP), which becomes a permanent part of the mature hair follicle structure that remains separated from the epidermal cells by a basement membrane (Fuchs, 2007).

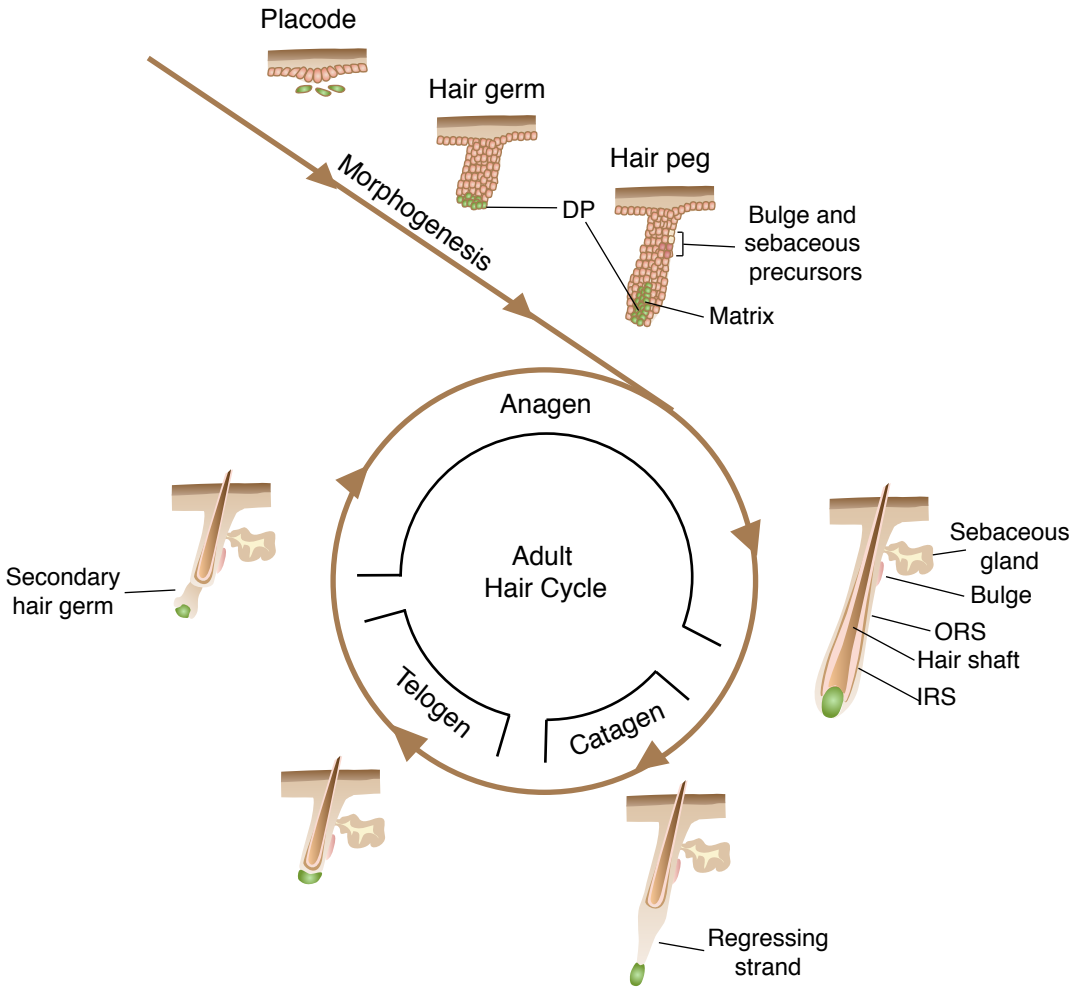

Illustration 1.3 Hair follicle morphogenesis and the hair cycle. Hair morphogenesis begins with the formation of placodes in the epidermal sheet. Placodes then grow down into the dermis as a hair germ, while dermal cells receiving signals from the placode condense to form the dermal papilla. The dermal papilla becomes surrounded by the proliferating matrix cells, and the follicle grows down through the dermis. After the growth phase, the follicle enters catagen, a phase of apoptotic regression, followed by telogen, a resting phase during which no proliferation occurs. After completion of telogen, the follicle re-enters the growth phase, or anagen. Abbreviations: DP, dermal papilla; ORS, outer root sheath; IRS, inner root sheath.

Rapidly dividing cells at the leading edge of the down-growing follicle form a bulb-like structure, referred to as the matrix, around the DP. As matrix cells move up and away from the DP and basement membrane, they commit to terminal differentiation in a process similar in some ways to that of the interfollicular epidermis. The matrix cells give rise to seven concentric cell layers that make up the hair shaft (HS) and its surrounding channel, the inner root sheath (IRS) (Fuchs and Horsley, 2008). IRS specification is regulated by Notch signaling and the transcription factor Gata3, while the hair shaft is specified by Wnt signaling and Lef1 (Gat et al., 1998; Kaufman et al., 2003). The outer layer of the hair follicle, or outer root sheath (ORS) is contiguous with the interfollicular epidermis. The upper portion of the ORS contains the "bulge" region, which forms the niche for the reservoir of hair follicle stem cells.

In the adult skin, the hair follicle cycles between phases of growth (anagen), destruction (catagen) and quiescence (telogen) and is regenerated by stem cells from the bulge (Illustration 1.3). After morphogenesis, the follicle ceases to proliferate and enters catagen. This phase is characterized by apoptosis of the lower two-thirds portion of the hair follicle and regression of the DP towards the bulge, which marks the permanent upper portion of the hair follicle (Müller-Röver et al., 2001). Once the DP reaches the bulge, the hair follicle enters the resting phase, marked by an absence of proliferation, apoptosis or differentiation (Alonso and Fuchs, 2006). After a period of rest, accumulating signals from the DP, including BMP antagonists and FGF7 promote stem cell activation and proliferation. This event marks the entry into the anagen phase, during which the lower portion of the follicle is regenerated (Greco et al., 2009).

The bulge cells divide infrequently and can regenerate the follicular, sebaceous and interfollicular epidermal lineages when transplanted onto the backs of immunodeficient mice (Blanpain et al., 2004; Cotsarelis et al., 1990; Tumbar et al., 2004). They do not appear to play a role in maintaining the interfollicular epidermis under conditions of homeostasis, but are mobilized to help regenerate skin upon wounding (Ito et al., 2005; Levy et al., 2005).

Label-retention studies in mice have suggested that the interfollicular epidermis also contains slower cycling basal cells. These cells have been posited to be the interfollicular stem cells that give rise to clones of transit amplifying (TA) cells, analogous to the matrix cells of the hair follicle, which undergo a limited number of divisions before differentiation (Clayton et al., 2007; Mackenzie, 1970; Potten, 1974). This hypothesis suggests the existence of an "epidermal proliferative unit" (EPU) consisting of a stem cell, its TA progeny, and their differentiated descendants. However, more recent studies using genetic labeling of basal cells and their progeny were more consistent with a model of a single epidermal progenitor that is capable of undergoing either symmetric or asymmetric divisions relative to the underlying basement membrane to maintain epidermal homeostasis (Clayton et al., 2007; Poulson and Lechler, 2010).

Cell-Cell Adhesion in Tissue Morphogenesis and Homeostasis

The flux of cells from proliferative to terminally differentiating compartments of the skin requires precise spatiotemporal coordination of the assembly and disassembly of cell-cell and cell-ECM adhesions. The important role of varying adhesive properties for cell sorting and tissue formation has been recognized since the beginning of the previous century, when zoologists and

embryologists began to observe the selective aggregation of distinct cell types from sponges, amphibians and chicken embryos in cell culture (Holtfreter, 1939; Moscona, 1962; Wilson, 1907). Subsequent studies have demonstrated that in both simple and stratified epithelia, the interactions between cells are primarily mediated by three junctional complexes: adherens junctions (AJ), tight junctions (TJ), and desmosomes. Desmosomes anchor to the intermediate filament network to provide the tissue with structural integrity, as described above, while tight junctions localize to the most apical sites of intercellular contact and are involved in sealing membranes to prevent interstitial fluid flow and also partition the apical and basolateral membrane domains to regulate epithelial cell polarity (Franke, 2009). Adherens junctions are dynamically regulated calcium-dependent adhesion structures that associate with the actin cytoskeleton at the intracellular surface. Although all three perform critical functions in an epithelial tissue, adherens junction formation precedes the other two at sites of initial cell-cell contact and adherens junctions can participate in numerous signaling pathways regulating cell survival, morphogenesis and growth control, making them particularly significant for tissue growth, homeostasis, and regeneration (Halbleib and Nelson, 2006; Perez-Moreno and Fuchs, 2006).

Composition of Adherens Junctions

Adherens junctions were first characterized ultrastructurally as electron-dense plaques at opposing cell-cell contacts (Farquhar and Palade, 1963). Seminal studies by Takeichi's group identified a single-pass transmembrane protein responsible for the formation of calcium dependent adhesions in Chinese hamster cells, mouse teratocarocarcinoma cells and during morula compaction.

The protein was named "cadherin" due to its calcium-dependent adhesion function (Boller et al., 1985; Hyafil et al., 1981; Takeichi, 1977; Yoshida and Takeichi, 1982; Yoshida-Noro et al., 1984). In mammals, the classical cadherin family contains several closely related proteins that exhibit tissue-specific expression: E-cadherin, primarily expressed in epithelial cells, is considered the prototypic cadherin, though other well-characterized family members include placental (P), neural (N), vascular-endothelial (VE), retinal (R), and kidney (K), cadherins (reviewed in (Stepniak et al., 2009). The extracellular domains of cadherins contain several calcium-binding repeats that mediate homophilic binding interactions with cadherins on adjacent cells (Overduin et al., 1995). The cadherin cytoplasmic domain contains highly conserved regions that mediate association with p120-catenin and β-catenin (or the closely related γ-catenin), which are members of a superfamily of proteins possessing "armadillo" domain repeats. p120-catenin binds cadherins at a juxtamembrane region of the cytoplasmic tail, while β-catenin associates with a distinct "catenin binding domain" at the carboxy-terminus of the protein (Davis et al., 2003; Nagafuchi and Takeichi, 1988; Ozawa et al., 1989; Ozawa et al., 1990; Reynolds and Carnahan, 2004; Yap et al., 1998).

In addition to its role in adherens junctions, β-catenin also plays a central role in Wnt signaling, as mentioned above (van de Wetering et al., 1997). Cytoplasmic β-catenin that is not associated with cadherins is normally phosphorylated by GSK3-β and targeted for degradation. Wnt signaling inhibits this degradation pathway, thereby promoting the accumulation of cytoplasmic β-catenin, which then translocates into the nucleus to regulate transcription

reviewed in (Clevers, 2006). At the adherens junction, β-catenin is protected from degradation and binds α-catenin, an actin binding and filament bundling protein that lacks armadillo repeats and is structurally unrelated to the other catenins (Illustration 1.4) (Rimm et al., 1995). Like the cadherins, α-catenin is one of a family of related proteins with tissue-specific expression patterns: α-E-catenin is the primary epithelial form, while α-N-catenin and α-T-catenin are expressed in neural tissues and the heart, respectively (Herrenknecht et al., 1991; Hirano et al., 1992; Janssens et al., 2001). A more distantly related protein, α-catulin is expressed ubiquitously, but may perform distinct functions in the cell (Janssens et al., 1999; Merdek et al., 2004). The complex between cadherin, p120-catenin, β-catenin, and α-catenin constitutes the core of the adherens junction, and is conserved throughout metazoans, including *C. elegans* and *Drosophila melanogaster*, where its role in development has been extensively studied (Reviewed in (Tepass et al., 2001)).

Regulation of the Actin Cytoskeleton by Adherens Junction Proteins

In epithelial sheets, adherens junctions are closely associated with a circumferential belt of actin cables that distributes mechanical tension and helps coordinate cell shape across the epithelium (Yonemura et al., 1995). The interaction with the actin cytoskeleton is critical for the maintenance of epithelial integrity as well as the initial assembly of adherens junctions. During the early stages of cell-cell adhesion, cells extend dynamic actin-rich membrane protrusions that become stabilized in puncta containing cadherins and catenins at sites of membrane contact between adjacent cells (Adams et al., 1998; Adams et al., 1996).

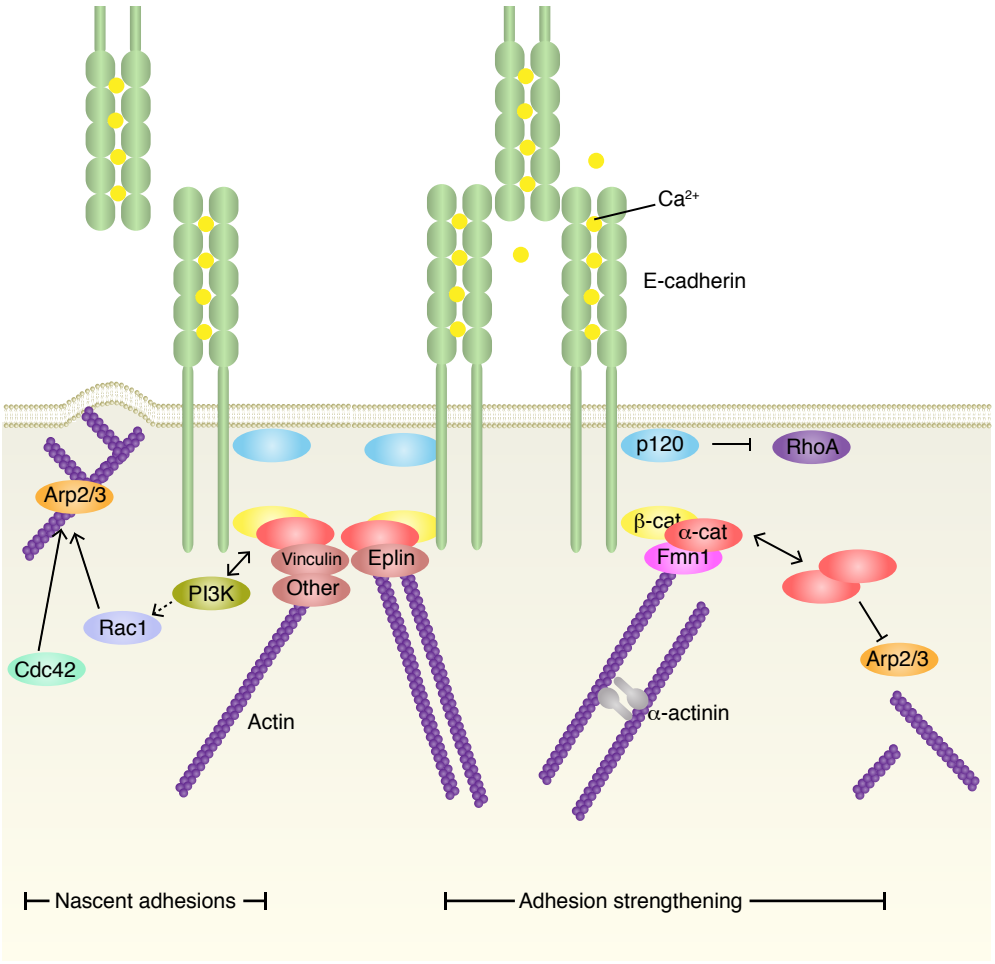

Illustration 1.4 Schematic of adherens junctions signaling. The core of the adherens junction (AJ) consists of a transmembrane protein of the cadherin family. Adhesion is mediated by calcium-dependent homophilic binding between cadherins on adjacent cells. The intracellular tails of cadherins associate with p120-catenin, b-catenin and indirectly, a-catenin, which along with other actin-binding proteins link the AJ to the actin cytoskeleton. During adherens junction formation, Arp2/3-mediated branched actin polymerization forms membrane protrusions that help bring membranes of apposing cells into close contact to allow cadherin interaction. Nascent adhesions are strengthened through remodeling and crosslinking of the cortical actin cytoskeleton. a-catenin facilitates this process and promotes linear actin polymerization by inhibiting Arp2/3, and recruiting Formin1, which generates unbranched filaments. Arrow, positive regulation; double arrow, dynamic association.

The formation of these membrane protrusions is mediated by the activity of Rho-family GTPases. These proteins function as molecular switches that cycle between an active GTP-bound state and an inactive GDP-bound state. The exchange of GDP for GTP (activation) and subsequent GTP hydrolysis (inactivation) steps are regulated by Guanine Exchange Factors (GEFs) and GTPase Activating Proteins (GAPs), respectively (Etienne-Manneville and Hall, 2002). In their active state, GTPases can bind a wide variety of effector proteins to regulate their behavior (Bishop and Hall, 2000). The best-characterized mammalian Rho GTPases are RhoA, Rac1 and Cdc42. Classical studies in fibroblasts demonstrated that these proteins promote distinct forms of actin assembly. RhoA promotes the formation of unbranched actin filaments by formins; these filaments can then be incorporated into contractile actomyosin fibers (Ridley and Hall, 1992). Rac1 and Cdc42 both promote branched actin filament polymerization by the Arp2/3 complex. However, they interact with different Arp2/3 regulators to produce morphologically distinct actin structures: Rac1 activation results in wide, flat membrane protrusions, or lamellipodia, while Cdc42 generates thin fingerlike membrane protrusions, or filopodia (Ridley et al., 1992). All three of these proteins play central roles in cell-cell adhesion, as well as in numerous other processes that depend on actin remodeling, such as migration, cell division and the establishment of polarity (Etienne-Manneville and Hall, 2002).

The process of adhesion formation and maturation can differ somewhat across cell types. In keratinocytes, adhesions are initiated through extension of filopodia, which embed into the membrane of apposing cells triggering puncta

formation. Double rows of these puncta on adjacent cells become associated with radial actin fibers and form a structure known as an adhesion zipper. As adhesion progresses, actin polymerization and actomyosin contractility pull the puncta into a single row; the puncta then coalesce into a linear adhesion structure and the cortical actin is remodeled into the actin belt that lies parallel to the junction surrounding the cell (Vaezi et al., 2002; Vasioukhin et al., 2000). In contrast, MDCK cells, which generate a non-stratified epithelium, initiate adhesion through extension of lamellipodia, which also become stabilized at puncta (Adams et al., 1996). Zones of RhoA and Rac1 activity at the edges of contacts drive the formation of new puncta and expansion of the region of cell-cell contact to maximize adhesion (Yamada and Nelson, 2007). Inhibition of Rho or Rac signaling either chemically, or through via expression of dominant negative constructs inhibits adherens junction formation in cultured cells, highlighting the importance of actin remodeling for cell-cell adhesion (Braga et al., 1997; Vaezi et al., 2002).

Because of the ability of α-catenin to bind both β-catenin and actin, the prevailing notion has been that the β-catenin/α-catenin interaction serves to directly link the adherens junction to the actin cytoskeleton (Hirano et al., 1992; Rimm et al., 1995). Indeed, numerous studies in cell culture have shown that α-catenin is indispensable for cadherin-mediated cell-cell adhesion (Hirano et al., 1992). Carcinoma cell lines lacking α-catenin form sparse cadherin puncta that fail to mature into linear adhesions, seal membranes, or to construct a circumferential actin belt (Watabe-Uchida et al., 1998). Expression of α-catenin in these cells can rescue the defect in actin organization and adherens junction

formation (Bullions et al., 1997; Watabe et al., 1994). However, more recent biochemical studies have brought this idea of a direct link into question by showing that α-catenin does not interact with both β-catenin and actin simultaneously (Yamada et al., 2005). Rather, α-catenin can exist in solution as either a monomer that preferentially binds β-catenin, or as a dimer that holds a stronger affinity for actin filaments. The α-catenin dimer can organize the actin cytoskeleton *in vitro* by inhibiting the polymerization of branched actin structures mediated by the Arp2/3 complex, most likely by competing with Arp2/3 for binding to actin filaments (Drees et al., 2005). This function of α-catenin appears to be independent of its role in cell-cell adhesion, as selective sequestration of cytosolic α-catenin to mitochondria in mammalian cells increases actin polymerization and lamellipodial membrane dynamics, which are hallmarks of Arp2/3 activity (Benjamin et al., 2010).

Rather than operating as a direct bridge between the adherens junction and actin, α-catenin may also link to the actin cytoskeleton indirectly, through its interaction with several actin-binding proteins. For instance, α-catenin has been shown to interact with Formin-1 to promote the assembly of the linear actin cables at adherens junctions. Forced recruitment of Formin-1 to adherens junctions via β-catenin can rescue the radial actin cables and adherens junction formation that are impaired in cells lacking α-catenin (Kobielak et al., 2004). The linkage between actin and adherens junctions may also be mediated by Eplin, a recently identified actin binding and bundling protein that interacts with α-catenin. In MDCK cells, Eplin localizes to adherens junctions and its depletion impairs the ability of adhesion zippers to mature into linear junctions with a

parallel belt of actin cables (Abe and Takeichi, 2008). Vinculin has also been shown to bind α-catenin at cell-cell contacts (Watabe-Uchida et al., 1998). It appears to be recruited to junctions in an actomyosin tension-dependent manner, and strengthens the adhesions in response to mechanical tension (le Duc et al., 2010; Yonemura et al., 2010). Other actin-binding proteins that associate with α-catenin include ZO-1, afadin and α-actinin (Harris and Tepass, 2010). However, these other proteins do not tend to consistently co-immunoprecipitate with the cadherin-catenin complex in a stoichiometric ratio, suggesting that they may not stably incorporate into the adherens junction. Ultimately, differences in expression and localization of these and other actin regulators may determine the contribution of these various mechanisms across different cell types.

Unlike α-catenin, p120-catenin does not directly bind actin. p120-catenin was initially discovered as a tyrosine kinase substrate found to associate with E-cadherin (Reynolds et al., 1994). It was subsequently shown to bind a juxtamembrane region of E-cadherin to promote lateral clustering of cadherins in the membrane to strengthen adhesion (Yap et al., 1998). p120-catenin may fortify adherens junctions by regulating cadherin turnover, as p120-catenin association serves to stabilize E-cadherin at the cell surface by inhibiting its endocytosis, while depletion of p120-catenin by siRNA in mammalian cells promotes the internalization and degradation of E-cadherin, accompanied by loss of cell adhesion (Davis et al., 2003; Reynolds and Carnahan, 2004). p120-catenin also controls actin assembly through inhibition of RhoA signaling (Anastasiadis et al., 2000; Noren et al., 2000).

Adherens Junction Function In Vivo

Cadherin-mediated cell-cell adhesion regulates tissue morphogenesis at many stages of development. Homophilic binding between cadherin extracellular domains often mediates sorting of cells expressing different types (or levels) of cadherins, facilitating tissue formation in embryogenesis (Godt and Tepass, 1998; Nose and Takeichi, 1986). For instance, expression of N-cadherin in the presumptive neural ectoderm allows it to separate from the non-neural ectoderm that expresses E-cadherin during neurulation (Gumbiner, 2005). E-cadherin subsequently continues to be the primary cadherin expressed in the epidermis. However, during hair follicle morphogenesis, hair placode cells reduce their expression of E-cadherin and up-regulate P-cadherin expression during their downgrowth into the dermis. This change in adhesion appears to be functionally significant, as over-expression of E-cadherin in the skin under a K14 promoter inhibits hair follicle formation (Jamora et al., 2003). Similarly, forced expression of E-cadherin in the intestine slows migration of enterocytes up the villus (Hermiston et al., 1996).

Conversely, proper adherens junction assembly is required for the formation and maintenance of epithelial tissues. During embryogenesis, down-regulation of cadherin expression is often associated with morphogenetic movements called epithelial-mesenchymal transitions, or EMTs, during which epithelial cells disassemble their cell-cell adhesions and take on a more migratory phenotype (Cano et al., 2000). This occurs during formation of mesoderm at gastrulation and in during migration of neural crest cells (Thiery et al., 2009). Similar phenotypic changes also occur during metastasis of epithelial tumors,

when tumor cells lose their epithelial characteristics and invade the surrounding tissue (Cano et al., 2000). Loss of cadherin adhesion can also lead to tissue degeneration, as early mouse embryos lacking E-cadherin are unable to form a blastocyst cavity or trophectoderm epithelium due to impaired cell junction formation, and die at the time of implantation (Larue et al., 1994a; Larue et al., 1994b; Ohsugi et al., 1997). In the skin, simultaneous depletion of both E- and P-cadherins results in impaired cell-cell adhesion and epidermal barrier formation, as well as increased apoptosis, perturbations in tissue architecture and disruption of cell polarity (Tinkle et al., 2008). In contrast ablation of E-cadherin alone results in a milder impairment of terminal differentiation and progressive loss of hair follicles (Tinkle et al., 2004; Tunggal et al., 2005; Young et al., 2003). This difference is likely due to the upregulation of P-cadherin in the basal layer, highlighting the potential for functional redundancy among some of the closely related family members (Tinkle et al., 2008). Similarly, in the mammary gland, conditional deletion of E-cadherin in the differentiating alveolar cells results in impaired terminal differentiation and lactation as well as increased apoptosis at the end of pregnancy (Boussadia et al., 2002).

Depletion of the catenin proteins *in vivo* has similar deleterious consequences for the tissue, although the phenotypes do vary due to the different adhesion-independent roles of the catenins. As in the case of E-cadherin, mouse embryos lacking α-catenin exhibit disruption of trophoblast development, arrest at the blastocyst stage and pre-implantation lethality (Torres et al., 1997). Conditional ablation of α-catenin in the epidermis using the K14 promoter to drive Cre recombinase results in striking defects in epidermal

architecture. Mouse embryos lacking α-catenin in the skin are born alive, but die within hours from dehydration due to failure to establish a functional epidermal barrier. These embryos do not develop normal hair follicles, and their skins show a discontinuous basement membrane and loss of epidermal cell polarity (Vasioukhin et al., 2001). Their epidermis also exhibits hyperproliferation, accompanied by increased MAP kinase, Nf-kappaB and Stat3 signaling and inflammation (Kobielak and Fuchs, 2006; Vasioukhin et al., 2001). Skins grafted from these embryos onto immuno-compromised *Nude* mice form large proliferative invaginations into the underlying dermis and progressively resemble human squamous cell carcinoma *in situ* (Kobielak and Fuchs, 2006).

α-catenin is also critical for the development of other tissues. In the mammary gland, deletion of α-catenin using WAP-Cre or MMTV-Cre results in arrested alveolar expansion, defects in cell polarity, functional differentiation and milk protein production as well as an increase in apoptosis (Nemade et al., 2004). In contrast, deletion of α-catenin in the brain using a CNS-specific Cre results in an abnormal activation of Sonic Hedgehog signaling, which results in a shortened cell cycle, reduction in apoptosis and cortical hyperplasia (Lien et al., 2006). Thus, the consequence of α-catenin deletion depends on cell type and stage of development.

In contrast to E-cadherin and α-catenin, the phenotypes of β-catenin deletion in mice tend to arise primarily from its adhesion-independent functions in Wnt signaling. This is likely due to some compensation by plakoglobin at adherens junctions (Haegel et al., 1995). For instance, epidermal deletion of β-catenin results in defects in hair follicle morphogenesis, but not epidermal barrier

formation (Huelsken et al., 2001). Deletion of β-catenin in the embryonic endoderm leads to the formation of multiple hearts and ectopic Bmp2 signaling, due to a conversion to pre-cardiac mesoderm cell fate in the absence of Wnt signaling (Lickert et al., 2002). Similarly, deletion of β-catenin in the central nervous system results in a shift of dorsal telencephalon cells to a ventral cell fate due to lack of Wnt signaling (Backman et al., 2005).

On the other hand, p120-catenin deletion phenotypes in mice more closely resemble those of cadherins and α-catenin. Epidermal deletion of p120-catenin results in reduced adherens junction components in the epidermis of newborn mice, but no gross disruption of differentiation or barrier formation. However, as the mice age, the epidermis becomes hyperproliferative and undergoes chronic inflammation. As in the case of α-catenin, the inflammation is due to increased NFkB activation; unlike the α-catenin mutant, the NFkB activation appears to result from increased Rho activation that occurs in the absence of p120-catenin (Perez-Moreno et al., 2006). Ultimately, grafted skins from these mice develop progressive epidermal neoplasias that exhibit mitotic alterations, due to the elevated NfkB and Rho activity levels (Perez-Moreno et al., 2008). Similarly, deletion of p120-catenin in hippocampal neurons results in increased RhoA activation and decreased synapse formation (Elia et al., 2006). Conditional ablation of p120-catenin in salivary glands results in defects in ductal differentiation, cell adhesion and morphology, and also produces hyperproliferative masses that resemble epithelial neoplasias (Davis and Reynolds, 2006).

It should be noted that although the above outlined examples have come from studies in mice, much of what we know about adherens junction biology is conserved in lower metazoa such as *D. melanogaster* and *C. elegans*. For instance, in *Drosophila,* the E-cadherin and β-catenin homologs encoded by the *shotgun* and *armadillo* genes, respectively, are also central to the formation of multiple epithelial tissues and morphogenetic movements during embryogenesis (Cox et al., 1996; Tepass et al., 1996).

Cross-talk Between Adherens Junctions and Other Signaling Pathways

During tissue development and homeostasis, it is critical to coordinate the regulation of cell-cell adhesion with that of other pathways that govern tissue architecture, rearrangements, growth and differentiation. These pathways include input from cell-matrix adhesions and growth factor receptors that must be integrated with signal cues from cell-cell contacts to guide cellular behavior. For instance, cells undergoing EMT during mesoderm formation concomitantly reduce their cell-cell adhesions and increase their migration over the ECM (Cano et al., 2000). A breakdown in the process of integration of these pathways can lead to defective tissue development, or to disease states, such as tumorigenic transformation and metastasis.

Cell-Matrix Adhesions and Control of Migration

A point of convergence between cell-cell and cell-ECM adhesion signaling occurs at the level of actin cytoskeleton regulation. Both adherens junctions and focal adhesions (FAs), the integrin-based structures that mediate ECM adhesion, control the activity of proteins that are involved in actin remodeling (Illustration

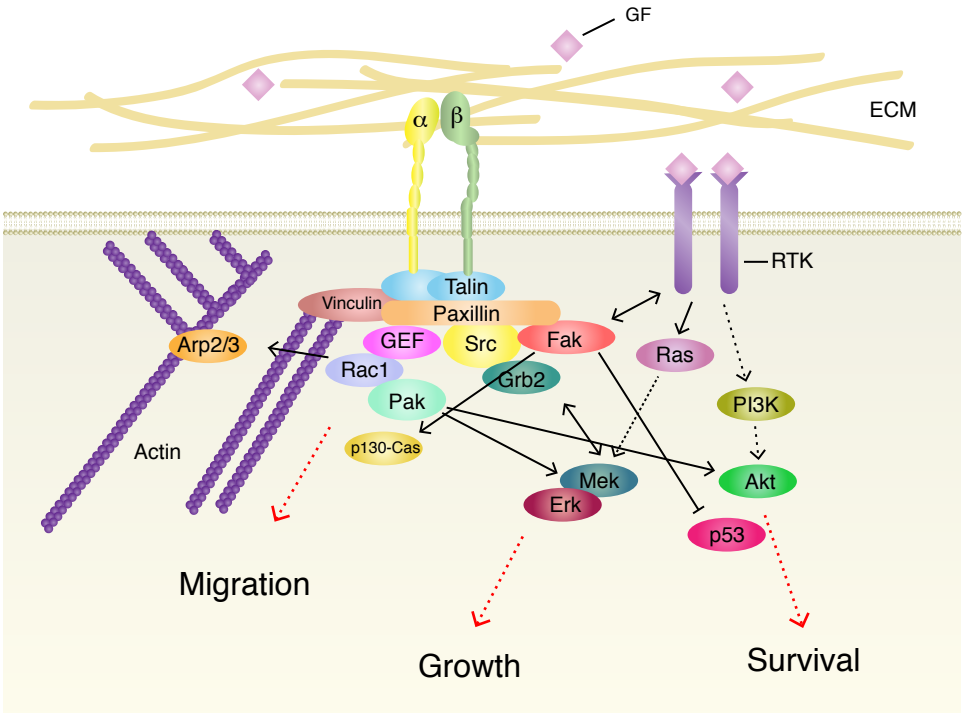

Illustration 1.5. Schematic of focal adhesion signaling centers. Integrin heterodimers form receptors for extracellular matrix (ECM) proteins and constitute the transmembrane core of the focal adhesion. Adhesion to ECM promotes the formation of a multiprotein complex at the cytoplasmic tail of integrins. Multi-domain adapter proteins such as Talin and Paxillin provide docking sites for the recruitment of kinases and actin regulators such as Rac Guanine Nucleotide Exchange Factors (GEFs). Rac activation promotes actin polymerization via Arp2/3 and leads to extension of membrane protrusions ahead of the adhesion site, enabling migration. Focal adhesion kinase (Fak) binds Paxillin and becomes activated upon integrin ligation. It phosphorylates many targets, including Paxillin and p130-Cas, which also regulate migration by promoting focal adhesion disassembly. Fak can also bind growth factor receptor tyrosine kinases, which often associate with focal adhesions. This interaction can promote their downstream signaling through the RAS-MAPK and PI3K pathways thereby enabling-convergence between migration, growth and survival pathways. Arrow, positive regulation; double arrow, dynamic association; dashed arrow, multi-step regulation.

1.5). These proteins, which include Rho family GTPases, along with their effectors and regulators, in turn can modify the assembly, stability and disassembly of both types of adhesion structures.

Integrin heterodimers, consisting of an α and β subunit, form the core of most cell-ECM adhesions and act as bidirectional mechanochemical links between the ECM and the actin cytoskeleton (Illustration 1.5). Binding to ECM components such as fibronectin, collagen or laminin triggers clustering of integrins in the plane of the cell membrane and the formation of the macromolecular structures called focal adhesions (Berrier and Yamada, 2007). At these locations, the cytoplasmic tails of integrins, which themselves lack enzymatic activity, recruit a vast array (over 160 to date) of cytoskeletal regulators and other signaling proteins that form a cytoplasmic plaque (Geiger et al., 2009). Regulation of FA turnover is of particular importance during cell migration. In general, cell migration proceeds through extension of lamellipodial or filopodial protrusions at the front, or leading edge of the cell, which become anchored to the ECM through the assembly of new FAs. The focal adhesions provide traction as the cell migrates over ECM and are disassembled at the rear of the cell and at the base of protrusions as the cell moves forward (reviewed in(Ridley et al., 2003).

Key regulators of integrin signaling include multi-domain adapter proteins such as Talin, Vinculin and Paxillin, which serve as docking sites for effector kinases and regulators of actin organization (Brown and Turner, 2004). For example, integrin engagement by ECM stimulates the activation and autophosphorylation of focal adhesion kinase (Fak) at Tyrosine 397. This

phospho-tyrosine provides a docking site for the kinase Src, which then phosphorylates additional Fak residues to potentiate its activity, ultimately resulting in the phosphorylation of Fak substrates such as p130Cas and Paxillin (Geiger et al., 2001; Miranti and Brugge, 2002). Fak and Paxillin phosphorylation are particularly important for FA disassembly; cells lacking these proteins, or expressing constructs that are not capable of being phosphorylated exhibit slower rates of FA disassembly and impaired migration in culture (Petit et al., 2000; Webb et al., 2004). Similarly, conditional ablation of Fak in the mouse epidermis results in impaired downgrowth of hair follicle cells into the dermis, (a process that involves collective migration of placode cells) and slowed keratinocyte migration out of a tissue explant due to reduced FA disassembly (Schober et al., 2007).

Phosphorylated Paxillin can also recruit other effectors, such as the GIT-PKL-Pix-Pak complex and Crk, both of which promote activation of the Rac1 GTPase (Brown and Turner, 2004). Pix, as a guanine nucleotide exchange factor (or GEF), is an activator for Rac1, while a Pak is a serine/threonine kinase that is also a Rac1 effector that phosphorylates Paxillin, among other substrates. Thus, this module can create a positive feedback loop to maintain localized Rac1/Pak signaling at the focal adhesion and couple adhesion turnover to the formation of new membrane protrusions (Nayal et al., 2006; Zhao et al., 2000). Rac1 activity at the leading edge is important for cell migration both *in vitro* and *in vivo* (Kraynov et al., 2000). As in the case of Fak, conditional deletion of Rac1 in the epidermis results in defective hair follicle morphogenesis and wound healing, as well as

impaired cell spreading and migration in cultured keratinocytes (Castilho et al., 2007; Chrostek et al., 2006; Tscharntke et al., 2007).

Rac1 activation is also regulated during cell-cell adhesion formation. Induction of cadherin adhesion in cultured cells by increasing the calcium concentration results in a transient activation of Rac1, which is inhibited by an E-cadherin neutralizing antibody (Nakagawa et al., 2001; Noren et al., 2001). Rac1 localization and activity are highest near nascent sites of cell-cell contact, but decrease as sites become stabilized (Ehrlich et al., 2002; Kovacs et al., 2002; Yamada and Nelson, 2007). The activation of Rac1 at nascent cell-cell contacts may recruit the Arp2/3 complex and promote the assembly of branched actin networks. This process may be inhibited by α-catenin during the subsequent stabilization phase, as branched actin is bundled into actin cables (Yamada et al., 2005). Inhibition of Rac1 may indeed play a role in junction stabilization as hyperactivation of Rac1 perturbs the localization and adhesion of E-cadherin in several different cell types (Braga et al., 2000; Pirraglia et al., 2006).

In addition to Rac1 itself, several of its regulators and effectors can localize to both cell-cell and cell-matrix adhesions. Examples of such dual localization patterns include Src, the Rac GEFs Tiam1 and β-Pix, as well as the Rac effectors Pak, IQGAP1 and the Arp2/3 complex (Brown and Turner, 2004; Geiger et al., 2009; Hamelers et al., 2005; Kuroda et al., 1998; Lozano et al., 2008; Malliri et al., 2004). These studies demonstrate that Src can phosphorylate AJ components and promote their dissociation, while IQGAP1 can compete with α-catenin for binding to β-catenin; Tiam1 and Pak proteins are required for the disassembly of AJs induced by Rac1 hyperactivation. Thus, their recruitment to one structure or

the other can coordinate a shift between stable cell-cell adhesion and dispersive migration, such as the one that occurs during epithelial-mesenchymal transitions in development.

Growth-Factor and Survival Signaling

In addition to their direct roles in physically anchoring cells to their microenvironment, both cell-cell and cell-matrix adhesions control cell proliferation and survival by interfacing with growth factor and MAP kinase-signaling (MAPK) pathways. Adhesion to the ECM sends a strong pro-survival signal, and untransformed cells require ECM adhesion to progress through the G1 phase of the cell cycle in response to mitogenic stimuli (Wary et al., 1998). Focal adhesion components such as integrins, Fak and Src can associate directly or indirectly with growth factor receptors to potentiate their downstream signaling pathways (Danen and Sonnenberg, 2003; Long et al., 2010). In general growth factor receptors are tyrosine kinases that dimerize and autophosphorylate upon ligand binding. The phosphotyrosines provide docking sites for adapter proteins such as growth factor receptor-bound protein 2 (Grb2) or insulin receptor substrate 1 (Irs1), which transmit the signal to the Ras/MAPK and PI3K pathways, among many others. Activation of MAPK and PI3K/Akt then phosphorylate numerous targets to promote proliferation and cell survival, respectively (Reviewed in (Lemmon and Schlessinger, 2010).

Integrin-mediated signaling may converge with receptor tyrosine kinase (RTK) signaling through Pak, Fak or Src-dependent phosphorylation of Raf or MEK (Chen et al., 1996; Renshaw et al., 1997). This phosphorylation may promote the assembly of Raf-Mek-Erk signaling complexes (Slack-Davis et al.,

2003). Additionally, the localization of RTKs to FAs, and their physical interaction with integrins, can amplify these phosphorylation cascades by bringing kinases and substrates in close proximity (Danen and Sonnenberg, 2003; Yamada and Even-Ram, 2002). In some cases, integrin-mediated adhesion can even cluster and activate RTKs in caveolae and lipid raft membrane domains in the absence of their specific ligands (Miyamoto et al., 1996; Wary et al., 1996). Integrin signaling can suppress Caspase and p53 activity via PI3K-mediated activation of Akt, thereby inhibiting apoptosis. Thus, integrin hyperactivation can promote some cell survival under conditions of growth factor starvation (Boudreau et al., 1995). In contrast, depletion of Fak or integrin β1 can lead to apoptosis in embryonic fibroblasts or endothelial cells (Braren et al., 2006; Shen et al., 2005). The net effect of this integrated signaling network depends on the specific complement of ligands, receptors, and adapters found in a particular tissue microenvironment. Conversely, IGF and EGF-dependent signaling pathways can also regulate cytoskeletal remodeling and cell migration through activation of Rac1, phosphorylation of Fak or myosin light chain (MLC) kinase (Haase et al., 2003; Klemke et al., 1997; Ridley et al., 1992).

Cadherin-mediated adhesion tends to promote cell survival, but also a density-dependent "contact inhibition" of cell proliferation (Fagotto and Gumbiner, 1996). This mechanism ensures that cells in an epithelial tissue do not overgrow indefinitely. Although this phenomenon is not yet well understood, several studies suggest that cadherin ligation can act to suppress RTK signaling. Studies indicate that the contact inhibition may depend on the translocation of a Pak-Pix complex from FAs to AJs (Liu et al., 2010; Zegers et al., 2003) E-cadherin

has been shown to form a complex with the EGF receptor, and cadherin-mediated cell adhesion was found to suppress EGF receptor signaling in human breast epithelial cells and MDCK cells (Qian et al., 2004; Takahashi and Suzuki, 1996). Conversely, cells treated with an E-cadherin blocking antibody concomitantly with EGF show increased Erk phosphorylation compared EGF-only treatment, suggesting that inhibition of E-cadherin adhesion can potentiate EGFR signaling (Damiano et al., 2010). Likewise, E-cadherin has also been reported to form a complex with the IGF1 receptor and negatively regulate its activity (Canonici et al., 2008; Guvakova and Surmacz, 1997).

In the skin, both EGF and IGF ligands are mitogenic stimuli for keratinocytes. The receptors for both ligands are expressed primarily in the basal layer and regulate its proliferation, migration and differentiation (Hodak et al., 1996; Vassar and Fuchs, 1991). Indeed, EGFR levels are upregulated during wound healing (Nanney et al., 1996). The IGF ligand is produced in dermal fibroblasts and is thought to transmit proliferation and survival signals to the basal layer through MAPK and PI3K pathways (Sadagurski et al., 2006). Conditional ablation of the IGF receptor in the epidermis has been shown to cause progressively decreased epidermal thickness and reduced proliferation; the proliferation could be rescued by expression of constitutively active Rac1, further highlighting the complex crosstalk between these pathways (Stachelscheid et al., 2008). Interestingly, cultured keratinocytes lacking α-catenin show increased sensitivity to insulin in growth media, as treatment with insulin results in sustained Erk phosphorylation of α-cat knockout (KO) cells as compared to controls (Vasioukhin et al., 2001).

Adherens Junctions and Cancer

Disruption of cell-cell adhesion coupled with aberrant cell matrix and growth factor signaling are not only detrimental to tissue development and homeostasis, but are also hallmarks of cancers. Epithelial tissue derived cancers, referred to as carcinomas, are some of the most common types of cancer, and more than half of all human cancers arise from squamous epithelia specifically (Jemal et al., 2010; Parkin et al., 2005). Numerous clinical and high-throughput genomics studies have characterized the reduction of E-cadherin, α-catenin and p120-catenin in a wide variety of cancers due to somatic or germline mutations, epigenetic or transcriptional repression, or post-transcriptional regulation (Cowin et al., 2005; Hajra and Fearon, 2002; Ochiai et al., 1994; Shiozaki et al., 1994). Functional studies have demonstrated that re-expression of the missing AJ proteins can suppress invasion and malignant conversion in cancer cells, suggesting a critical tumor suppressive role for AJs (Perl et al., 1998). Indeed, the loss of cell-cell adhesion markers generally correlates with tumor grade and patient mortality (Cavallaro and Christofori, 2004; Yoshida et al., 2001).

Squamous cell carcinomas (SCCs) and other epithelial cancers also often carry mutations in key regulators of cell proliferation and survival: Ras and p53. The p53 pathway becomes suppressed in nearly all human cancers, often as a result of inactivating missense mutations in its DNA binding domain (Oren and Rotter, 2010; Soussi et al., 2006). Activating point mutations in H-Ras are the frequent oncogenic mutations in human skin and in mouse models of chemical carcinogenesis (Quintanilla et al., 1986). Hyperactivation of Ras-MAPK signaling has been observed in over 30% of all human cancers (Hoshino et al., 1999; Leon et

al., 1987; Quintanilla et al., 1986). In mouse models, epidermal deletion of p120-catenin or α-catenin induces neoplasia and SCC *in situ* (Kobielak and Fuchs, 2006; Perez-Moreno et al., 2008). Alteration of either, or both of these pathways can cooperate with AJ destabilization to accelerate tumorigenesis. For instance, while conditional of E-cadherin in the mammary gland leads to tissue degeneration and increased apoptosis, deletion of both E-cadherin and p53 leads to metastatic lobular mammary carcinoma through increased cell survival (Derksen et al., 2006).

The primary cause of patient mortality is usually not the primary tumor itself, but metastatic lesions (Jemal et al., 2010). Metastasis is a multistep process during which the tumor cells must leave the primary tumor site to invade neighboring blood or lymphatic vessels (intravasation), survive in circulation, exit the circulatory system (extravazation) and colonize a secondary tissue (Nguyen et al., 2009). The early stages of metastasis, during which tumor cells reduce their cell-cell adhesion and become more migratory and invasive, resemble the EMT mechanisms utilized to break apart the epithelial sheet during development. Thus, in addition to a reduction in cell-cell adhesion, these cells often concomitantly exhibit hyperactivation of integrin/Fak and RTK signaling to enable their migration and survival (Desgrosellier and Cheresh, 2010; Guasch et al., 2007).

Both *in vitro* and *in vivo* studies have demonstrated that these pathways, and in particular, the genes that mediate their convergence are critical for tumor progression. For instance, the Rac1-Pak signaling axis is required for maximal activation of the MAPK pathway, likely through Pak-mediated phosphorylation

of Mek. In support of this, deletion of Rac1 in models of K-Ras induced lung cancer or colorectal carcinoma cell lines suppresses tumor formation (Espina et al., 2008; Kissil et al., 2007). In the skin, mice lacking Rac1, or its activator Tiam1, are resistant to Ras-induced tumorigenesis (Malliri et al., 2002; Wang et al., 2010). Conversely, Rac1 upgregulation has been observed in tumors and cancer cell lines, and its overexpression can accelerate tumorigenesis (Espina et al., 2008; Lozano et al., 2003). Similarly, Fak is often overexpressed in invasive carcinomas (Cance et al., 2000; Lark et al., 2003; Owens et al., 1995). Fak hyperactivation promotes cell migration and proliferation through its regulation of actin and MAPK signaling. It can also promote cell survival through inhibition of p53 by directly binding p53 and targeting it for proteasomal degradation (Lim et al., 2008). Deletion of Fak in the epidermis or mammary gland suppresses tumor formation and invasion (Luo et al., 2009; McLean et al., 2004; Pylayeva et al., 2009). These studies illustrate the complex and integrated nature of oncogenic signaling networks.

The Tissue Morphogenesis and Cancer Toolbox

As our understanding of the complex interconnections between pathways governing tissue biology expands, we continue to need more sophisticated tools to dissect these integrated networks. Our current understanding of tissue development and homeostasis comes from decades of research using a variety of experimental systems, each with its own advantages and drawbacks.

Lower Eukaryotes: Simpler Genetics

Many of the key pathways governing tissue development, such as the Wnt, Hedgehog and Notch pathways are highly conserved and have been characterized in depth in *Drosophila melanogaster*. Their rapid life cycle and ability to produce large numbers of offspring, combined with a relatively low level of functional redundancy between genes make *Drosophila* a particularly advantageous system for mutagenesis screens. Sophisticated genetic screens can be designed not only to test the function of individual genes, but also to identify genes that function in common pathways through "second site modifier" screens and analysis of epistasis (Bier, 2005). For instance the RTK-Ras-MAPK signaling network was initially worked out in a series of second site modifier screens, looking for modifiers of the *sevenless* RTK mutant allele (Dickson et al., 1996; Margolis and Skolnik, 1994; Simon et al., 1991). The ease of transgenic delivery of genetic constructs facilitates analysis of gene misexpression, overexpression, knockdown by RNA interference (RNAi) or tagging with fluorescent proteins, while the fast breeding time facilitates various combinations of these approaches (McGuire et al., 2004; Yao and White, 1994). More complex genetic systems, such as heat shock or tetracycline inducible expression and the UAS-Gal4 system, enable precise spatiotemporal control over gene expression (Bello et al., 1998; Brand and Perrimon, 1993; Lis et al., 1983; Wilder, 2000). Additionally, using a FLP/FRT recombinase system, experimenters are able to perform mosaic analysis on clones of mutant tissue that are interspersed with wild-type control cells in the same animal. This has enabled analyses of competitive growth and

the distinction between cell-autonomous and non-autonomous phenotypes (Nellen et al., 1996; Struhl and Basler, 1993).

Despite these advantages, the *Drosophila* system also has its limitations. Certain structures or pathways, such as beaks, feathers, or an elaborate central nervous system have evolved in vertebrates that are not be found in lower eukaryotes. Other characteristics, such as mammary glands and hair are specific to mammals. Moreover the phenotype for a gene mutation in *Drosophila* does not always correlate with the mammalian phenotype. An example of this is the p120-catenin gene, whose ablation in mammalian tissues results in disassembly of cell-junctions and striking perturbation of epithelial integrity. In contrast in *Drosophila*, p120-catenin is not required for cell-cell adhesion (Myster et al., 2003). Conversely, some genes may be required for a process in *Drosophila*, but its homolog may have functional redundancy in mammals, as in the case of E- and P-cadherin in the mammalian skin (Tinkle et al., 2008).

Cell Culture

Advances in cell culture technology have facilitated the study of many cellular processes involved in development and disease in mammalian cells. Many cell lines and primary cells can recapitulate processes that occur *in vivo*, including intercellular junction formation in keratinocytes and Madin-Darby canine kidney (MDCK) cells, as well as differentiation and synapse formation in cultured neurons. The ability to control growth media formulations facilitates probing signaling pathways by the addition or removal of growth factors or chemical inhibitors. Transfection with plasmid DNA and infection with viral vectors with various constitutive and tetracycline-inducible promoters allows

control over exogenous gene expression and knockdown (Gossen et al., 1995). Cultured cells are also amenable to videomicroscopy and high-throughput screens. Additionally, cells may often be grafted into immunocompromised mice after manipulations in culture to study tissue regeneration or tumorigenesis (Blanpain et al., 2004; Welm et al., 2008).

Since the 1980s, the development of 3D culture methods has enabled more accurate studies of tissue regeneration. 3D organotypic culture of keratinocytes has been used to study skin neoplasia and even invasion (Asselineau et al., 1989; Kopan et al., 1987; Reuter et al., 2009; Ridky et al., 2010). Isolated intestinal stem cells can regenerate entire crypt-villus structures *in vitro* (Sato et al., 2009), and MDCK cells can form spherical cysts that enable the study of cell polarization and lumen formation (O'brien et al., 2002). However, despite the extensive advances that have been brought about through studies in cell culture, these systems still do not fully recapitulate developmental signaling in the native microenvironment, and even grafting cannot reproduce the interaction with ECM and immune cells that occurs *in vivo.*

Mammalian Genetics

Genetic analyses in mice provide the closest approximation of our gene function and tissue biology. Over the last 25+ years, the resources for this system have expanded exponentially. As in *Drosophila*, transgenic technology enables the expression of genetic constructs in a tissue specific or inducible manner (Brinster et al., 1982; Furth et al., 1994; Hanahan, 1985). In the skin, the use of the Keratin 14 and Keratin 5 promoters has enabled epidermis-specific expression of a variety of proteins (Nguyen et al., 2006; Vassar et al., 1989). There are now

numerous lines carrying fluorescent proteins (such as GFP-actin), signaling reporter genes (e.g. TOP-GAL), along with gain of function and dominant negative mutants (Gat et al., 1998; Vaezi et al., 2002; Vassar et al., 1991). Additionally, site-directed mutagenesis by gene targeting in combination with the Cre-LoxP recombinase system allows for tissue-specific loss-of-function studies of gene function *in vivo* (Rajewsky et al., 1996; Thomas and Capecchi, 1987). However, the system also has its drawbacks, primarily due to the long development and breeding cycle of mice, which requires 19 days from conception to birth, and approximately eight weeks from birth to sexual maturity. This makes it more difficult to perform exploratory genetic screens, or to conduct more sophisticated analysis of genetic interactions between multiple genes in a hypothesized pathway. However, it is these kinds of studies that are becoming increasingly necessary as we begin to grasp the network complexities of morphogenetic and oncogenic signaling *in vivo.*

Specific Aims

The well-characterized architecture, spatially segregated cell types and ease of accessibility make the mammalian epidermis an attractive system to study the complex signaling mechanisms governing tissue growth. These mechanisms include signaling pathways originating from cell-cell adhesions as well as cell-matrix adhesions to regulate cell survival and the precise balance between proliferation and differentiation that are required to maintain the integrity of the epidermal barrier. Studies in mice are able to closely recapitulate the cellular behaviors and molecular pathways that take place in human tissue and can provide major insights into potential treatments for cancers and other

diseases. However, studies in mouse skin have been hampered by a lack of tools that enable the rapid analysis of genetic interactions and mid- to high-throughput genetic studies. This is due to the difficulties in generating targeted mouse mutants and the long breeding time of mice.

In my thesis work, I aimed to circumvent these difficulties by developing technological and genetic tools to enable rapid mechanistic dissection of pathways regulating epidermal development and homeostasis. To achieve this aim, I explored whether the mammalian epidermis can be efficiently transduced with lentiviral vectors *in vivo* using an ultra-sound guided delivery microinjection system. Since lentivirus infects the first cell layer it encounters, I had to identify a time window when the proliferative basal cells would be accessible to the virus. Additionally, in order for the methodology to be useful as a tool, it was necessary to show that the viral genome becomes specifically and stably integrated in the epidermal precursor cell DNA and is propagated to their progeny in the epidermis and hair follicles.

Having established that the *in utero* infection approach can produce efficient and stable expression in the epidermis, my 2nd aim was to develop the system for modulating gene expression *in vivo* using lentiviral shRNA vectors, to label infected cells with fluorescent proteins and to excise floxed alleles using lentivirally-expressed Cre recombinase. In order to determine whether this system could be utilized to circumvent genetic redundancy or to analyze genetic interactions, I co-injected embryos with up to four different fluorescently labeled viruses and quantified infection by flow cytometry. Additionally, in order to accurately quantify the effect of a gene deletion on cellular growth, I developed a

flow-cytometry-based assay that measures the relative growth of mutant cells compared to wild-type cells in a mosaic tissue. As the entire process, from mouse fertilization to embryo/newborn analysis can be completed in under three weeks, and with multiple genes analyzed simultaneously, this approach extends our current genetic toolbox for epidermal analysis.

In order to demonstrate the utility of the system, I conducted a proof-of-principle study using the adherens junction protein α-catenin. Skin-specific deletion of α-catenin using transgenic expression of Cre under the Keratin 14 promoter results in a dramatic perturbation of epidermal architecture, loss of cell polarity, disruption of skin barrier function, and hyperproliferation. I examined whether these phenotypes could be recapitulated by either lentiviral shRNA-mediated knockdown or lentiviral Cre-mediated excision.

In order to test whether the system could be utilized to probe genetic interactions, I assessed whether the hyperproliferative behavior of α-catenin knockout skin could be modified by concomitant knockdown of H-ras or Erk1, which are hyperactivated upon genetic deletion of α-catenin. To assess the effect of α-catenin ablation on cellular growth, I utilized the above-mentioned cellular growth assay and uncovered a net growth disadvantage in α-catenin mutant clones. In order to search for the reason for this disadvantage, I measured the frequency of apoptosis in control and mutant clones, and observed a striking increase in apoptosis upon the loss of α-catenin. To address the mechanism of the apoptosis induction and to further highlight the utility of the system for analyzing genetic interactions, I co-depleted α-catenin and Trp53 in the

epidermis, and observed that simultaneous depletion of Trp53 mitigated the increased apoptosis and cellular growth defect.

Finally, to further probe the relationship between α-catenin loss, the disruption of epithelial integrity and the regulation of cell survival, I studied the interplay between cell-cell and cell-matrix signaling pathways in the skin. To do so, I analyzed the biochemical activation status of Fak-Pak signaling pathway components *in vivo* and *in vitro*, and found an increased activation of this signaling axis in α-catenin mutant tissue. To correlate this with cell behavior, I used videomicroscopy to analyze cell growth out of skin explants and found an increase in cell migration in α-catenin null tissues that depended on Fak and Pak signaling. Additionally, to analyze the effect of this signaling on cell survival *in vivo,* I compared frequency of apoptosis between the basal layer, where integrin signaling is active, and the suprabasal layers, which lack integrin signaling, and found that in the α-catenin null, apoptotic cells localize primarily to the suprabasal layer, whereas in control tissue, they tend to be basal. To determine whether this was dependent on focal adhesion signaling, I simultaneously depleted α-catenin and Fak in the epidermis and found that this removed the survival advantage and increased basal apoptosis in the wild type, suggesting that in the absence of proper cell-cell adhesion, cells become more dependent on cell-ECM signaling for their survival.

CHAPTER 2: DEVELOPMENT OF AN *IN UTERO* EPIDERMAL INFECTION SYSTEM

Dissecting the complex cellular behaviors regulating tissue growth in embryogenesis and cancers necessitates a physiologically relevant *in vivo* model and a method for exploring gene function in the context of signaling pathways that govern homeostasis. In *C. elegans* and *Drosophila,* studies of normal tissue balance and growth control have been aided by an array of genetic approaches including RNA interference (RNAi). In higher eukaryotes, where the relation to human cancers is often clearer, functional analyses of genes regulating cellular growth have been limited to labor-intensive knockout technologies.

Several groups have recently turned to *ex vivo* organ culture to bridge the gap between these approaches. Explants of mammary and salivary glands can undergo branching morphogenesis in culture, and this process can be manipulated through treatment with chemical inhibitors, soluble proteins and growth factors (Fata et al., 2007; Knox et al., 2010; Wiseman et al., 2003). Additionally, explants from these and other tissues can be transfected with siRNAs or infected with viral vectors for loss-of-function, gain of function and imaging studies (Feng et al., 2010; Knox et al., 2010; Matsumoto et al., 2010).

The use of viral vectors, and in particular lentivirus, has also proven to be an effective method for delivery of relatively small genes *in vivo* to several organs and tissues (Naldini et al., 1996). A number of studies have reported intra-amniotic ultrasound-guided microinjections of viruses to deliver genes *in vivo* to mammalian organs and tissues of early embryos *in situ* (Endo et al., 2008; Holzinger et al., 1995; Liu et al., 1998; Lu et al., 1997; Punzo and Cepko, 2008;

Slevin et al., 2006). While promising, such studies have not yet achieved cell type-selectivity and targeting efficiency suitable for functional analyses and probing the physiological relevance of genetic interactions in mammals. My goal was to develop a highly efficient method for manipulating gene expression in the context of intact epidermal tissue, due to its position as a classical model for studies of tumorigenesis and epithelial biology. Such a method should ideally be non-invasive, cell-type specific and should take advantage of existing generic RNAi libraries to facilitate larger scale genetic studies (Moffat et al., 2006; Silva et al., 2005). Here, I describe the developed methodology and document its feasibility for novel quantitative investigations of mouse tissue growth, morphogenesis, homeostasis and cancer.

Results

Ex vivo manipulation of skin explants

In order to determine whether culture of skin explants could provide a suitable method for rapid chemical and genetic manipulation for the skin as it is in other tissues, I developed an *ex vivo* culture system optimized to support proper development of epidermal architecture and hair follicle morphogenesis. I found that skins from E14.5 embryos could be cultured on membrane filters at the air-liquid interface for at least four days. At this stage, the epidermis consists of a basal and suprabasal layer and specification of guard hair placodes has just been initiated (Figure 2.1a). During the four-day culture, the epidermis completes stratification and barrier formation undergoes waves of hair follicle morphogenesis (Figure 2.1b). To test if the explants could be manipulated through chemical treatment, I cultured explants in the presence or absence of PI3

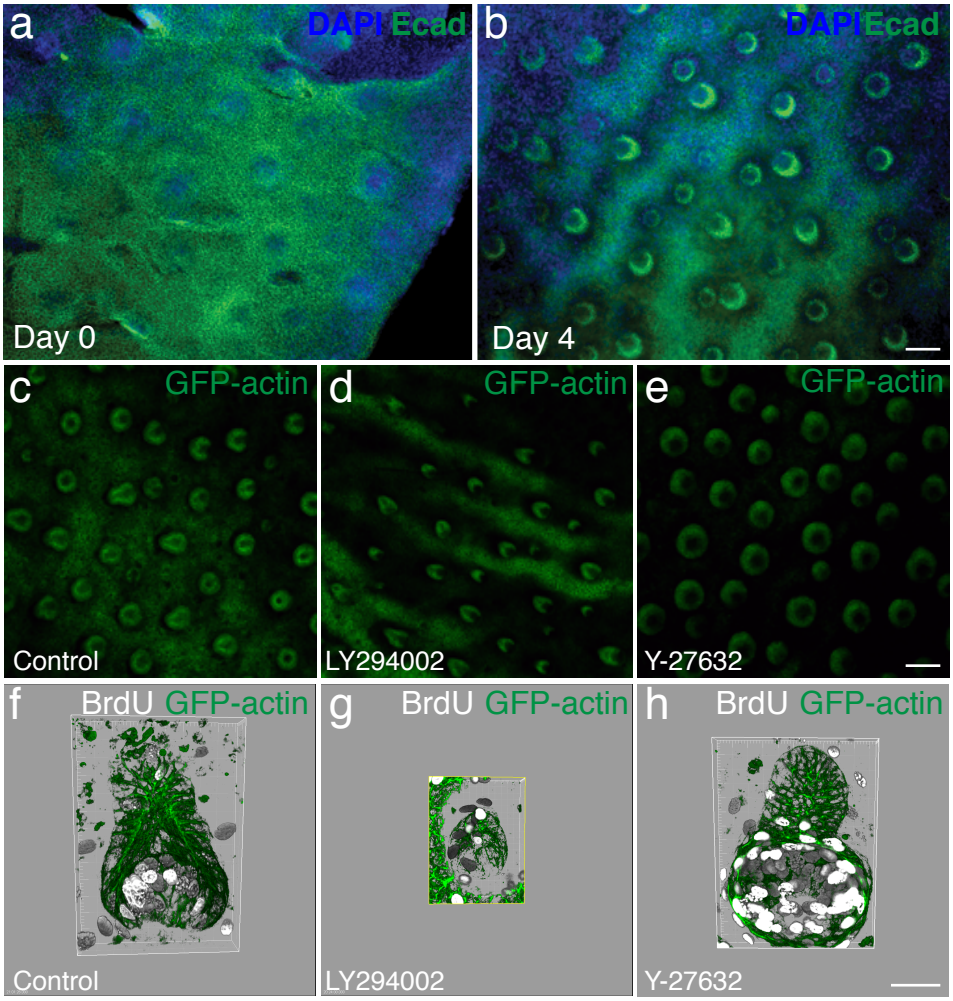

Figure 2.1 Embryonic skin explants continue to develop in culture and can be manipulated through chemical inhibitors. (a,b) Skin explants from E14.5 placed into culture (a) and allowed to develop for four days (b) undergo waves of hair follicle morphogenesis, maintain epithelial integrity and express epithelial markers. (c-e) Four day culture of skin explants in the absence (c,f) or presence of 20μM LY294002 (PI3 kinase inhibitor, d,g) or 20μM Y-27632 (ROCK inhibitor, e,h). Note the changes in hair follicle morphology in the treatment conditions. (f-h) 3D reconstructions of explants treated as in (c-e), and pulsed wtih BrdU for 1 hour to demarcate proliferating cells. Note differences in number and location of $BrdU^+$ cells in tissues treated with inhibitors. Images are planar view from dermal side. Scale bars, (a-e) 100μm (f-h) 30 μm.

kinase or ROCK inhibitors (Figure 2.1c-h). These pathways have been shown in other systems to be critical for lung and ureteric bud branching in organ culture (Liu et al., 2004; To et al., 2006). Control explants developed hair follicles with robust actin cables, polarized cells and a proliferative matrix compartment, marked by BrdU incorporation (Figure 2.1c,f), which parallel hair follicle development *in vivo*. In contrast, explants treated with either of the inhibitors formed either small or aberrantly shaped follicles that did not display an appropriate proliferative compartment (Figure 2.1d,e,g,h). These results suggested that epidermal explants were in fact amenable to mechanistic probing using chemical inhibitors. However, attempts to infect skin explants with adenoviral, retroviral or lentiviral vectors only resulted in a highly inefficient transduction of dermal fibroblasts or peridermal cells, suggesting that even by E14.5, the multiple epidermal layers formed a barrier that precluded access of virus to the basal progenitors. This greatly limited the utility of the explant system for genetic analysis and suggested that a more optimal time for targeting basal precursors might be prior to periderm formation. As the embryonic ectoderm is too fragile to dissect and culture prior to stratification, this would necessitate an *in vivo* targeting approach.

Transduction of surface epithelium with lentiviral vectors

Ultrastructural analysis of skin sections from mid-gestation embryos revealed that periderm formation had initiated at E10.5 and was complete by E12.5 (Figure 2.2a-c). To determine the functional consequences of this architectural development, embryos from E9.5 to E17.5 were analyzed for their ability to internalize lentivirus-sized fluorescent beads from the surrounding

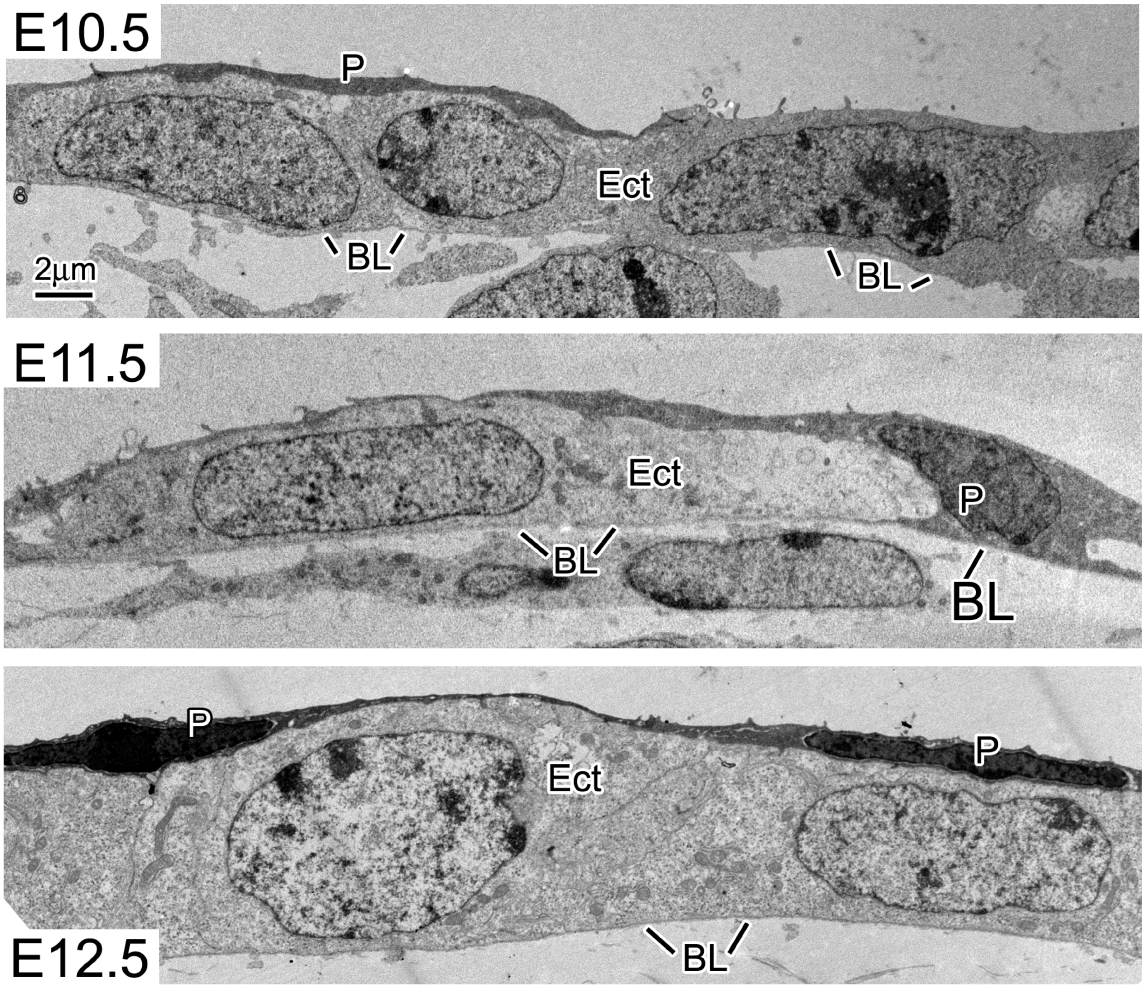

Figure 2.2 Transmission electron microscopy of periderm development during embryogenesis. (Top panel) At embryonic day 10.5, ectoderm cells (Ect) form a single layer over the basal lamina (BL) with rare individual periderm cells (P) detectable above. (Center panel) By day E11.5, more periderm cells extend intermingling processes to cover the ectoderm. (Bottom panel) At E12.5, ectodermal cells are completely covered by a layer of periderm cells connected by junctions. Scale bar, 2 μm. EM performed by H.A. Pasolli.

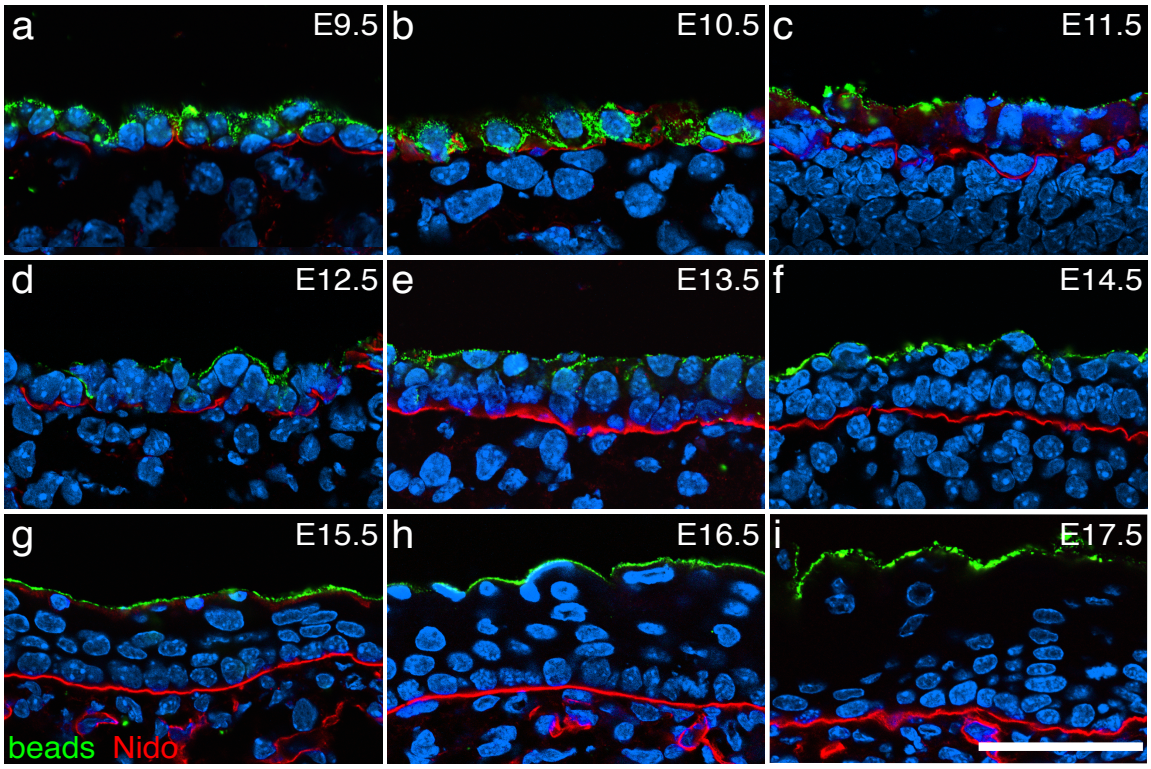

Figure 2.3 Basal epidermal cells selectively take up microspheres until E11.5 when they become fully covered by protective peridermal cells. (a–i) E9.5-E17.5 embryos were carefully separated from the extraembryonic tissue and placed in a PBS solution containing 200 nm fluorescent microspheres for 30 min, followed by sectioning and analysis of backskin tissue. Shown are representative sections illustrating the distribution of microspheres. The basal layer, resting atop the basement membrane marked by Nidogen (Nido), took up beads at E9.5 and E10.5, but subsequently microsphere uptake was restricted to the periderm. Note absence of microspheres in dermal cells. DAPI (blue) labels the nuclei. Scale bar, 50 μm.

medium (Fig. 2.3). Beads were internalized by E9.5–E10.5 surface epithelium, composed of a single layer of non-neural ectoderm, and were thereafter confined to the periderm layer, consistent with the results of the ultrastructural analysis. Importantly, even at E9.5-E10.5, the beads were only internalized by cells of the ectodermal layer, and never penetrated into the underlying mesenchyme. These results were recently corroborated by Endo *et al*., who employed ultrasound-guided lentiviral microinjection into the amniotic cavity of mouse embryos at 8–12 days post-coitum (E8–E12) to achieve postnatal expression of an epidermal-promoter-driven GFP transgene (Endo et al., 2008). However, the results of the bead uptake assay suggested that epidermal specificity might be achieved by the delivery mechanism itself.

To explore this possibility more rigorously, I performed microinjections into the amniotic cavity of E9.5 embryos, using ultrasound to visualize the position of the embryos inside the uterus (Figure 2.4a-c). Injection of fluorescent beads into the amniotic sac resulted in their deposition on the embryo surface, while mis-injection outside the amniotic sac led to retention of the beads on the amniotic membrane, highlighting the importance of proper targeting (Figure 2.4 d). Using pLKO.1, a generic lentiviral vector designed for *U6* promoter-driven short hairpin RNA (shRNA) expression, I replaced its *PGK* promoter-driven puromycin-resistance gene with *histone-H2B* fused to *Gfp, Rfp*, *Cfp* and *Yfp* cDNAs (LV-XFP; Figure 2.5a) to enable visualization *in vivo* (Kanda et al., 1998; Moffat et al., 2006; Tumbar et al., 2004). I also generated a lentiviral Cre recombinase construct (LV-Cre), harboring an nls-Cre fusion gene driven by the cytomegalovirus (CMV) promoter, to be injected onto Rosa26-YFP or Rosa26

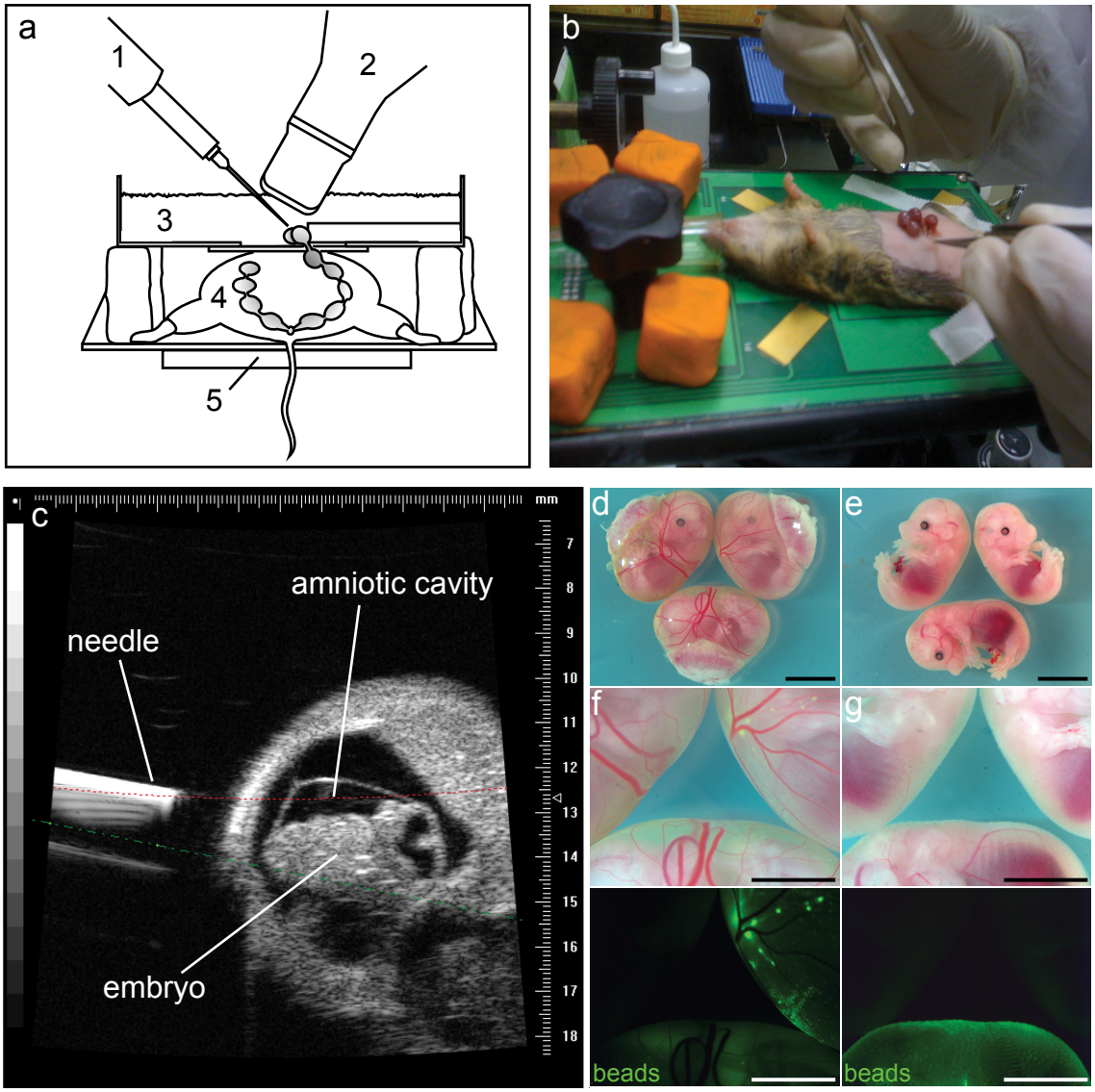

Figure 2.4 Ultrasound-guided embryonic injections successfully target the amniotic cavity. (a) Schematic of microinjection set-up. Microinjection needle, 1; ultrasound transducer, 2; modified membrane bottom dish filled with PBS, 3; anesthetized female mouse 9.5 days post conception, 4; heated stage, 5. (b) Uterine exposure during surgery. (c) Ultrasound view of the E9.5 embryo and amniotic sac just prior to injection. (d,e) Gestational sacs injected at E9.5 with 200 nm green fluorescent microspheres and analyzed at E15.5 were imaged directly (d) or following removal of extraembryonic tissue (e). (f,g) Close-up views of boxes in (d) and (e), respectively, imaged either by light or epifluorescence microscopy. Note that while two sacs received fluorescent beads, only one successfully targeted the amniotic cavity, enabling the embryo to take up the beads. Scale bars, 3 mm.

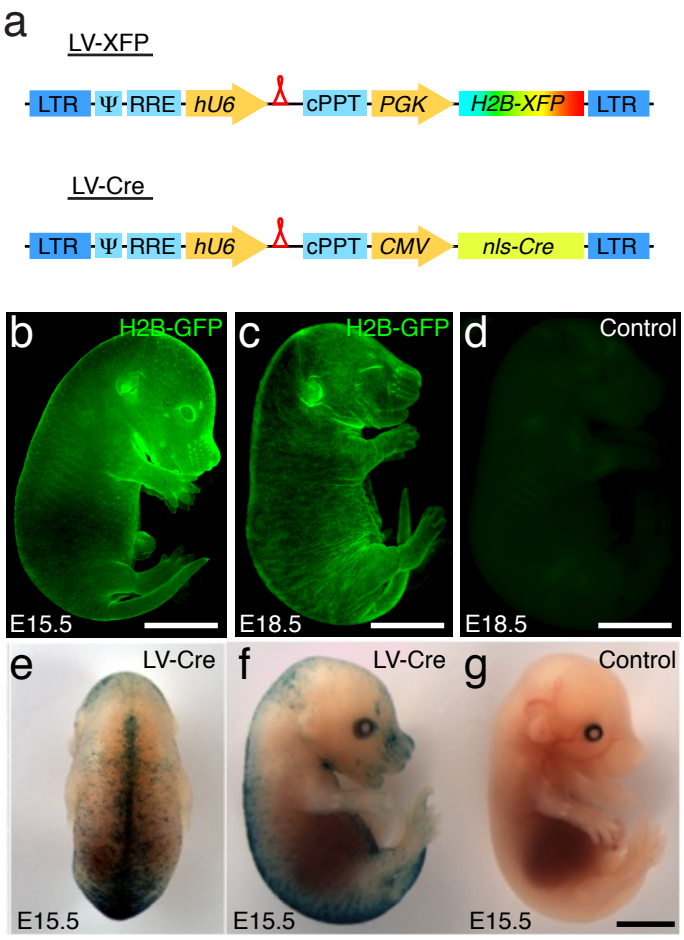

Figure 2.5 Intra-amniotic injection of lentivirus can achieve epidermal transduction and gene expression. (a) Lentiviral constructs used in the study. Modifications are of pLKO.1, a generic lentiviral vector for expressing human U6 (hU6) promoter-driven short-hairpin RNAs (shRNAs; red loop). The vector's puromycin resistance cassette is replaced by H2B fused to GFP, YFP, CFP or RFP (denoted LV-XFP). Alternatively, Cre recombinase driven by the CMV promoter is inserted, (b–d) LV-GFP infection of E9.5 embryos analyzed at E15.5 (b) or E18.5 (c) relative to non-infected control (d). (e-g) LV-Cre infection of E10.5 r26lacz+ Cre reporter embryos, analyzed at E15.5, relative to non-infected control littermate. Note the different patterns of infection at E9.5 versus E10.5 transductionScale bars, 3 mm (b,d-g), 5 mm (c,d).

LacZ Cre-reporter embryos ($r26^{yfp/+}$, $r26^{lacZ/+}$) (Soriano, 1999; Srinivas et al., 2001). Intra-amniotic injection of high-titer preparations of these viral species resulted in detectable and efficient infection epidermis upon gross examination of the embryos at E15.5 and E18.5 (Figure 2.5b-g). Empirically, infection at E9.5 achieved higher infection efficiency than at E10.5, despite the lack of a complete periderm covering at that stage. This may be due to a difference in the ratio of embryo surface area to amniotic fluid volume between the two stages that increases the relative concentration of the virus at E9.5 versus E10.5. Thus, infections were performed at E9.5 for the remainder of the study.

Examination of tissue sections transduced at E9.5 with LV-GFP revealed that by E18.5, H2B-GFP was detected throughout multilayered backskin epidermis and developing hair follicles (HFs, Figure 2.6 a). Expression was maintained in adult skin, indicating that lentiviral transductions achieved stable incorporation of DNA into the host genome, and that expression of viral transgenes was not silenced in the tissue (Figure 2.6b). Analysis of YFP expression in LV-Cre infected Rosa26-YFP embryos similarly showed YFP expression throughout the skin epithelium of E18.5 and adult mice, demonstrating that lentiviral delivery of Cre can efficiently excise loxP-flanked (floxed) sequences in single-layered embryonic epidermis (Figure 2.6c,d).

Under high infection rates, large regions of skin epithelium expressed YFP (Figure 2.6e), with an occasional YFP^- hair follicle and overlying epidermis (Figure 2.6e, inset). Conversely at lower infectivity rates, discrete areas encompassing a uniformly or partially YFP^+ hair follicle and adjacent epidermis could be visualized (Figure 2.6d-g). As the system provides control over the

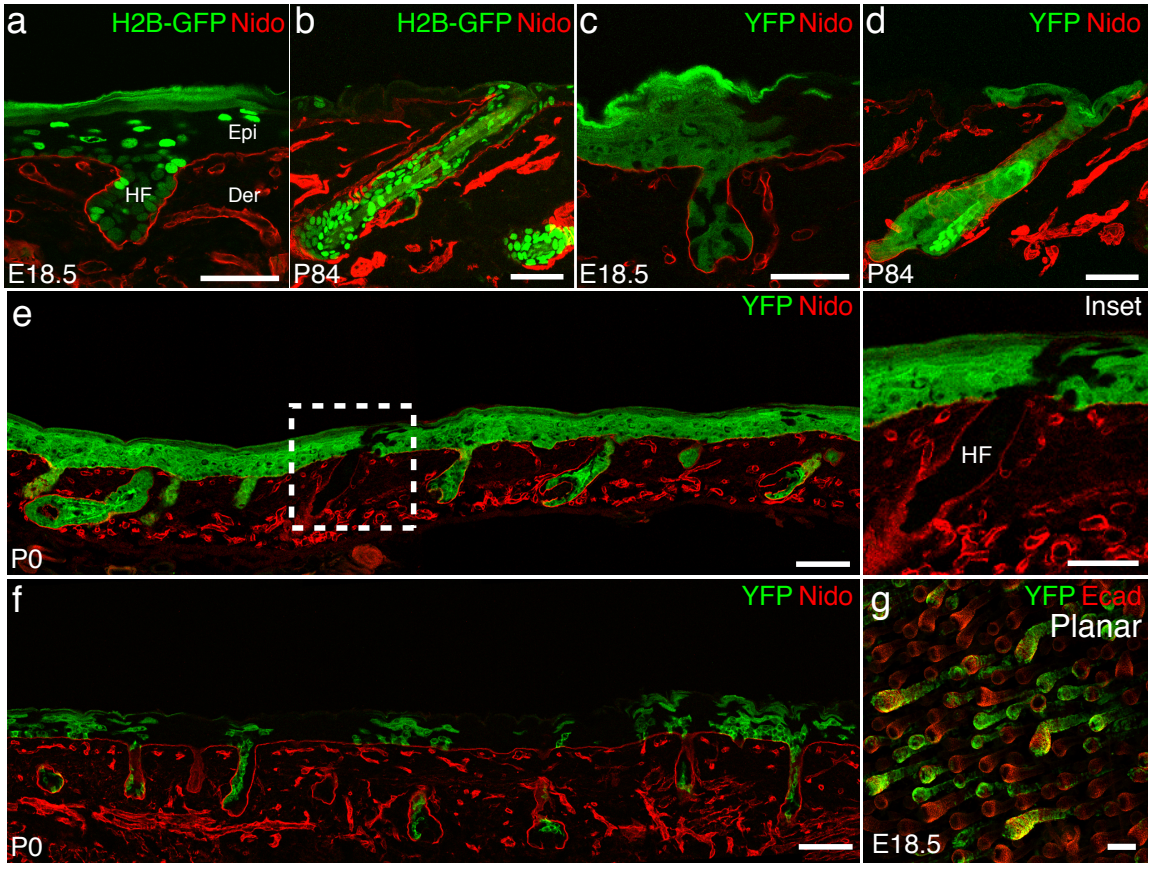

Figure 2.6 Intra-amniotic injection of lentivirus at E9.5 results in non-invasive, high-efficiency, stable and epidermally restricted transduction. (a-d) Backskin sections of E9.5 LV-GFP infected control (a,b) and LV-Cre infected $r26^{yfp/+}$ Cre-reporter embryos (c,d) analyzed at E18.5 (a,c) or 12 weeks (b,d). Transduced cells are YFP^{+} or $H2B\text{-}GFP^{+}$. Nidogen (Nido) demarcates basement membrane and dermal blood vessels. (e) Newborn backskin section at high LV-Cre infection efficiency; boxed area, enlarged and shown as an inset, shows a single non-infected hair follicle with an overlying patch of YFP^{-} epidermis. (f) Newborn backskin section at 10% infection efficiency, when individual clones may be distinguished. (g) Planar view of E18.5 backskin of $r26^{yfp/+}$ Cre reporter embryos infected with LV-Cre at E9.5, viewed from the dermal side. Transduced cells are YFP^{+} and hair follicles are labeled with anti-E-cadherin antibodies. Abbreviations: Epi, epidermis; Der, dermis; HF, hair follicle; LTR, long terminal repeat; ψ, retroviral packaging element; RRE, rev response element; cPPT, central polypurine tract; PGK, phosphoglycerate kinase promoter; H2B-XFP, histone-H2B fused to Gfp, Rfp, Cfp or Yfp; nls, nuclear localization signal; CMV, cytomegalovirus promoter; LV, lentivirus; Cre, bacterial Cre recombinase. Scale bars, (a-d, inset) 50 μm, (e,f,g) 100 μm.

degree of labeling these lineage-tracing studies (Figure 2.6f-g), it affords means to explore issues such as the arrangement of epidermis into discrete units in the future (Clayton et al., 2007).

Most importantly, the transductions led to apparent surface epithelial-specific expression without the use of tissue-specific promoters. To explore this further, I injected LV-RFP into E9.5 transgenic mouse embryos expressing actin-GFP under an epidermal-specific *Krt14* (*K14*) promoter (*K14-GFPactin*) (Vaezi et al., 2002). When subjected to fluorescence activated cell sorting (FACS), H2B-RFP$^+$ newborn backskin cells were all GFP$^+$ (Figure 2.7a) confirming that the skin transductions are epidermal-specific. Moreover, FACS quantification revealed that high infection rates were consistently achieved over the entire embryo surface in both HF and overlying epidermis, with highest transduction in the head region (Figure 2.7b,c). High head-skin infectivity at E9.5 resulted in a 2–3 day earlier excision achieved by LV-Cre (E10.5) versus transgenic K14-Cre (E12.5–E13.5) (Figure 2.8). This difference could be useful for functional analyses of genes involved in early epidermal development. Interestingly, with higher viral titers, progressively smaller increases in overall infection levels were observed. For instance, with injections of $>10^6$ cfu, a further 700% increase in viral titer elevated head-skin infection by only 30%. This raised the intriguing possibility that at high infectivity, cells might be transduced with multiple viruses (Figure 2.7b).

To monitor multiple viral deliveries, I injected E9.5 embryos with four different fluorescently tagged viruses and analyzed the tissues at E18.5 (Figure 2.9a-d). Even at low levels of infection (30%), ~1% of epidermal cells co-

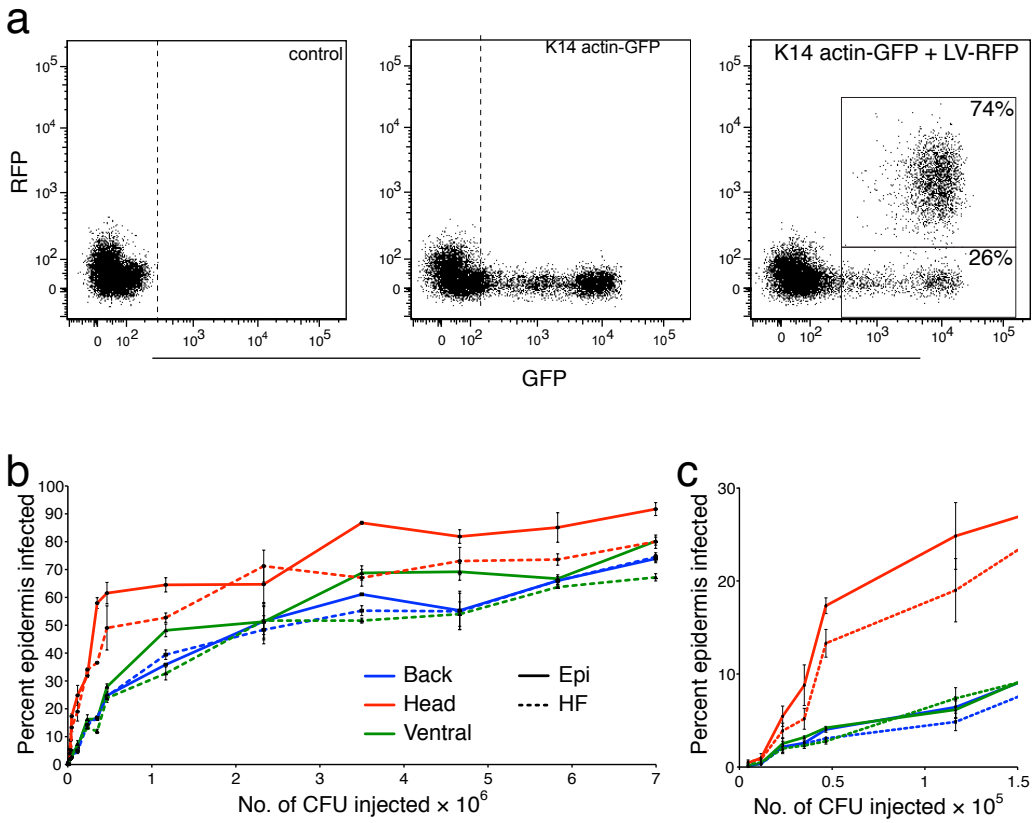

Figure 2.7 Epidermal infection depends on viral titer and is permissive for delivery of multiple viral constructs. (a) FACS analysis of control and K14actin-GFP embryos infected at E9.5 with LV-RFP and analyzed at E18.5. Note the absence of RFP signal in non-infected samples, and that only GFP+ cells are RFP+, consistent with epidermally-restricted transduction. (b) Relation between viral titer and epidermal infection efficiency as determined by FACS analysis of hair follicle and epidermal compartments of different skin regions of E18.5 embryos infected with LV-RFP. (c) Close-up view of lower titer part of the graph in (b). Note the more efficient transduction of head skin at lower viral titers.

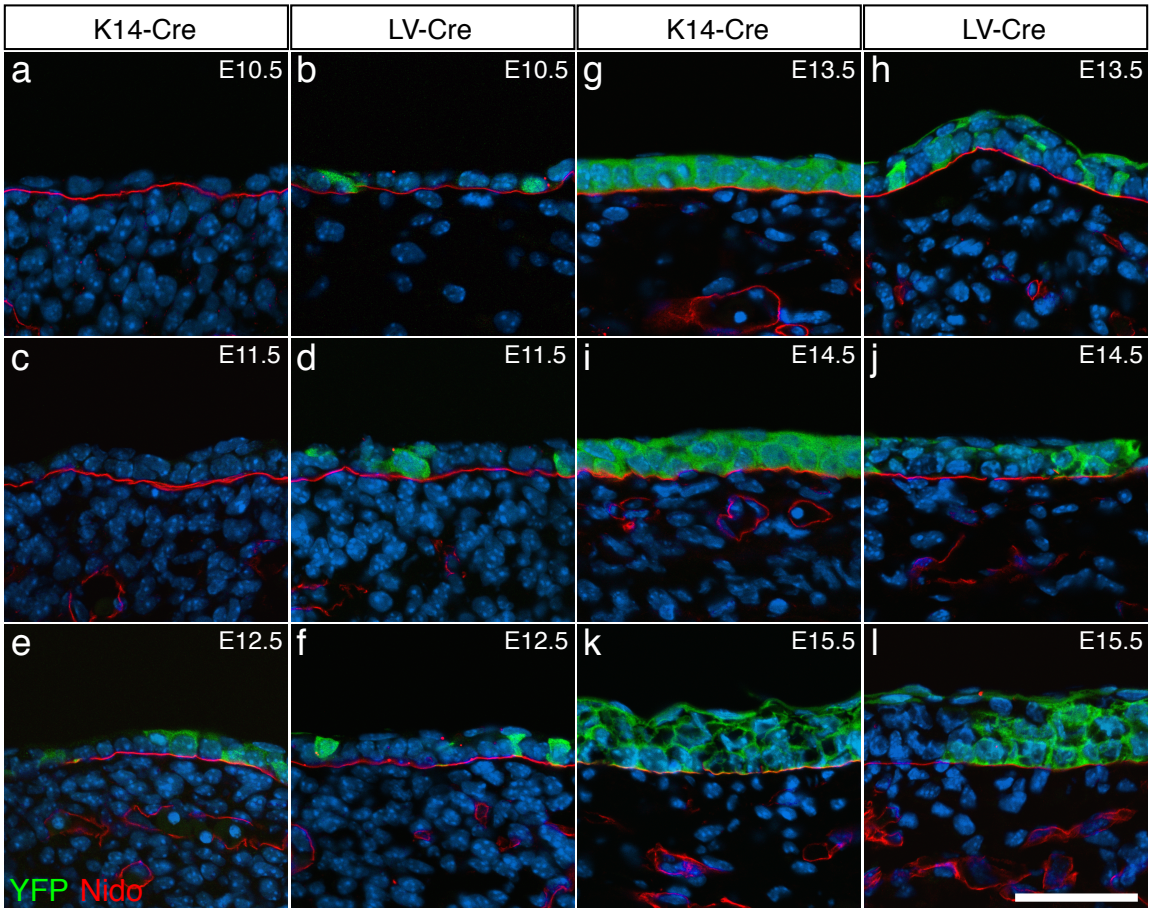

Figure 2.8 Lentiviral-Cre mediated excision precedes that achieved by K14-Cre by 2-3 days. (a–l) $r26^{yfp/+}$ embryos were either bred on a K14-Cre background or infected with LV-Cre at E9.5, and YFP expression was used to detect active Cre-mediated excision. Shown are representative backskin sections of these embryos. Note that YFP is expressed in LV-Cre infected embryos as early as E10.5 (b). By contrast, YFP is initially expressed in K14-Cre embryos by E12.5 (f) and is not fully attained until E13.5 (g). Nidogen (Nido) marks the basement membrane and blood vessels in dermis. DAPI (blue) labels the nuclei. Scale bar, 50 μm.

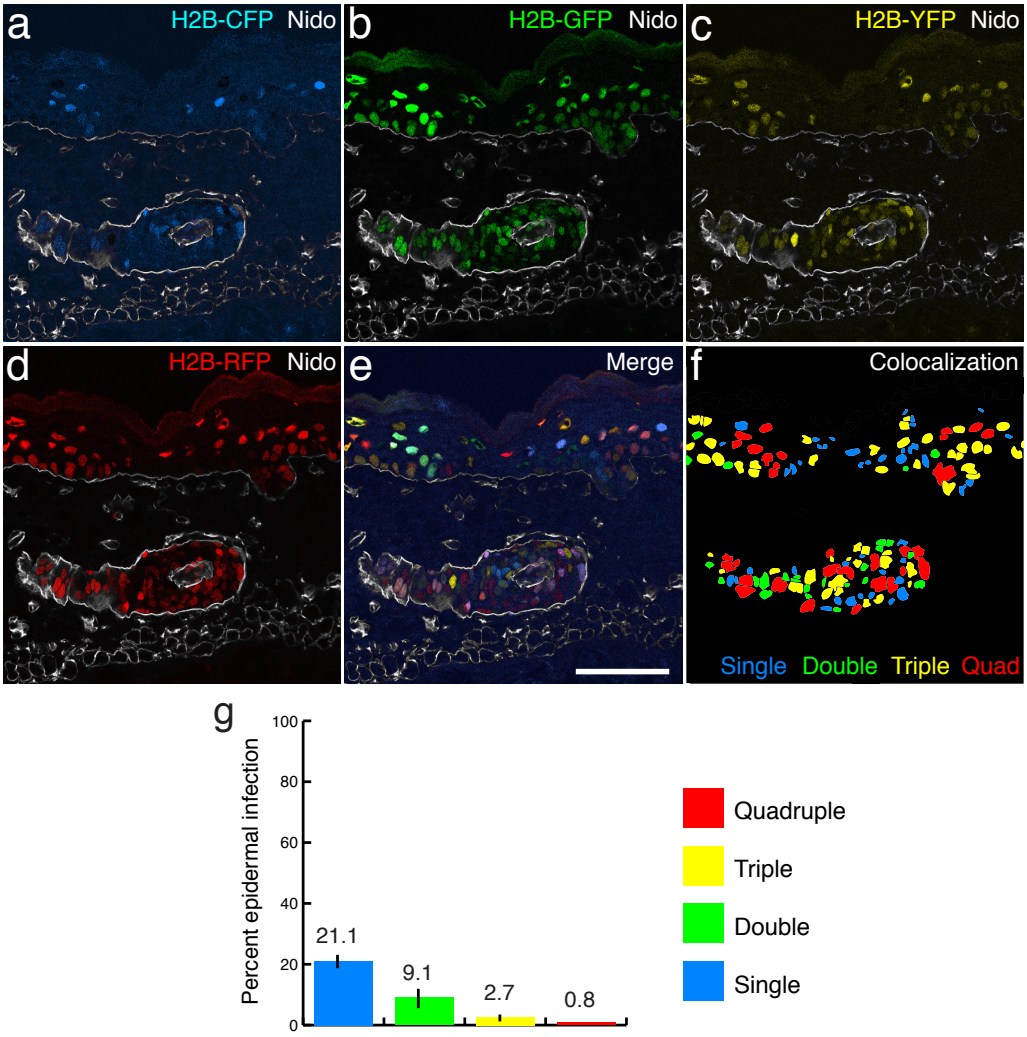

Figure 2.9 Epidermal infection permits delivery of multiple viral constructs simultaneously. (a-f) Representative backskin section from an E18.5 embryo simultaneously infected with LV-CFP, LV-GFP, LV-YFP, and LV-RFP. Shown are single color (a-d), and merged (e) images. Note that for this particular embryo, overall infection was ~34% and ~66% of the cells were uninfected. (f) Colocalization of binarized single fluorescence images, color-coded to mark single, double, triple and quadruple infection.(g) FACS quantification of co-infection efficiency, color-coded as in (f). Abbreviations: Epi, epidermis; HF, hair follicle; CFU, colony-forming units of lentivirus. Nidogen (Nido) demarcates basement membrane and dermal blood vessels. Scale bar, 50 μm.

expressed all four fluorescently tagged histones (Figure 2.9e-g). Since the backbone of each of these viruses can accommodate additional features, including multiple shRNAs and transgenes, the potential for rapid analysis of multiple gene functions far exceeds the practicality of conventional mouse genetics.

In evaluating the efficacy of the lentiviral delivery system, it was critical to verify that these viral transduction tools did not elicit adverse side effects. It is noteworthy that the described micromanipulations yielded high survival rates (79%) and efficient targeting to the amniotic cavity (81%). Moreover, lentiviral infection did not affect tissue proliferation, apoptosis, as judged by FACS analyses of BrdU incorporation and active Caspase-3 labeling of LV-Cre and LV-GFP infected epidermal cells, that showed no significant difference from uninjected control littermates (Figure 2.10a-d). Epidermal morphology and the program of differentiation were also not perturbed in infected tissues (Figure 10e-g). Additionally, leukocyte and lymphocyte numbers were comparable and low in lentivirally-infected and non-infected P0 mouse skins (Figure 2.11). This contrasted with the high level of leukocyte infiltration in skins from newborn K14-Cre p120-catenin conditional knockout mice, which display a robust pro-inflammatory response and hence served as a positive control (Perez-Moreno et al., 2006). This was particularly important, as retroviral-based vectors have been reported to elicit innate and/or adaptive immune responses in gene therapy trials (Follenzi et al., 2007). Lastly, lower levels of lentiviral transduction were detected at other sites including corneal, oral, nasal, otic and mammary epithelia (Figure 2.12). These areas arise from placodes and invaginations that are

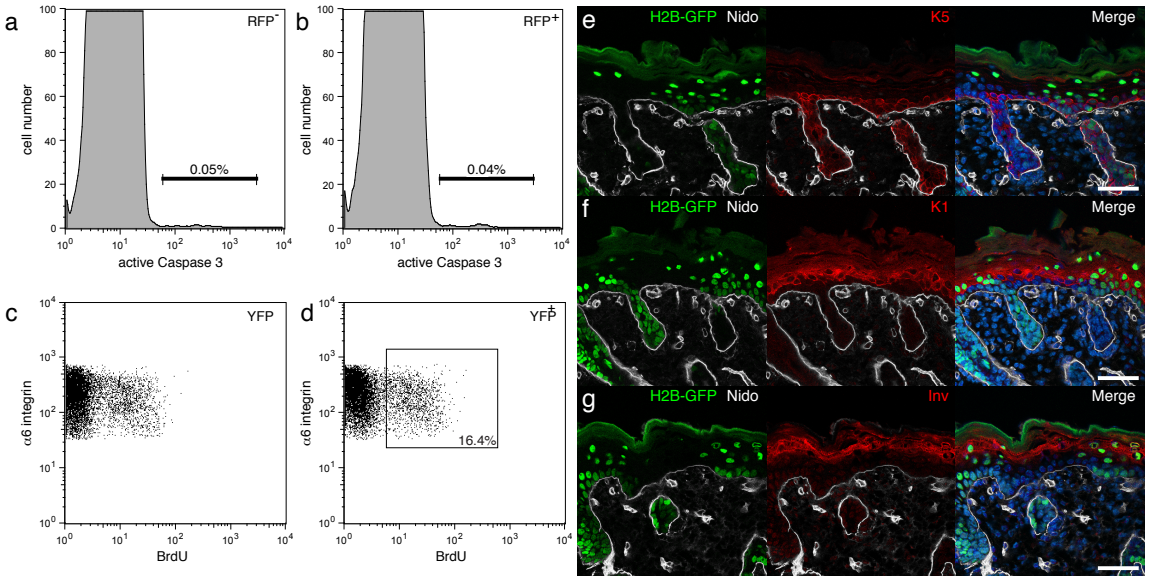

Figure 2.10 Lentiviral transduction of the epidermis shows no spurious effects on apoptosis, proliferation and tissue differentiation. (a,b) FACS analysis of active Caspase 3 expression in backskin epidermal cells from P0 animals, which were either uninfected (a) or infected at E9.5 with LV-RFP (b). Note similar rates of apoptosis. (c,d) BrdU incorporation in transduced and non-transduced α6 integrin^{+} basal epidermal cells FACS-isolated from P0 r26$^{yfp/+}$ animals that had been infected with LV-Cre at E9.5. Note that the percentages of BrdU positive cells are comparable. (e–g) Differentiation markers, including basal keratin 5 (K5), spinous keratin 1 (K1) and granular Involucrin (Inv) show normal distributions in the epidermis of P0 animals that had been infected with LV-GFP at E9.5. H2B-GFP marks the transduced clones. Nidogen (Nido) marks the basement membrane. DAPI (blue) labels the nuclei. Scale bar, 50 μm.

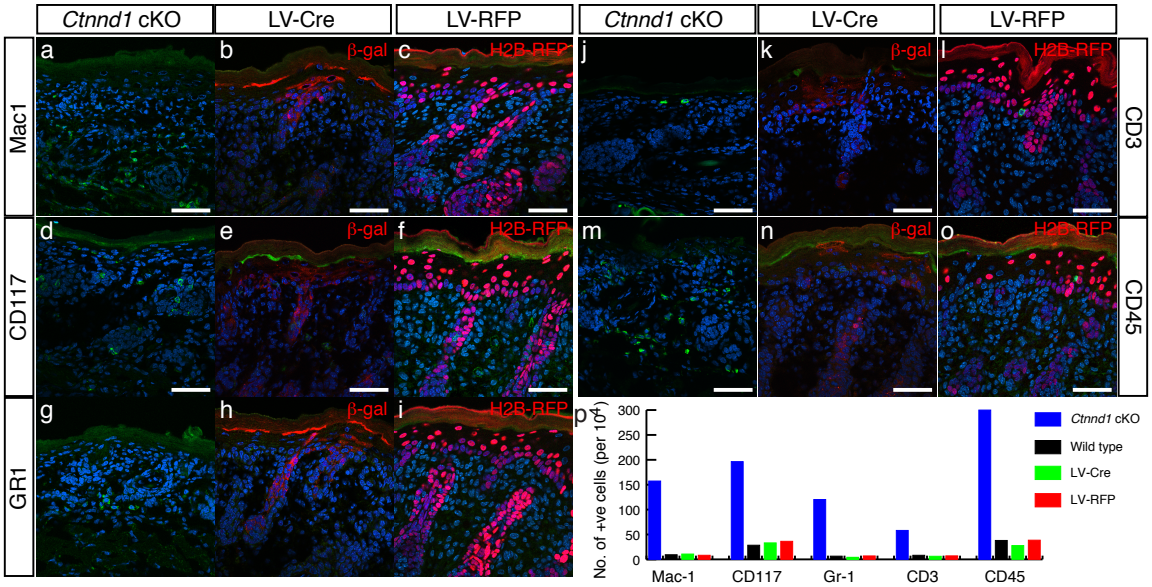

Figure 2.11 Lentiviral transduction of the developing epidermis does not trigger an overt immune response. (a–o) Expression of innate (Mac1, CD117, GR1) and adaptive immunity (CD3, CD45) markers in the backskins of Cre-reporter $r26^{LacZ/+}$ P0 mice that had been infected with LV-Cre at E9.5 and also wild-type P0 mice that had been infected with LV-RFP at E9.5. For a positive control, we used K14-Cre $Ctnnd1^{lox/lox}$ mice (Ctnnd1 cKO), shown to elicit a marked proinflammatory response by P0[15]. (p) Quantification of the immuno-positive cells detected in the P0 skins of each animal. β-gal marks the cytoplasm of LV-Cre transduced clones and H2B-RFP marks the LV-RFP transduced cells. Immune cells are labeled in green. DAPI (blue) labels the nuclei. Scale bar, 50 μm.

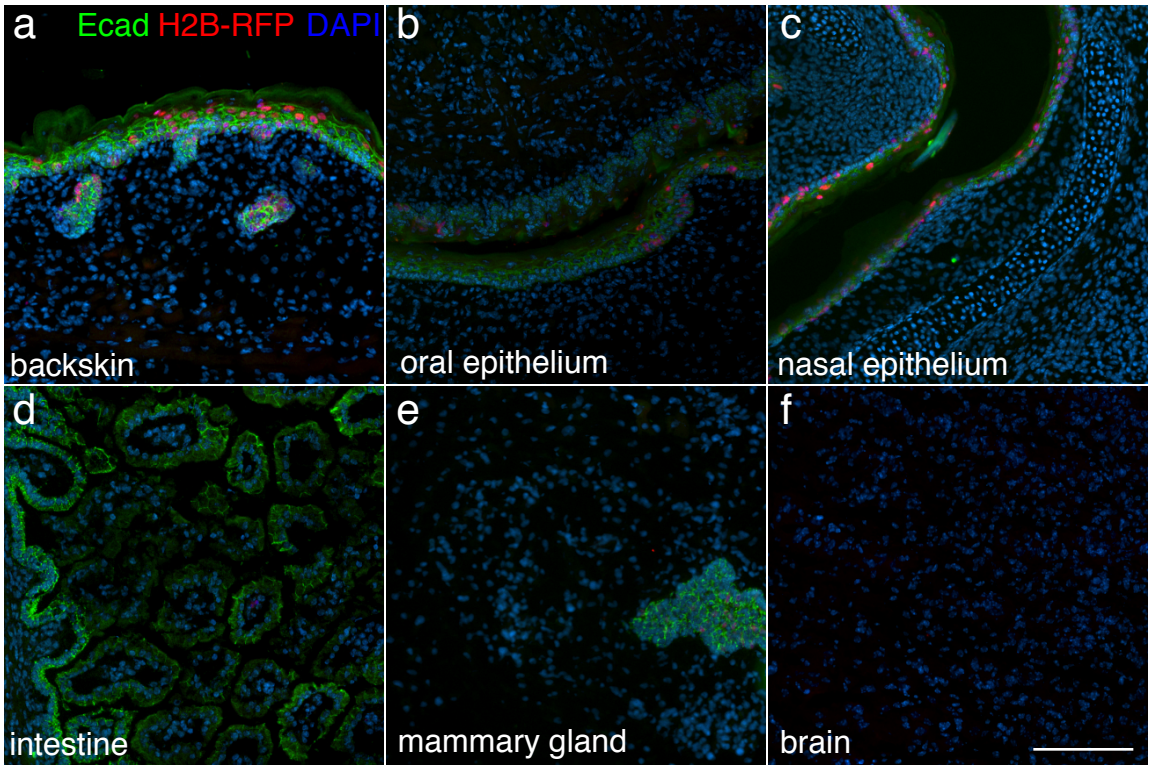

Figure 2.12 Lower levels of lentiviral infection in other ectoderm-derived tissues (a–f) Embryos were transduced with LV-RFP at E9.5 and tissues were analyzed at E18.5 for RFP expression. At a moderate level of epidermal infection (a), oral (b), nasal (c) and mammary (e) epithelia show detectable RFP expression. (d) Rare RFP$^+$ cells are found in the intestine. (f) No RFP expression can be detected in the brain. Note, RFP expression is limited to epithelial compartments in the tissues. Scale bar, 100 μm.

exposed to the amniotic fluid at the E9.5 stage of development, suggesting that this approach may be suitable for studying these tissues as well. A few rare positive cells could be detected in the intestine, and no infected cells were observed in the brain, consistent with the completion of neural tube closure by the time of injection.

Development of a quantitative cellular growth assay

The ability to co-infect epidermal cells with multiple viruses and accurately quantify infection levels by FACS facilitated the adaptation of the system to assay whether a genetic deficiency results in a growth advantage or disadvantage in the context of tissue development or homeostasis *in vivo*. The general principle is outlined, and should be particularly useful in the cancer field, where skin carcinogenesis is frequently the model of choice (Figure 2.13). Briefly, E9.5 embryos are infected with two lentiviruses: (i) LV-Cre, which, depending on the genetic background, marks control ($r26^{yfp/+}$) or mutant ($gene^{lox/lox}r26^{yfp/+}$) cells, and (ii) LV-RFP, which labels a corresponding group of cells to serve as internal control for overall infection levels (Figure 2.13a,b). By FACS-quantifying H2B-RFP$^+$ and YFP$^+$ cells in control and mutant E18.5 embryos, a Cellular Growth Index (CGI) is obtained, defined as the ratio between YFP$^+$ cells observed in the test condition ($gene^{lox/lox}r26^{yfp/+}$) and YFP$^+$ cells in the control ($r26^{yfp/+}$), for an equivalent infection level (H2B-RFP$^+$ cells). A CGI of 1 reflects no effect of gene deficiency on cellular growth, while an increase or decrease indicates an advantage or disadvantage, respectively (Figure 2.13c). As depicted by regression analysis, the ratio of H2B-RFP$^+$ to YFP$^+$ cells in a control tissue remains linear across a range of infection levels (Figure 2.13d).

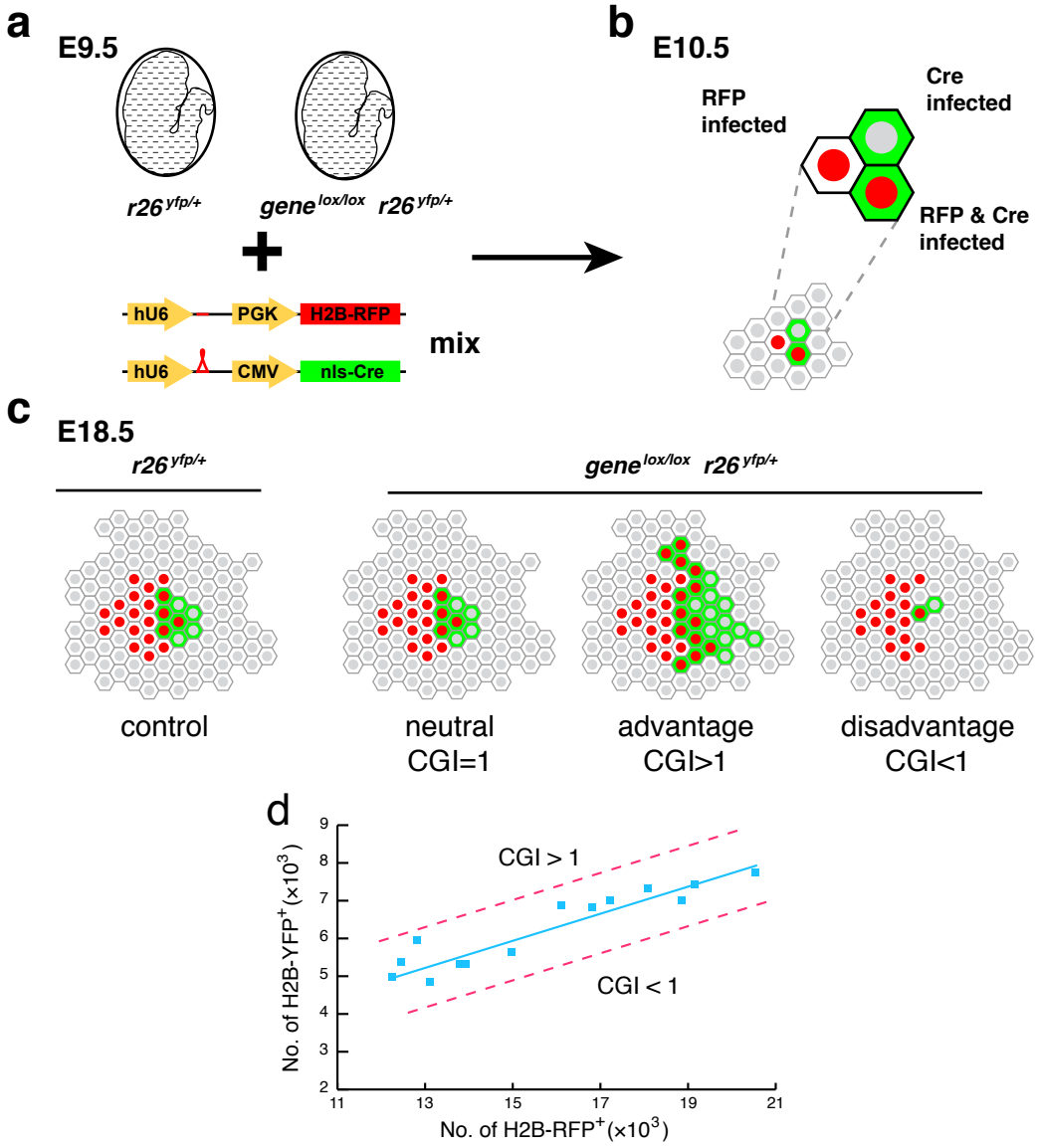

Figure 2.13 Rapid assay for measuring an epidermal growth advantage or disadvantage conferred by a gene mutation. (a–c) Schematic of the Cellular Growth Index (CGI) assay. (a,b) E9.5 Cre-reporter embryos are infected with a mix of LV-Cre and LV-RFP resulting in epidermal cells that have been transduced and express H2B-RFP, YFP or both. (c) At E18.5, the relative numbers of H2B-RFP+ to YFP+ cells in control (r26yfp/+) and gene knockout (genelox/lox r26yfp/+) mice are compared. Phenotypes are scored as either being neutral or having a growth advantage or disadvantage depending on the CGI value. (d) Graph of FACS quantified numbers of H2B-RFP+ cells relative to YFP+ cells in control mice at E18.5. Genes whose depletion results in a growth advantage or disadvantage would shift the curve towards the upper or lower dashed red lines, respectively.

Additionally, an shRNA hairpin can be incorporated into the LV-Cre vector, to enable the quantitative assessment of the effect of the depletion of two genes simultaneously on relative tissue growth *in vivo*.

Discussion

Although primary keratinocyte cultures have been instrumental for elucidating many features of epidermal biology, they undergo significant morphological and biochemical changes that limit their value for studying normal tissue physiology. This is true even for organotypic cultures and *in vivo* engraftment approaches, which generate wound-like perturbations in tissue integrity. The use of *ex vivo* tissue explants facilitates the use of chemical inhibitors and growth factors to probe the mechanistic requirements of various signaling pathways for tissue development. Additionally, explant culture has been successfully combined with videomicroscopy approaches, thereby enabling visualization of the kinetics of organ development. These approaches have been useful in elucidating the morphogenesis of several epithelial organs including the salivary and mammary glands. However, in the case of the skin, it appears that the explant culture system cannot clear the hurdle of targeted gene delivery to the epidermal tissue. While this system has recently proven useful in our laboratory for analyzing the tissue-extrinsic regulation of the establishment of planar cell polarity, the inability to achieve genetic manipulation severely limits its utility for mechanistic analysis (Devenport and Fuchs, 2008).

While chemical inhibitors can provide useful hints as to the requirements for a particular pathway activity in a growth process, inhibition of signaling in a heterogeneous culture made up of multiple cell types, such as in the case of the

skin, makes it difficult to tease apart which cell type is being affected by the inhibitor or growth factor. Thus, for instance, in the case of treatment of tissue explants with an inhibitor of PI3 kinase signaling, it is difficult to distinguish whether the smaller hair follicle morphology and reduction in proliferation is due to signaling inhibition in epidermal portion, or an indirect effect due to loss of proper function of the dermal papilla or another dermal structure. The same case can be made for "straight" knockout animals, where unless a particular gene exhibits a highly limited expression pattern in a specific tissue, it is difficult to discern the primary consequence of its deletion. In the case of PI3 kinase inhibition, clearer insight comes from conditional ablation of its major upstream regulator, the IGF-1 receptor in the epidermis, which in agreement with my explant studies, also causes hypoproliferation and hair follicle hypoplasia (Stachelscheid et al., 2008).

In vivo xenotransplantation permits specific genetic manipulation of the cells of interest in culture, followed by grafting onto mice to return the cells to an *in vivo* environment. This approach enables testing the relations between human and mouse biology (via engraftment of human tumor cells) and hence represents an important approach for skin cancer research. However, engraftment procedures require immunocompromised mice, thereby restricting the full complement of cellular behaviors likely to play a role in cancers, which show extensive interaction with the tumor microenvironment and immune system (Reuter et al., 2009).

The strength of the methodology described here lies in the fact that it enables rapid manipulation of gene expression *in vivo*, while retaining an

unperturbed endogenous microenvironment. This can allow for the study of epidermal signaling during embryonic development, when reciprocal signaling interactions between the epidermis and underlying dermis drive cellular behavior, such as hair follicle morphogenesis. Due to the spatiotemporal complexity of these interactions, it is currently quite difficult to fully recapitulate these signaling events using organotypic culture or cell engraftment approaches.

An additional advantage of the technology is that it eliminates the need for a skin specific promoter due to the fact that infection is limited to the epidermal layer. This is particularly important for lentiviral vectors, which have a packaging limit of approximately 5-6 kilobases (kb), including the necessary viral genes and packaging signals, which also amount to approximately 2 kb. Lentiviral vectors carrying inserts above this cutoff show a steep drop in packaging and infection efficiency, which correlate with insert length. As the keratin-14 promoter is 2 kb in length on its own, this greatly limits the options for genes that could be successfully expressed in a high titer lentivirus, especially if they are to be fused to GFP or another fluorescent protein to facilitate *in vivo* tracking. Although a shorter fragment of the keratin 5 promoter, of approximately 0.8 kb has also been used to drive epidermal expression, it appears to be activated later during embryogenesis, after initiation of stratification and hair follicle morphogenesis, thus precluding the study of early events in skin development (Endo et al., 2008).

The ability to selectively target and label epidermal progenitors enabled development of the CGI assay as a quantitative tool for dissecting pathways that regulate cell growth. Given that the epidermis has long served as a major model

in cancer studies, this new strategy becomes particularly powerful. In addition, a combination of RNAi-mediated knockdown and lentiviral-Cre mediated knockout allows for a rapid assessment of genetic epistasis. Moreover, at least four different viruses can be used for simultaneous tissue infection, expanding the utility of this system for e.g. eliminating functional redundancies or conducting knockdown/replacement studies.

It is noteworthy that epidermal transduction with LV-Cre provides temporal and spatial benefits over the existing epidermis-specific Cre lines. A clear benefit is the elimination of a need for multiple matings to generate homozygous floxed mice carrying an epidermal-specific Cre. This can be particularly difficult and inefficient if the homozygous mutant is not viable or fertile, due to a barrier defect. In this case, the parent carrying K14-Cre must be heterozygous, and as a result, at most ¼ of the progeny could be both Cre^+ and homozygous. In mouse strains such as C57Bl6, which is commonly used to generate targeted ES cells, but tends to carry only 6 or so pups per litter, this can lead to inefficiency of mating and high costs to maintain and breed mice to achieve sufficient numbers of the desired genotypes.

Moreover, earlier and more uniform generation of epidermal-specific gene knockouts with LV-Cre permits future exploration of early developmental functions, e.g. stratification, planar cell polarity and epithelial-mesenchymal interactions. The ability to control infection levels by varying lentiviral titers offers a number of additional benefits. Partially infected tissue can serve as an ideal source of animal-matched internal control cells. This is particularly useful for analysis of cell proliferation via BrdU injection, as incorporation of BrdU, as

well as rates of growth in general can vary somewhat between embryos. Additionally, by generating a mosaic tissue, it is possible to distinguish between cell autonomous and non-autonomous roles of a protein *in vivo*, by assessing whether gene ablation in a given cell confers phenotypic changes on its wild-type neighbors and vice versa. Finally, the ability to control the proportion of mutant and wild-type cells in the skin provides a means of analyzing gene function in adult skin, which may be precluded by newborn lethality due to impaired epidermal barrier function.

Materials and Methods

Lentiviral vector constructs

For construction of LV-RFP, LV-GFP, LV-CFP and LV-YFP, the puromycin resistance cassette of the pLKO.1 vector (The RNAi Consortium Library, Sigma) was replaced between *BamHI* and *NsiI* sites with *histone H2B-mRfp1, H2B-eGfp, H2B-cfp, and H2B-yfp* cDNAs amplified by PCR using *BglII* and *NsiI* flanked primers. LV-Cre was constructed by ligation of PCR-amplified *NdeI*/*MluI* flanked *CMV* promoter and *MluI*/*NsiI* flanked *nlsCre* fragment (Addgene plasmids 12265) into *NdeI*/*NsiI* cut pLKO.1. All plasmids were sequenced prior to use.

Large-scale lentivirus production and concentration

Large-scale production of VSVg pseudotyped lentivirus was performed by calcium phosphate transfection of 293FT cells (Invitrogen) with pLKO.1 and helper plasmids pMD2.G and pPAX2 (Addgene plasmid 12259 and 12260). 293FT cells below passage 10 were cultured in D10 medium, consisting of DMEM

(Lonza) supplemented with 10% v/v FBS, 1% v/v Pen-Strep-Glutamine (Lonza), 1% v/v 100 mM sodium pyruvate, 1% v/v 7.5% sodium bicarbonate, and 500 μg/ml G418. For transfection of each pLKO.1 construct, cells were plated in at least 2 500cm^2 plates (Nunc) pre-coated with poly-L-lysine (Sigma) diluted ten-fold in PBS. Cells were transfected at 90% confluence with 137.5 μg pLKO.1, 137.5 μg pPAX2, and 90 μg pMD2 per plate. Media was changed 12 hours after transfection and after 16 hours, cells were switched to serum-free viral production media (VPM) consisting of Ultraculture (Lonza 12-275F) supplemented with 1% v/v Pen-Strep-Glutamine (Lonza), 1% v/v 100 mM sodium pyruvate, 1% v/v 7.5% sodium bicarbonate and sodium butyrate to a final concentration of 5 mM.

Viral supernatant was collected 48 hours after transfection, filtered through a Stericup-HV PVDF 0.45 μm filter (Millipore), and then concentrated ~2,000-fold, first by passage through a Centricon Plus-70 100KD centrifugal filter (Millipore) in a table-top centrifuge spun at 2500g, and then by ultracentrifugation in a MLS-50 rotor (Beckman Coulter) at 45,000 rpm at 4°C for 1.5 hours. Viral titers were determined by FACS analysis of infected cultured keratinocytes. The relation between viral titer and *in vivo* infection efficiency was determined by injecting decreasing amounts of a single viral aliquot of known titer, diluted for a constant volume of 1.5 μl per embryo. Embryos were collected at E18.5 and percent infection was determined by FACS.

Mice and in utero ultrasound-guided microinjection.

The following mice were used: CD1 (Charles River Laboratories), *Gt(ROSA)26Sor*$^{tm1(EYFP)Cos/+}$ (Jackson Laboratories, donated by A. McMahon),

Gt(ROSA)26Sor$^{tm1(LacZ)Cos/+}$ (Jackson Laboratories, donated by P. Soriano), *K14-GFP-Actin* (Fuchs lab (Beronja et al., 2010)). Day 0.5 of gestation was determined by detection of a vaginal plug after overnight mating. Females at E9.5 of gestation were anesthetized with isoflurane (Hospira) and maintained with constant oxygen and isoflurane on a heated stage for the duration of the surgery. Hair was removed from the abdominal area by chemical hair removal (Nair). Pregnancy was ascertained prior to incision by ultrasound visualization (Vevo, VisualSonics). After confirmation of pregnancy, the abdomen was cleaned with 70% ethanol and opened via a midline incision. Forceps were used to carefully displace the intestines and to bring one uterine horn to the surface. A modified tissue culture dish with a 2.5 cm hole in the center that was sealed with a transparent membrane was placed on the abdomen and supported by clay blocks. Forceps were inserted into a 10 mm slit in the center of the membrane used to pull 3 embryos inside their uterine horn through the slit and into the dish. The dish was subsequently filled with room temperature PBS to serve as an ultrasound-conducting medium and to keep the uterine tissue moist. The membrane formed a watertight seal with the abdominal skin to prevent leakage of the PBS. Finally, a semi-circular sheet of silicone rubber (cast in a tissue culture dish) was placed laterally to the exposed uterus to stabilize the embryos in position throughout injection (Figure 2.4a).

The microinjection apparatus was set up as follows: glass microcapillary tubes (Drummond Scientific) were pulled to an inner diameter of 40-50 μm and sharpened at a 20° angle using a needle grinder (Sutter Instrument Co.) for 15 minutes. Tips were inspected under a microscope, rinsed once with water and

allowed to air dry. A sharpened needle was labeled with calibration marks at 1 μl intervals, back-filled with mineral oil (Sigma) and loaded onto the microinjection apparatus according to manufacturer's instructions (Nanoject II, Drummond Scientific). The needle was then loaded with an aliquot of high titer lentivirus, inserted into the dish near the embryos and visualized by ultrasound. During injection, both the needle and the embryos were repositioned as needed using X-Y-Z control knobs on the microinjector and stage, respectively. Each embryo was injected with 1.5 μl of lentivirus, and up to eight embryos were injected per litter. After injection, the uterine horns were replaced into the abdominal cavity, the peritoneal membrane was sutured with absorbable sutures (Chromic), and the skin was closed with surgical staples. Surgical procedures were limited to 30 min for high survival rates, and mice resumed activity within 5 minutes after surgery. The Rockefeller University Animal Care and Use Committee approved animal experimentation protocols used in the study.

Immunostaining and β-galactosidase detection.

The following primary antibodies were used: chicken GFP (1:2,000; Abcam); rat Ecad (ECCD-1, 1:500; M. Takeichi), Nidogen (ELM1, 1:2,000; Santa Cruz), Mac1 (M1/70, 1:100; Pharmingen), CD117 (2B8, 1:100; Pharmingen), GR1 (RB6-8C5, 1:100; Pharmingen), CD3 (KT3, 1:200; Chemicon) and CD45 (30-F11, 1:100; Pharmingen); rabbit α1-catenin (C8114, 1:2,000; Sigma), Caspase 3 (AF835, 1:1,000; R&D), K6 (1:500; P. Coulombe), K5 (1:500; E. Fuchs), K1 (1:500; E. Fuchs) and Involucrin (1:500; Covance). Secondary antibodies were conjugated to Alexa-488 (Molecular Probes), Cy3, or Cy5 (Jackson Laboratories). F-actin was detected

by Alexa-546 phalloidin (Molecular Probes). The senescence-associated β-galactosidase assay was performed as as recommended (Cell Signaling).

For immunofluorescence of sagittal sections, embryo skins were fixed in 4% formaldehyde in PBS for 2 hours, washed in PBS and embedded in OCT. 10 μm cryosections were cut, mounted on slides and rehydrated in PBS. Sections, cells and explants were blocked for 1 hour at room temperature in PBS containing 2.5% normal goat serum, 2.5% normal donkey serum, 1% BSA, 1% fish gelatin and 0.1% Triton. Primary antibodies were incubated in blocking buffer for 2 hours at room temperature or overnight at 4°C. Secondary antibodies were incubated in blocking buffer for 1 hour at room temperature. For whole-mount microscopy of skins with intact hair follicles, tissues were incubated while shaking in 0.25% collagenase (Sigma) in 4 mls of HBSS (HyClone) at 37°C for 1.5 hours, prior to fixation in 4% formaldehyde in PBS and extensive washing with PBS containing 1% triton (PBST). Tissues were blocked for 2 hours, primary antibody incubation was performed overnight and secondary antibody incubation was performed for 2 hours at room temperature. Tissues and cells were mounted in Vectashield with DAPI (Vector). Confocal images were captured by a scanning laser confocal microscope (LSM510 Meta; Carl Zeiss, Inc.) using C-Apochromat 40×/1.2 water lens. Analysis of colocalization following tissue transduction with 4 separate fluorophores was performed using Metamorph (Molecular Devices). Images were processed using Adobe Photoshop.

Explant culture for tissue morphogenesis

Backskins were dissected from E14.5 *CD-1* and *K14-GFP-actin* embryos in cold PBS. Skins were placed dermis side down in a droplet of keratinocyte media on Nuclepore membranes (1 μm pore size, SPI supplies) coated with 10 μg/ml fibronectin and allowed to attach for 5 minutes. Explants were then cultured for 2-4 days in E-media supplemented with 15% serum with a final Ca^{2+} concentration of 0.3 mM at 37°C and 7.5 % CO_2 (Blanpain et al., 2004). For inhibitor experiments, explants were incubated in media containing a final 20 μM concentration of LY294002 or Y-27632 (Sigma), or an equivalent volume of DMSO for control.

Flow cytometry

Primary keratinocytes were isolated by digesting backskins from E18.5 embryos with dispase (Gibco, 0.4 mg/ml in PBS) for 1 hour at 37°C to separate the epidermis from dermis. Epidermal sheets were then minced and shaken in a 1:1 mixture of 0.25 % trypsin/EDTA (GIBCO) to versene to release basal keratinocytes. Trypsin was inactivated with keratinocyte culture media and after trituration, cells were passed through a 40 μm cell strainer to achieve a single cell suspension. Cells were purified using BD FACSAria II (BD Biosciences). I injected BrdU (50 μg g^{-1} body weight) intraperitoneally 6 h prior to processing, and BrdU incorporation and active Caspase 3 assays were performed as recommended (BD Pharmingen). FACS analysis was performed on BD LSR II and BD FACSCalibur (BD Biosciences).

Statistics.

All quantitative data were collected from experiments performed in at least triplicate, and expressed as mean ± standard deviation. Differences between groups were assayed using Student t-test. In analyses of CGI data, slopes of data distribution were compared using analyses of covariance (ANOCOVA) in Matlab Statistics Toolbox (Mathworks). Significant differences were considered when $p<0.05$.

CHAPTER 3: USE OF THE LENTIVIRAL EPIDERMAL DELIVERY SYSTEM TO DISSECT A GENETIC NETWORK

The ability to rapidly manipulate gene expression and function in the mammalian epidermis *in vivo* is particularly useful for understanding how perturbations of epithelial integrity can impinge upon tissue development and homeostasis. To illustrate the power of the approach, I focused on α-epithelial-catenin (referred to here as α-catenin), an essential actin-binding component of adherens junctions that is encoded by the *Ctnna1* gene (Nagafuchi et al., 1991). In epithelial cells, α-catenin is recruited to E-cadherin via its association with β-catenin. At cadherin-based adhesions, α-catenin can dynamically interact with itself and other actin regulators to promote polymerization and bundling of linear actin cables and inhibit formation of branched actin (Drees et al., 2005; Kobielak et al., 2004). These functions serve to promote the formation and stability of adherens junctions to enable epithelial sheet formation. Reduction in α-catenin expression has been reported in numerous human carcinomas as well as mouse models of cancer (Ding et al., 2010; Nozawa et al., 2006; Xiangming et al., 1999). Loss of adherens junction proteins has been associated with breakdown of epithelial integrity and epithelial mesenchymal transitions (EMTs) during cancer metastasis (Bajpai et al., 2009). However, whether the disruption of epithelial integrity and homeostasis induced by AJ destabilization has an effect on the early stages of cancer formation and tissue growth dynamics remains unclear. Interestingly, recent high-throughput sequencing and bioinformatics analysis designed to identify causal "driver" mutations in recessive cancer genes

(tumor suppressors) identified homozygous deletions in the *Ctnna1* gene, lending support the notion of its function as a tumor suppressor.

Previous conditional targeting of α-catenin in the epidermis by K14-Cre resulted in a striking epidermal phenotype. Mutant epidermis was characterized by aberrant cellular morphology, loss of hair follicle morphogenesis, defective barrier establishment and formation of hyperproliferative epithelial invaginations (Vasioukhin et al., 2001). This set of phenotypes can easily be identified in infected cells to determine the effectiveness of the lentiviral targeting approach. However, deletion of α-catenin throughout the epidermis also resulted in inflammation and recruitment for immune cells (Kobielak and Fuchs, 2006). The inflammation could potentially be a non-cell autonomous response to the widespread lack of an epidermal barrier, such as occurs during skin wounding. Localized depletion of α-catenin in clones within the context of a mosaic tissue provides a means of distinguishing cell-autonomous versus non-cell autonomous phenotypes. Additionally, how loss of α-catenin could impinge upon tissue growth and result in a pre-cancerous state has remained unclear. *In vitro* defects included aberrant actin cytoskeleton dynamics and MAPK mediated hyperproliferation. However, whether this was the case *in vivo* has yet to be determined.

Using a combination of lentiviral Cre-mediated knockout and lentiviral shRNA-mediated knockdown approaches, I demonstrate the efficiency of the *in utero* lentiviral delivery system for gene depletion in the epidermis and uncover genetic interactions between α-catenin and RAS-MAPK signaling that regulate proliferation *in vivo.* Additionally, I find that despite their hyperproliferation, α-

catenin-depleted cells are at a net growth disadvantage *in vivo* relative to their wild-type neighbors due to an increased sensitivity to p53-dependent apoptosis.

Results

To establish the fidelity of $r26^{yfp/+}$ Cre reporter as an indicator of *Ctnna1* knockout clones, LV-Cre was used to infect $r26^{yfp/+}$ E9.5 embryos that were also either wild-type or homozygous for the floxed *Ctnna1* allele (Vasioukhin et al., 2001). At E18.5, YFP^+ basal backskin epidermal cells were FACS-isolated for YFP and α6 integrin expression and analyzed by immunoblot. α1-catenin protein levels were ~7% of the control, suggesting that lentiviral delivery of Cre can result in efficient excision in the epidermis, and that YFP expression faithfully correlates with ablation of *Ctnna1* ablation (Figure 3.1a). Moreover, by immunofluorescence, clonal patches of YFP^+ epidermis were always negative for α1-catenin expression and vice versa (Figure 3.1b).

The tight correlation between YFP expression and loss of α-catenin allowed for direct comparison of the relative growth between the two cell types in the same tissue using the CGI assay. When I analyzed the $Ctnna1^{lox/lox}r26^{yfp/+}$ mice with the $r26^{yfp/+}$ controls using the described CGI assay, the ratio of H2B-RFP^+ cells and *Ctnna1* mutant (YFP^+) cells was independent of overall infection levels, as observed for the controls. However, the calculated CGI was 0.6, indicating a significant ($p<0.001$) 67% reduction in YFP^+ cells observed in *Ctnna1* mutant background relative to wild-type (Figure 3.1c,d). Consistent with the results of the CGI assay, a progressive loss of YFP^+ *Ctnna1* mutant but not control cell clones occurred during postnatal development, with surviving animals never

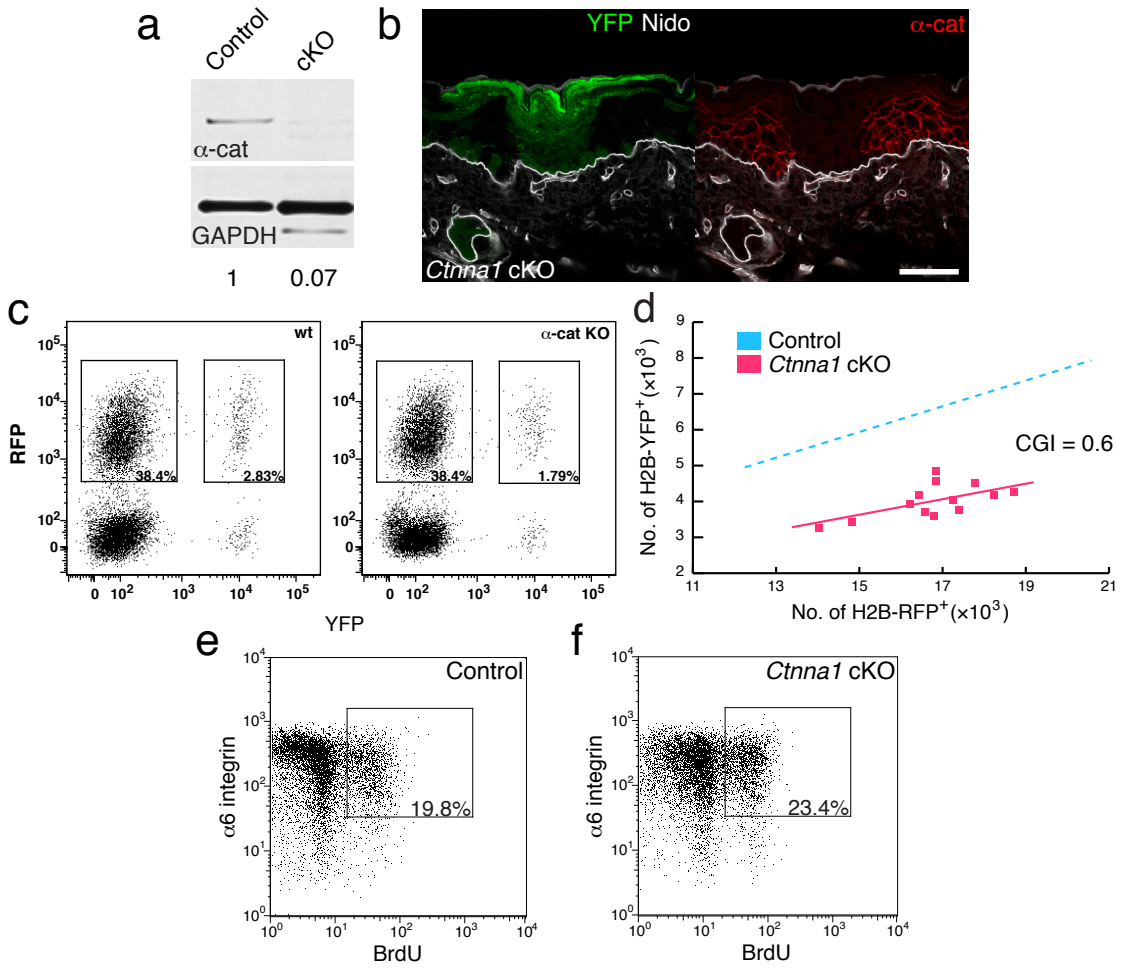

Figure 3.1 Lentiviral Cre infection and CGI analysis reveals an unexpected growth disadvantage following α1-catenin loss despite hyperproliferation. (a) Quantified anti-α1-catenin (α-cat; test) and glyceraldehyde phosphate dehydrogenase (GAPDH; control) immunoblots of protein lysates from cells FACS-sorted from LV-Cre infected control and *Ctnna1* floxed (cKO) embryos. (b) Back-skin sections of LV-Cre *Ctnna1* lox/lox r26yfp/+ (*Ctnna1* cKO) embryos immunolabeled with α1-catenin antibody. Transduced cells are indicated by their YFP expression. (c) FACS plots and quantification of RFP$^+$, YFP$^+$(and double positive epidermal cells for CGI assay of wild-type versus LV-Cre *Ctnna1* cKO mice at E18.5 (as in Fig. 2.13) (d) Graph of numbers of H2B-RFP+ cells relative to YFP+ cells in control (as in c) and *Ctnna1* cKO mice at E18.5. Note the reduced CGI (0.6; $p<0.001$) in the *Ctnna1* cKO clones. (e,f) FACS plots and quantification of % basal (α6-integrin+) cells which incorporated BrdU after a 6h labeling of E18.5 embryos. Note elevated BrdU incorporation despite the growth disadvantage in Ctnna1 cKO skin. Nidogen (Nido) marks the epidermal-dermal boundary as well as dermal blood vessels. Scale bar, 50 μm.

developing tumors. Thus following loss of α1-catenin, epidermal cells are at a growth disadvantage relative to their wild-type neighbors.

The growth disadvantage of α1-catenin null clones seemed at odds with the elevation in proliferating nuclear antigen Ki67 reported previously (Vasioukhin et al., 2001). To verify that α1-catenin deficiency indeed leads to hyperproliferation in the LV-Cre infected embryos, (or if it might be a non-cell autonomous consequence of widespread tissue dysplasia in the K14-Cre conditional mutants), I administered BrdU to $r26^{yfp/+}$ and $Ctnna1^{lox/lox}r26^{yfp/+}$ E18.5 embryos that had been infected at E9.5. After a six-hour pulse of BrdU, basal epidermal cells were FACS-sorted for α6-integrin$^+$ ± YFP$^+$. For control LV-Cre infected $r26^{yfp/+}$ embryos, the animal-matched ratio of BrdU$^+$YFP$^+$ versus BrdU$^+$YFP$^-$ cells remained constant as expected, indicating that LV-Cre or YFP expression alone had no effect on proliferation. By contrast, a significant increase (~20%, $p<0.001$) was seen in BrdU$^+$YFP$^+$ versus BrdU$^+$YFP$^-$ cells in LV-Cre infected $Ctnna1^{lox/lox}r26^{yfp/+}$ animals (Figure 3.1e,f).

While revealing the power of the lentiviral targeting strategy, the results unveiled an unexpected conundrum: how does α-catenin loss result in a cellular growth disadvantage and yet promote proliferation and tumorigenesis (Benjamin and Nelson, 2008; Kobielak and Fuchs, 2006)? To dissect the cellular mechanisms responsible, I first needed to demonstrate the utility of the system for conducting rapid functional and genetic interaction analyses *in vivo* by RNAi.

Efficient gene knockdown using lentiviral RNAi in vivo

The utility of the developed system for rapid RNAi-mediated loss-of-function studies requires efficient gene knockdown and faithful recapitulation of the knockout phenotype. As a proof-of-principle, I again used *Ctnna1*, as I could directly compare the phenotypic consequences of lentiviral Cre-mediated excision and lentiviral shRNA knockdown. The TRC mouse lentiviral library carried three *Ctnna1* shRNA constructs (Figure 3.2a) (Root et al., 2006). When introduced into cultured wild-type epidermal keratinocytes and after selection for puromycin resistance, they reduced *Ctnna1* mRNA levels to ~70% (shCtnna1-186), 30% (shCtnna1-1764) and 9% (shCtnna1-912) of levels seen with a control scrambled shRNA (shScram; Figure 3.2b,c).

After cloning these shRNAs into the LV-GFP backbone, amniotic injections were performed on E9.5 embryos. At E18.5, H2B-GFP$^+$ backskin cells were isolated by FACS, sorting for α6 integrin and GFP, followed by immunoblot analyses. In agreement with the transcript reductions observed *in vitro*, α1-catenin protein levels *in vivo* were reduced to ~70% (shCtnna1-186), 45% (shCtnna1-1764) and 18% (shCtnna1-912) of control levels (Figure 3.2b,c). Immunofluorescence analyses corroborated these results, revealing the strongest reduction in α-catenin in H2B-GFP$^+$ epidermal patches from embryos transduced with shCtnna1-912, which was the most efficient hairpin in *in vitro* studies (Figure 3.2d).

Previous *Ctnna1* gene targeting by transgenic K14-Cre expression resulted in defects in intercellular adhesion and actin dynamics, as well as disorganized epidermal stratification, MAPK-mediated hyperproliferation, and precancerous

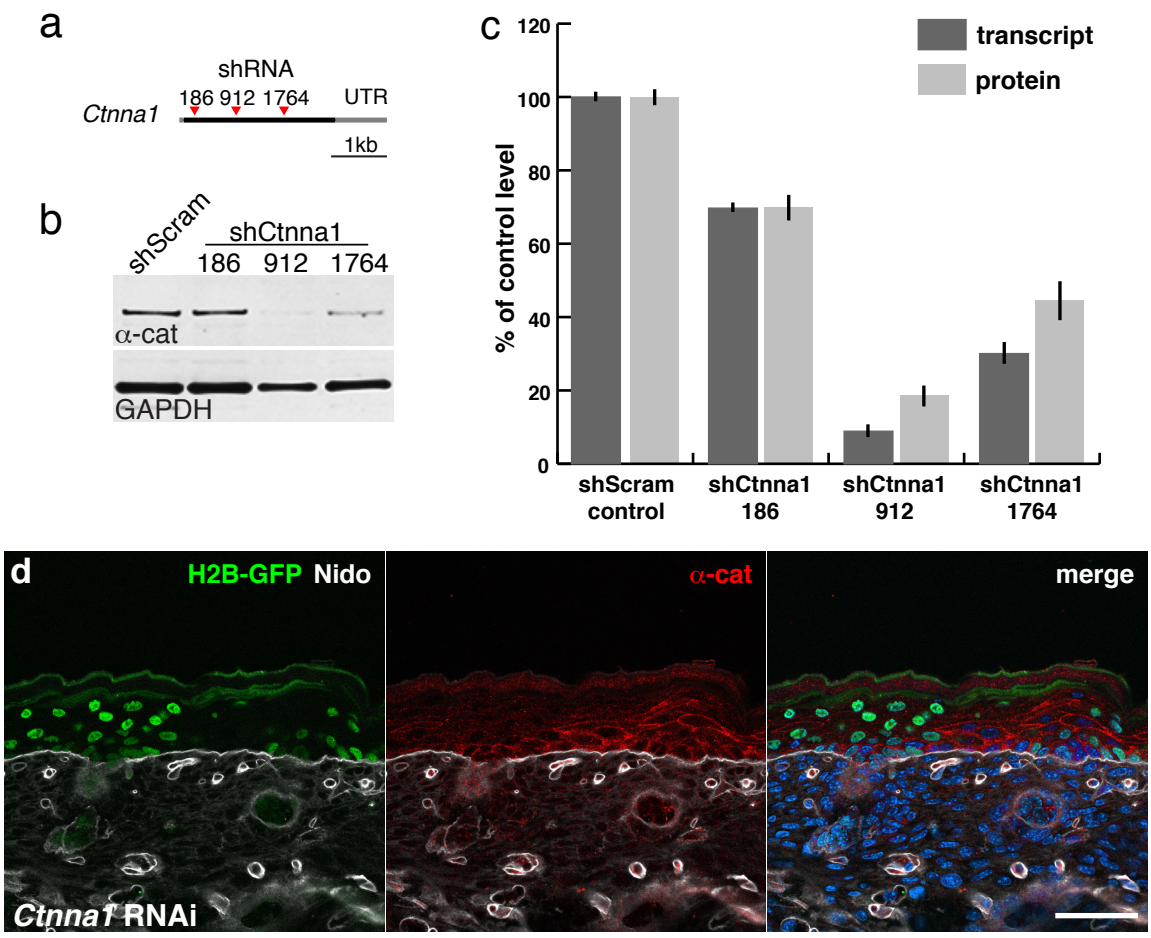

Figure 3.2 Efficient epidermal-specific lentivirus RNAi-mediated knockdown of Ctnna1 *in vivo*. (a) TRC RNAi library shRNA constructs (arrowheads) corresponding to Ctnna1. Numbers correspond to TRC nomenclature; utr, 3′ untranslated region. (b) Anti-α1-catenin and glyceraldehyde phosphate dehydrogenase (GAPDH) immunoblots of protein lysates of cells FACS-sorted from embryos infected with LV-GFP harboring Ctnna1-specific shRNAs (shCtnna1) and control scrambled shRNA (shScram). (c) Quantification of α1-catenin levels from blot in (b). (d) α1-Catenin immunolabeling reveals efficient knockdown (Ctnna1 RNAi) in all shCtnna1-912 infected (H2B-GFP+) but not uninfected cells in a representative mosaic P0 skin section. Scale bar, 50 μm.

epithelial invaginations (Kobielak and Fuchs, 2006; Vasioukhin et al., 2001). To verify that *in vivo* RNAi-mediated gene knockdown and LV-Cre mediated knockout can phenocopy these known loss-of-function consequences, I compared LV-GFP shCtnna1-912 knockdown and LV-Cre *Ctnna1* knockout with conditional K14-Cre *Ctnna1* knockout. For gene targeting, $Ctnna1^{lox/lox}r26^{yfp/+}$ mice were used so that levels of LV-Cre and K14-Cre-mediated knockout cells could be quantified by measuring the proportion of α6-integrin$^+$ basal epidermal cells that were YFP$^+$. Similarly, α6-integrin and H2B-GFP$^+$ were used to score the proportion of knockdown cells.

Ctnna1 knockdown, LV-Cre knockout and conditional K14-Cre knockout embryos shared an open-eye phenotype, curled tail, shortened limbs, fused digits and skins that were shiny, taut and fragile (Figure 3.3). Only *Ctnna1* knockdown and LV-Cre-mediated *Ctnna1* knockout embryos displayed a paucity of skin in the head region (Figure 3.3c,d). This increased severity in headskin phenotype gained by lentiviral versus K14-transgenic Cre phenotype was consistent with the high infectivity at this site (as shown in Figure 2.7) and with a 2–3 day difference in excision achieved by LV-Cre (E10.5) versus K14-Cre (E12.5–E13.5; Figure 2.8). Similarly, the phenotypic severity of K14-Cre conditional *Ctnna1* mutants tends to follow the developmental patterns of K14 expression; thus as K14 becomes expressed earlier in the flank than along the midline, K14-Cre *Ctnna1* mutants often exhibit a loss of stratified epithelium along the flank (Vasioukhin et al., 2001).

In addition to recapitulating the gross defects caused by α1-catenin loss of function, the knockdown also generated tissue defects characteristic of their

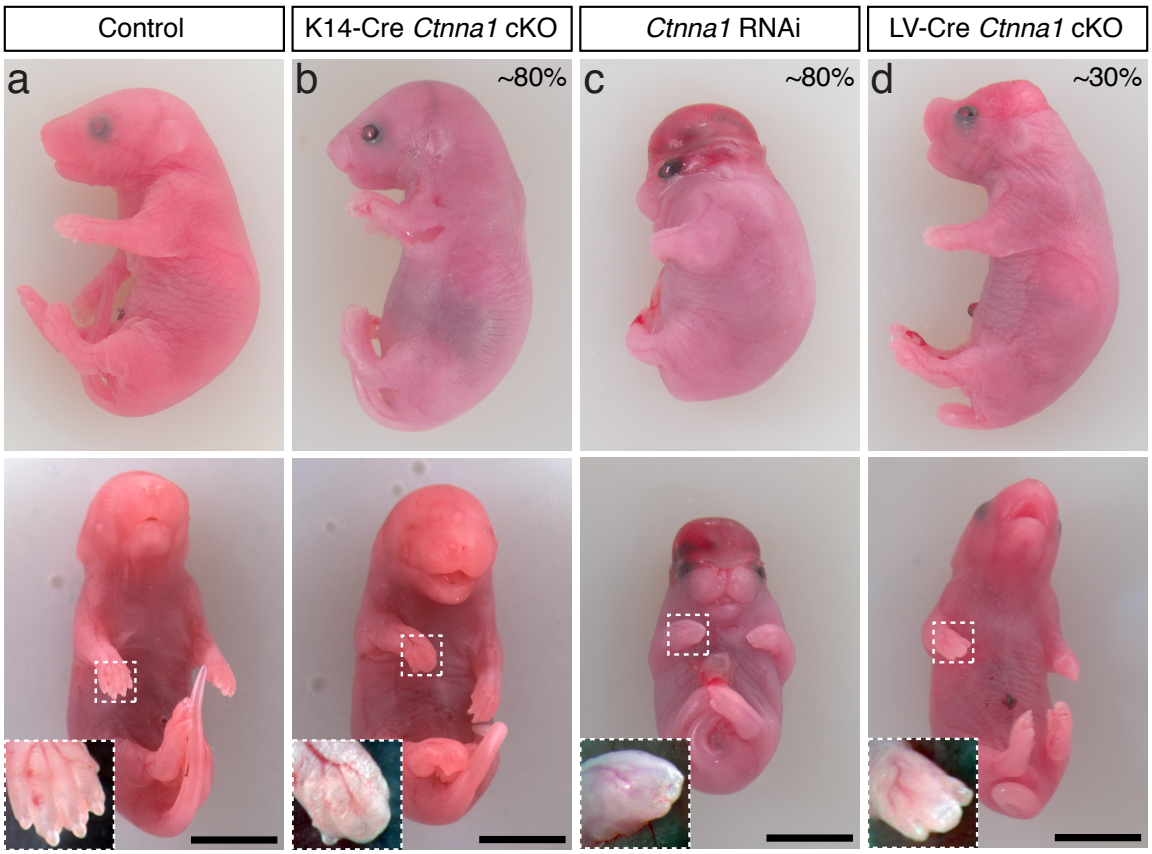

Figure 3.3 *Ctnna1* knockdown recapitulates gross LV-Cre and K14-Cre *Ctnna1* knockout phenotypes. Side (top panels) and face (bottom panels) views of representative newborn mice: (a) Control; (b) conditional K14-Cre-mediated *Ctnna1* knockout (K14-Cre *Ctnna1* cKO); (c) shCtnna1-912 knockdown (*Ctnna1* RNAi) and (d) LV-Cre mediated *Ctnna1* knockout (LVCre *Ctnna1* cKO). Percentages indicate overall levels of epidermis infected. Note the similarities between lentivirus-mediated RNAi knockdown and conditional LV-Cre-mediated knockout targeting of *Ctnna1* particularly in the head region, where the virus elicits early targeting, not achieved with the K14 promoter, which is active in headskin only several days later. Note also the limb (insets) and curled tail defects in *Ctnna1*-compromised (b–d) but not in control (a) embryos. Scale bars, 5 mm.

Ctnna1 knockout counterparts. This included perturbations in epidermal architecture and stratification. In wild-type tissue, or tissue infected with shScram-H2B-GFP expressing lentivirus, the basal cells form a uniform sheet with cuboidal cell morphology, while the suprabasal layers exhibit a progressively flattened morphology as they approach the skin surface (Figure 3.4a). In both the *Ctnna1* knockdown and lentiviral Cre knockout, GFP^{+} and YFP+ cells, respectively, the basal layer appeared disorganized and the suprabasal layers failed to adopt the flattened morphology (Figure 3.4b,c). Furthermore, in control tissue, hair follicles invaginate into the dermis in a polarized fashion, with the leading edge pointing in the direction of the anterior, due to the activity of a planar cell polarity (PCP) signaling pathway that orients epidermal cells along the anterior-posterior axis (Figure 3.4a) (Devenport and Fuchs, 2008). General hair follicle growth was impaired in tissues lacking α-catenin, as buds formed, bud often failed to form mature follicles in areas of mutant tissue. Additionally, the hair buds that did form grew straight down (Figure 3.4c) rather than at an angle, suggesting a defect in PCP signaling. Hair buds were more often found in α-catenin knockdown rather than LV-Cre knockout tissue, which like the K14-Cre conditional mutant shows a near complete lack of follicle initiation in highly infected areas. Thus, this represents an instance in which an incomplete depletion adds a new dimension to loss-of-function phenotype. The requirement of α-catenin for the establishment of proper planar cell polarity and regulation of cell fate within the hair follicle was also corroborated by the fact lentiviral depletion of α-catenin by shRNA resulted

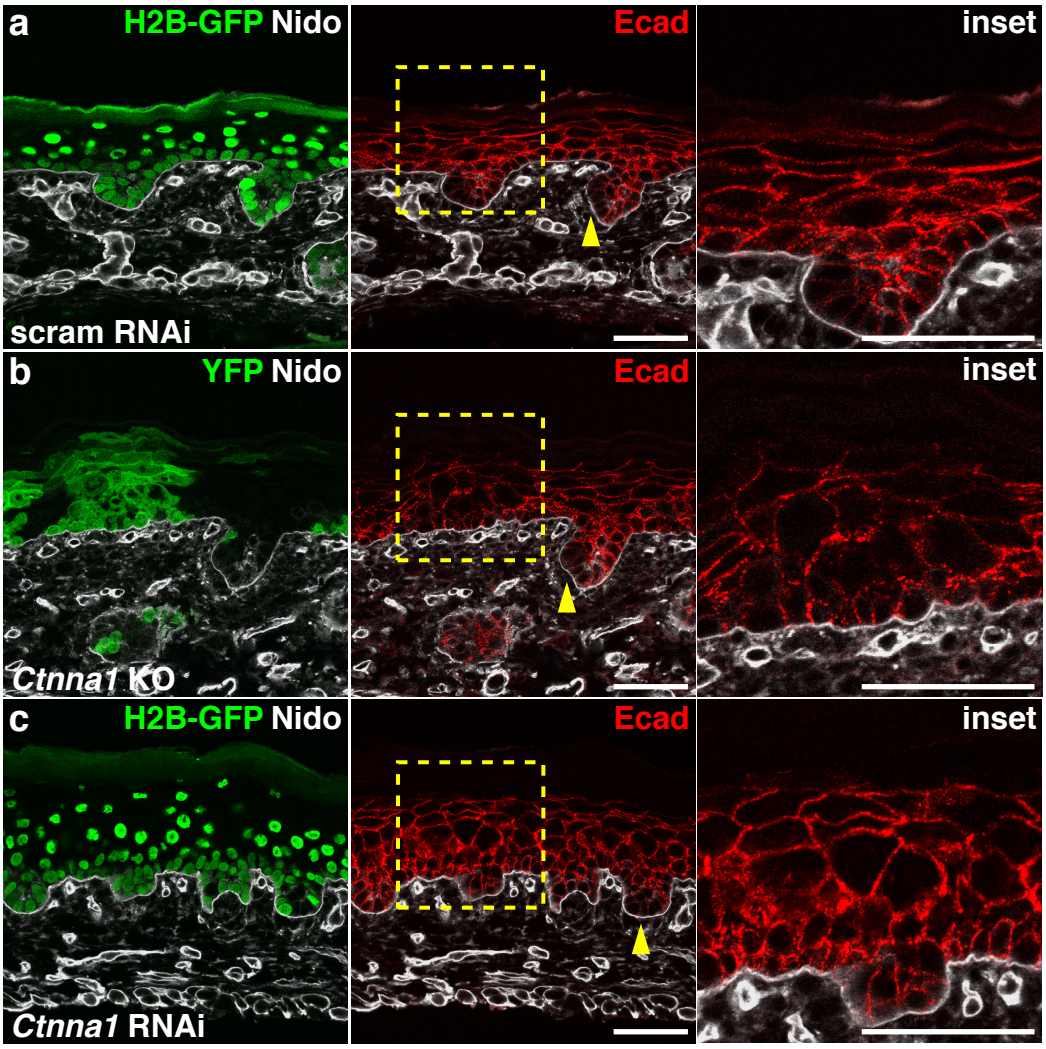

Figure 3.4 Lentiviral RNAi-mediated knockdown of Ctnna1 faithfully recapitulates morphological phenotypic abnormalities displayed by K14-Cre conditional and LV-Cre induced knockout counterparts. (a–c) Morphological and adherens junction defects, not found in Scram RNAi infected skin (a), are similar between Ctnna1 cKO (b) and Ctnna1 RNAi (c) infected cells. Boxed areas are shown in insets. Arrowheads denote hair follicles derived from infected epidermis. Note that asymmetric E-cadherin localization seen in Scram RNAi-infected (a) or uninfected areas (b) is consistently lost in Ctnna1 RNAi-infected skin (c), indicative of a planar cell polarity defect. Scale bar, 50 μm.

in a symmetric expression of Ncam, which is normally restricted to the posterior side of hair follicles (Figure 3.5a,b).

Additionally, depletion of α-catenin by lentiviral Cre expression on the homozygous floxed background or by lentiviral knockdown induced expression of keratin 6 in the suprabasal layers of the epidermis (Figure 3.5c,d). In wild-type tissue and in uninfected skin regions of injected embryos, K6 is normally restricted to the inner root sheath of the hair follicle. However, it becomes expressed in the epidermis upon hyperproliferation. Suprabasal K6 expression was observed in the K14-Cre conditional α-catenin mutant, and thus the lentiviral depletion approach successfully recapitulated this phenotype as well (Vasioukhin et al., 2001).

Previous studies of cultured keratinocytes identified defects in the organization of the actin cytoskeleton and establishment of adherens junctions in α-catenin knockout cells (Vasioukhin et al., 2000). This defect is also observed in primary keratinocytes migrating out of skin explants; wild-type keratinocytes migrate out of an explant as a continuous sheet with intact intercellular junctions, a coordinated actin cytoskeleton and a polarized leading edge, whereas keratinocytes from α-catenin knockout tissue break down any intercellular adhesions and migrate as non-coordinated single cells (Vaezi et al., 2002). In order to determine whether this cellular phenotype was recapitulated by lentiviral depletion of α-catenin, I analyzed explants of E18.5 tissue from mice injected with either LV-Cre on an $r26^{Yfp/+}$ Cre reporter background alone or with homozygous floxed *Ctnna1*. As expected, uninfected tissue or infected tissue from control animals retained its intercellular adhesions and migrated as a sheet

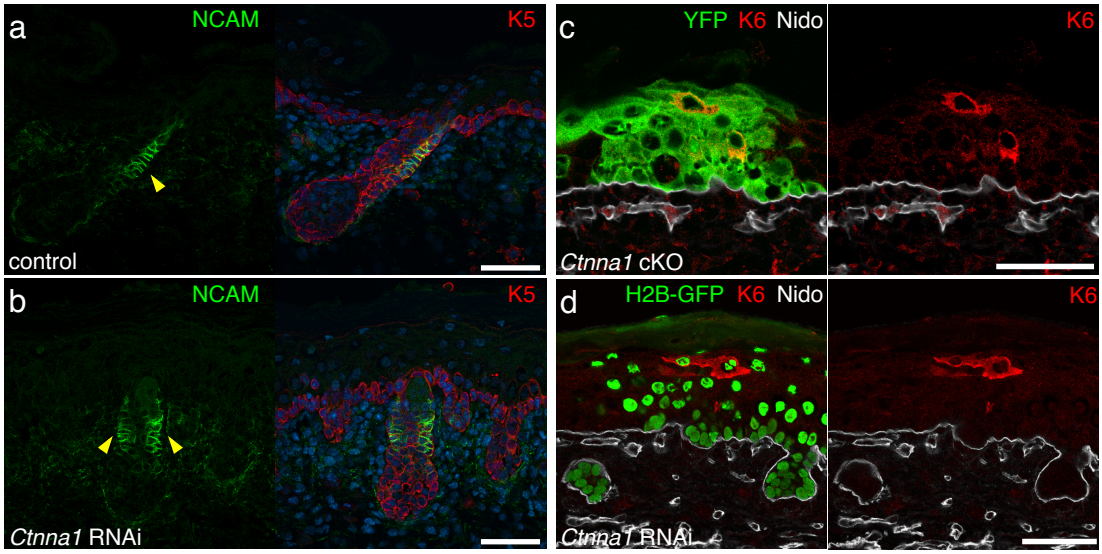

Figure 3.5 Lentiviral knockdown of *Ctnna1* is accompanied by changes in cell fate and gene expression. (a,b) Restricted NCAM expression, normally found on the posterior side of follicles, is distributed on both sides of follicles in Ctnna1 knockdown (Ctnna1 RNAi) tissue, consistent with a planar cell polarity defect (see Fig. 3 for additional PCP defects). K5 marks epidermal cells in contact with the basement membrane which demarcates the epidermis and dermis; DAPI (blue) labels the nuclei. (c,d) Suprabasal keratin 6 (K6), often reflective of enhanced basal cell proliferation, is detected in Ctnna1 cKO (h) and Ctnna1 RNAi (i) cell clones. Transduced cells are identified by their YFP or H2B-GFP expression. Nidogen marks the basement membrane and dermal blood vessels. Epidermal adherens junctions are marked by antibody to E-cadherin (Ecad). Primary antibodies are noted on each frame, with color coding according to secondary antibodies used. Scale bars, 50 μm.

(Figure 3.6a), while LV-Cre α-catenin knockout cells lost their cell-cell adhesions (Figure 3.6b). Importantly, this effect was phenocopied by knockdown of α-catenin with lentiviral shRNA (Figure 3.6c). Altogether, the striking phenotypic parallels between *Ctnna1* RNAi-mediated knockdown and loss-of-function mutation, but not control scrambled RNAi, made off-target effects unlikely and underscored the efficiency of this strategy for dissecting physiological mechanisms. In subsequent experiments, possible off-target effects are guarded for by using shScram RNAi controls and multiple shRNA hairpins against each gene transcript.

Using RNAi in vivo to dissect a genetic network

The ability to conduct knockdowns for functional studies provided the means to probe deeper into why *Ctnna1* mutant cells exhibit a growth disadvantage despite being hyperproliferative. I first tested whether RAS-MAPK activity, previously found to be elevated in cultured *Ctnna1* null cells, might be responsible for the elevated proliferation in these embryos (Vasioukhin et al., 2001). shRNAs were selected against a) *Hras1*, encoding the most abundant Ras family member and predominant target of oncogenic mutations in skin, and b) *Mapk3*, encoding ERK1, the most downstream component of the MAPK signaling cascade governing epidermal proliferation (Khavari and Rinn, 2007; Leon et al., 1987; Quintanilla et al., 1986). In keratinocytes *in vitro,* shHras1-267 and shMapk3-357 resulted in 86% *Hras1* and 93% *Mapk3* transcript reductions, respectively (Figure 3.7a).

After modifying the LV-Cre vector to express these shRNAs, I infected $r26^{yfp/+}$ embryos with these and control viruses. Quantitative immunoblot

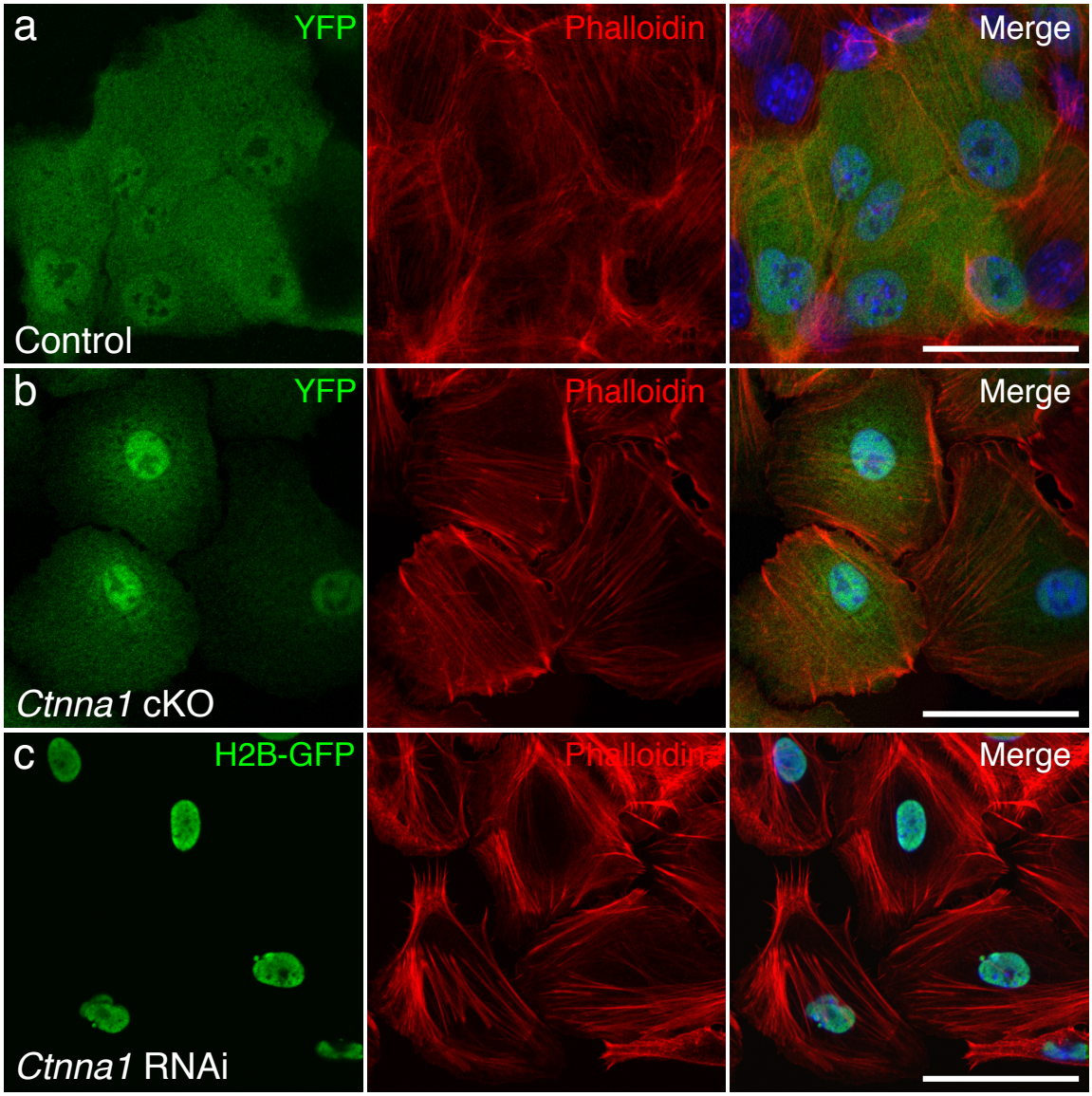

Figure 3.6 Lentiviral RNAi-mediated *Ctnna1* knockdown recapitulates *Ctnna1* knockout perturbations in actin organization and intercellular adhesion. Primary epidermal keratinocytes were grown out of E18.5 cultured skin explants from: (a) $r26^{yfp/+}$ embryos transduced with LV-Cre at E9.5 (Control); (b) $Ctnna1^{lox/lox}$ embryos transduced with LV-Cre at E9.5 (*Ctnna1* cKO) and (c) wild-type embryos transduced with shCtnna1-912 LV-GFP (Ctnna1 RNAi). Note that both knockout and knockdown cells, but not the control, show an aberrant actin cytoskeleton organization and a paucity of cell-cell adhesion, despite close intercellular contacts. F-actin is labeled with Phalloidin. YFP and H2B-GFP mark transduced cells. DAPI (blue) labels the nuclei. Scale bar, 50 μm.

analyses of lysates from FACS-purified infected (YFP^+) cells revealed marked reductions of HRAS (79%) and ERK1 protein levels (86%, Figure 3.7b). Newborn mice with strongly reduced HRAS and ERK1 were viable and displayed normal skin, consistent with their non-essential function in skin morphogenesis and embryonic development (Ise et al., 2000; Pagès et al., 1999).

To investigate the effects of *Hras1* and *Mapk3* knockdowns on the hyperproliferative behavior of *Ctnna1* mutant cells, I again analyzed BrdU incorporation, this time in $r26^{yfp/+}$ and $Ctnna1^{lox/lox}r26^{yfp/+}$ E18.5 embryos that had been infected with shRNA-modified LV-Cre at E9.5 (Figure 3.7c). For each animal, BrdU incorporation in YFP^+ cells was normalized to that of animal-matched YFP^- cells. In *Hras1* knockdown control animals, the proportion of $BrdU^+$ cells in YFP^+ and YFP^- populations was constant, indicating that this level of HRAS reduction alone did not affect proliferation. By contrast, equivalent *Hras1* knockdown in *Ctnna1* mutant cells abolished the increase in BrdU incorporation. *Mapk3* knockdown also restored normal proliferation to *Ctnna1* mutant cells, while exhibiting no effect on control cells. These data imply that the hyperproliferation following α-catenin loss *in vivo* is dependent upon downstream RAS-MAPK activity. These experiments further illustrate the strength of this new system, where a combination of RNAi-mediated knockdown with Cre-mediated knockout, can be used for rapid assessment of physiologically significant genetic interactions.

While these findings established a pathway whereby α-catenin deficiency leads to enhanced RAS-MAPK signaling and hyperproliferation *in vivo*, this mechanism acted counter to the decreased CGI. To explore the underlying

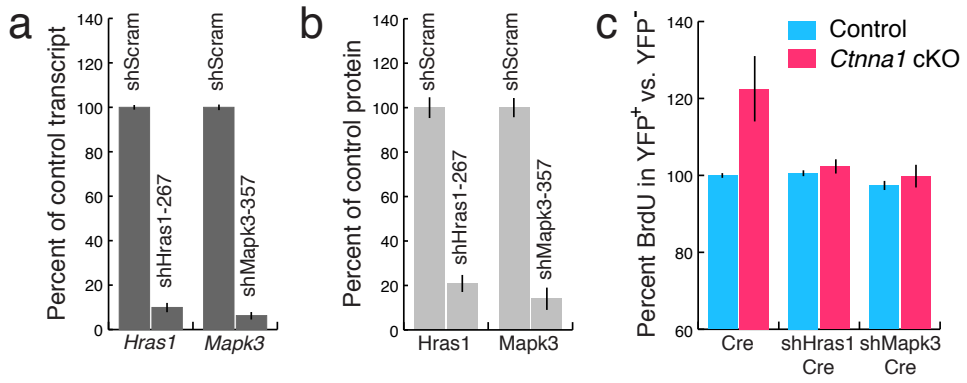

Figure 3.7 Hyperproliferation of *Ctnna*1 mutant cells is dependent upon RAS-MAPK signaling *in vivo*. (a,b) Efficiency of Hras1 and Mapk3 RNAi knockdowns in vitro and in vivo. Embryos and cultured keratinocytes were subjected to lentivirus-mediated RNAi knockdowns with shHras1-267, shMapk-357 or control scrambled shRNA (shScram). (a) Following keratinocyte infections, Hras1 and Mapk3 transcripts were quantified by real-time PCR. (b) Following embryo infections, HRAS and ERK1 protein levels were determined by immunoblot analyses (data are normalized to control values of 100%). (c) Effects of Hras1 and Mapk3 RNAi on BrdU incorporation in control and LV-Cre Ctnna1 cKO cells. Embryos were infected with LV-Cre vectors containing Hras1, Mapk3 or scrambled shRNAs as indicated. Prior to harvesting, embryos received a 6h pulse of BrdU. Shown are data after quantification by FACS.

reason for this difference, I first checked for senescence following α1-catenin loss. Previous studies have demonstrated that sustained RAS-MAPK signaling can induce senescence and growth arrest in primary cells, and that disruption of senescence induction is needed for malignant transformation (Collado et al., 2005; Wang et al., 2002). Additionally, primary non-passaged keratinocytes depleted of α-catenin show impaired colony formation and growth efficiency in culture (Figure 3.8a), which could perhaps be due to growth arrest. An assay for senescence-associated β-galactosidase activity (SA-β-gal), detected no signs of enhanced senescence in *Ctnna1* mutant tissue (Figure 3.8b,c). As a positive control, sebaceous gland tissue of older mice testsed positive in this assay (Dimri et al., 1995). I next addressed whether the hyperproliferation might be counterbalanced by enhanced apoptosis. Immunofluorescence analysis of LV-Cre infected *Ctnna1*$^{lox/lox}$r2*6*$^{yfp/+}$ tissues showed a 960% increase in active Caspase 3 positive cells relative to control r2*6*$^{yfp/+}$ tissues (Figure 3.8d,e).

TRP53 is a central regulator of apoptosis in epithelia as well as other cell types, and loss of TRP53 has been reported to rescue the apoptotic defects in *Cdh1* mutant mammary gland cells *in vivo* (Derksen et al., 2006). Additionally, a variety of human epithelial cancers show reduced E-cadherin and α-catenin levels along with TRP53 activation (Nozawa et al., 2006; Xiangming et al., 1999). To test whether TRP53 is activated following α-catenin loss in skin, mRNA was isolated from FACS-purified YFP^{+} cells of LV-Cre infected *r26*$^{yfp/+}$ and *Ctnna1*$^{lox/lox}$r2*6*$^{yfp/+}$ E18.5 embryos and profiled them for known TRP53 targets. The highest transcript increases in *Ctnna1* mutant embryos were *Bbc3* (1,130%) and *Pmaip1* (530%), encoding PUMA and Noxa, respectively (Figure 3.8f). In addition

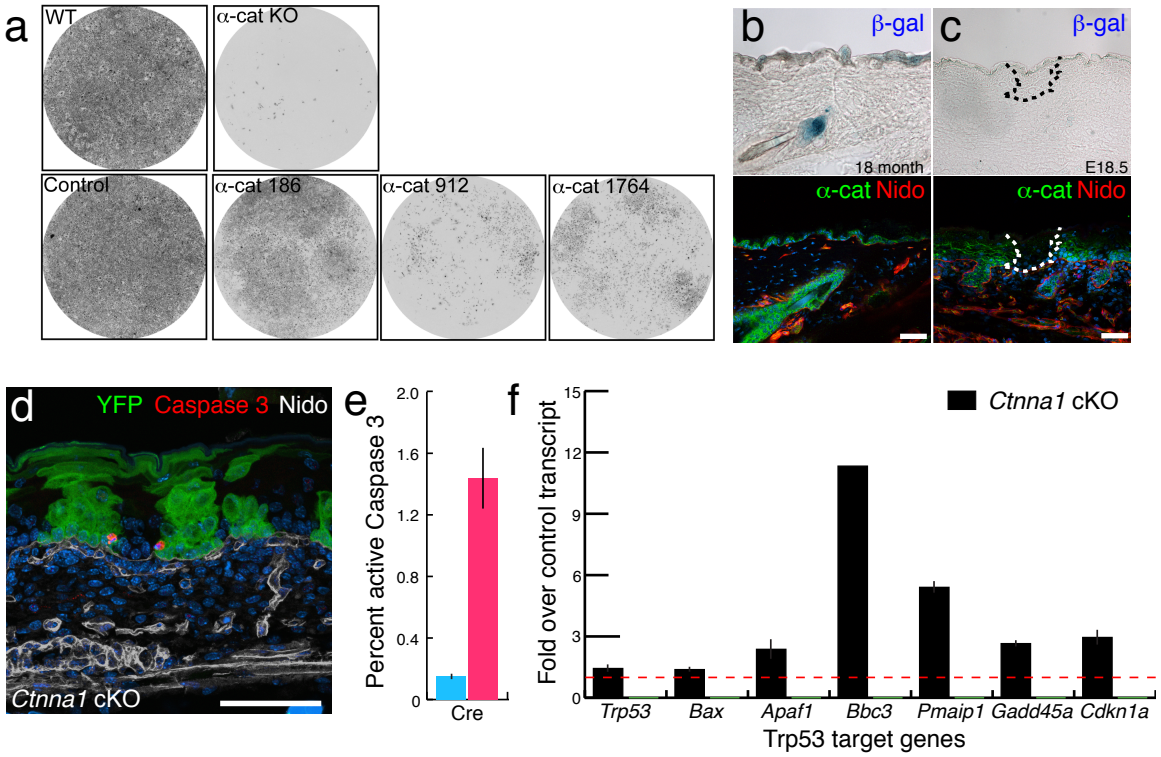

Figure 3.8 Loss of α1-catenin does not result in cell senescence, but does result in apoptosis and activation of p53 signaling. (a) Wild-type, scramble control, *Ctnna1* knockout and Ctnna1 knockdown primary keratinocytes in a colony growth assay. Note the reduction in growth that correlates with strength of knockdown hairpin. (b) Backskin sections of an 18 month old mouse served as a positive control for the assay, and shows senescence-associated β-galactosidase staining in the hair follicle and sebaceous gland. (c) Representative LV-Cre *Ctnna1* knockout cell clone, encased by the dotted line and marked by the absence of α1-catenin immunolabeling, shows no β-gal signal. Nidogen (Nido) marks the basement membrane. DAPI (blue) labels the nuclei. Scale bar, 100 μm. (d) Apoptotic cells (marked by active Caspase 3) in clonal patches of *Ctnna1* cKO skin, marked by YFP expression. Quantifications are shown in (e). Nidogen marks basement membrane and dermal blood vessels. DAPI (blue) labels the nuclei. (e) Percentage of Caspase 3 positive cells in control and *Ctnna1* cKO cells *in vivo*. (f) Fold changes in in vivo transcript levels of TRP53 signature target genes in cells FACS-sorted from Ctnna1 cKO embryos.

to being TRP53 targets, these proteins act as the primary mediators of TRP53-dependent cell death (Villunger et al., 2003). Smaller increases in the TRP53 targets *Cdkn1a*, *Gadd45a* and *Apaf1* were also detected.

To test for functional interactions between α-catenin and TRP53-mediated apoptosis, I depleted *Trp53* assessed the consequence of *Trp53* knockdown on apoptosis in *Ctnna1* mutant cells. First, I selected shTrp53-1223 and shTrp53-9132, which showed ~50% reduction in *Trp53* transcripts in keratinocytes and embryonic skin (Figure 3.9a). Next, I infected E9.5 $Ctnna1^{lox/lox}r26^{yfp/+}$ along with $r26^{yfp/+}$ only control embryos with LV-Cre harboring shTrp53 and analyzed them at E18.5. In control animals, concomitant knockdown of *Trp53* with LV-Cre expression did not change TRP53 target expression, suggesting that TRP53 activity was low in under normal conditions. However in *Ctnna1* mutant cells, TRP53 reduction *in vivo* reduced *Bbc3* and *Pmaip1* transcripts 190% and 350%, respectively, relative to LV-Cre alone (Figure 3.9b, green bars). Furthermore, while *Trp53* knockdown in control clones showed no measurable effect on apoptosis, comparable *Trp53* knockdowns in *Ctnna1* mutant cells resulted in a 300% decrease in active Caspase 3 positive cells (Figure 3.9c). This phenomenon was not attributable to off-target effects, since knockdown with two different Trp53 shRNAs gave similar results.

Finally, I tested whether the observed reduction in CGI could be reversed upon *Trp53* knockdown in *Ctnna1* mutant animals. Indeed when the mix of LV-RFP and LV-Cre expressing shTrp53-1223 was injected into $Ctnna1^{lox/lox}r26^{yfp/+}$ test and $r26^{yfp/+}$ control embryos at E9.5 and analyzed at E18.5, the calculated CGI was 0.8 (Figure 3.9d). Although this value was still <1, the difference from control

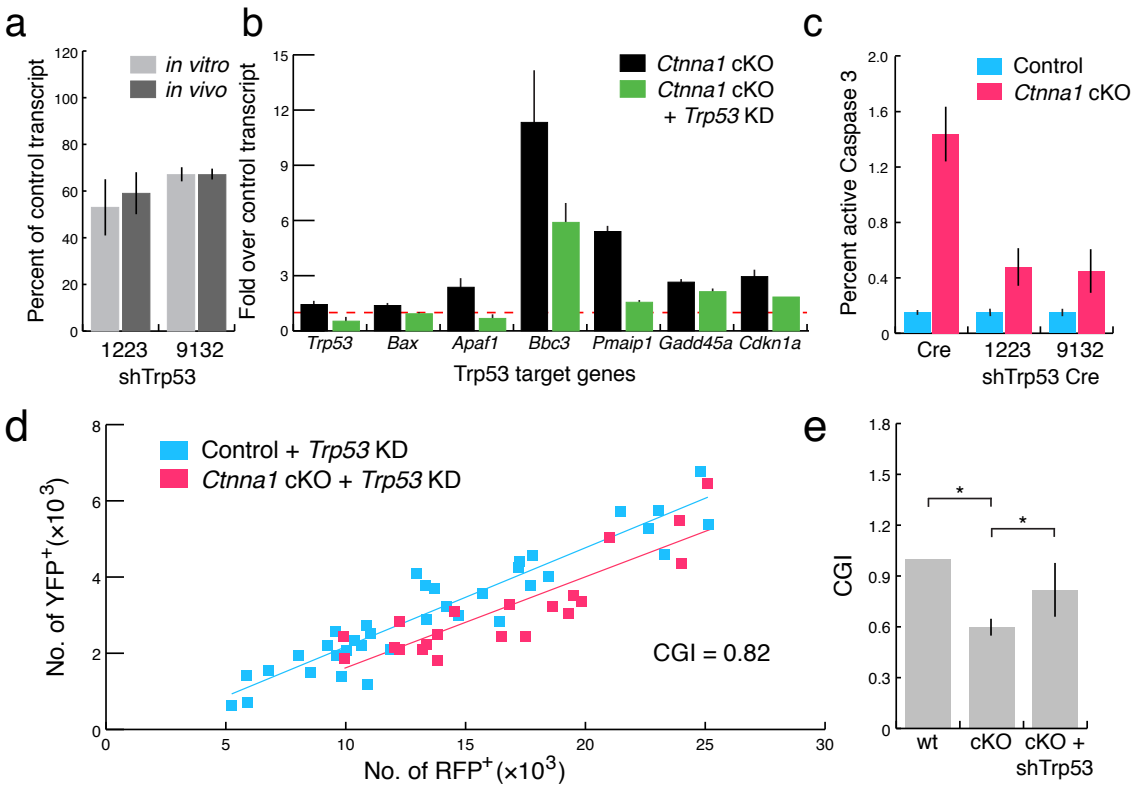

Figure 3.9 Concomitant depletion of Trp53 rescues apoptosis and CGI in *Ctnna1*-null tissue. (a) Levels of *Trp53* transcripts *in vitro* and *in vivo* following lentivirus mediated RNAi knockdown in keratinocytes and embryos. Two different *Trp53* shRNAs are tested. (b) Fold changes in *in vivo* transcript levels of TRP53 signature target genes in cells FACS-sorted from *Ctnna1* cKO embryos and from *Ctnna1* cKO embryos infected with shTrp53-1223 (*Ctnna1* cKO + Trp53 KD). Values are normalized to LV-Cre infected control embryos (red dashed line). (c) Percentage of active Caspase 3 positive cells in control and *Ctnna1* cKO cells in the presence and absence of *Trp53* RNAi *in vivo*. (d) Graph of numbers of RFP+ cells relative to YFP+ cells at E18.5 in control and *Ctnna1* KO mice infected with shTrp53-1223. CGI=0.8 ($p<0.001$). (e) Comparison of CGI for control (wt), *Ctnna1* knockout (cKO) and Ctnna1 knockout with *Trp53* knockdown (cKO + *Trp53* KD) embryos. *denotes CGI values that show significant differences ($p<0.001$).

was not statistically significant at $p<0.05$. This result differed significantly when compared to the CGI following loss of α1-catenin alone (Figure 3.9e; $p<0.001$). Together, these findings provide compelling evidence that TRP53 activation is responsible for the growth disadvantage following loss of α1-catenin.

Discussion

The described strategy for conducting comprehensive functional analyses couples the accessibility of epidermis with the utility and expediency of RNAi and commercially available shRNA libraries, and greatly expands the molecular toolbox for dissecting complex genetic pathways in mammalian tissue biology. In its simplest form as a single-gene functional analysis, this method necessitates only a few weeks between target-selection and phenotypic analysis. As such, it offers a distinct advantage over classical mouse genetics, the conventional method currently employed to study embryonic development and tissue homeostasis in an unperturbed physiological setting. This is particularly advantageous for the study of lesser-known genes, which are commonly found in microarray profiles and high-throughput screens. These genes are less likely to be studied *in vivo* due to the large amount of resources and time required to generate a targeted mouse mutant. The ability to quickly knock down a gene of interest *in vivo* and analyze the phenotypic consequences can provide a useful hint as to whether the study is worth pursuing further.

Unlike classical mouse genetics, the addition of experimental complexity in this system, such as analyzing the consequences of multiple gene knockdowns or a combination of knockout and knockdown approaches, does not significantly increase the experimental time. Injecting embryos with a combination of two or

more viruses does not take any longer than a single virus, whereas generating a conditional double knockout mouse requires several rounds of mouse matings and can take several months to a year. Additionally, the modular nature of the pLKO.1 vector facilitates rapid and efficient cloning. This can allow for the introduction of multiple shRNA hairpins targeting the same gene, to maximize knockdown efficiency. Alternatively, multiple hairpins within the same vector can target different genes, to eliminate redundancy between closely related genes or to analyze genetic interactions. Hairpins can also be carried on different viral vectors, to enable a combinatorial approach.

Using *Ctnna1* as a paradigm, I have shown how the technology can be used to reproduce known loss-of-function phenotypes, an essential step in demonstrating the utility of a new genetic tool. Lentiviral depletion of α-catenin protein either via Cre-mediated excision of floxed alleles or by shRNA-mediated knockdown recapitulated the morphological and biochemical phenotype observed in the K14-Cre conditional mutant at the tissue and cellular levels. The pattern of increased phenotypic severity corresponded with the regions of highest infectivity, as determined by FACS analysis.

I have also used this approach to uncover new insights into the genetic interplay between intercellular adhesion and growth control. Conditional ablation of α-catenin throughout the epidermis resulted in hyperproliferation, epidermal thickening and overgrowth in dermal invaginations. The ability to manipulate viral titer to achieve α-catenin deletion in discrete clones enabled me to dissect the cell-autonomous consequences of α-catenin loss. Despite their intrinsic increase in proliferation rate, *Ctnna1*-mutant cells were at a measurable

and significant growth disadvantage and did not outcompete their wild-type neighbors. Perhaps in the absence of neighboring wild-type cells, as in the conditional knockout situation, the widespread lack of a functional barrier may induce inflammatory and pro-proliferative signaling throughout the tissue, thereby further promoting the proliferation of α-catenin mutant cells. Additionally, the absence of competing wild-type cell may place additional pressure on the mutant cells to survive and sustain the epithelium.

This phenotypic difference between tissue-wide and focal deletion of α-catenin has also been reported in the mouse cortex. Tissue-wide deletion of α-catenin in the cortical neuroepithelium led to cortical hyperplasia and epithelial disorganization accompanied by activation of the hedgehog signaling pathway (Lien et al., 2006). In contrast, deletion of α-catenin in discrete clones within the cortical neuroepithelium caused cells within those clones to prematurely exit the ventricular zone and to undergo differentiation (Stocker and Chenn, 2009). Similarly, in *Drosophila*, zygotic mutants lacking adhesion proteins *Scribble, Discs-large* or *Lethal giant* exhibit loss of epithelial polarity, hyperproliferation, tissue overgrowth and invasion, leading to lethality at the third instar larval stage (Bilder et al., 2000). However, individual clones of cells lacking *Scribble* in the *Drosophila* eye disc show increased proliferation but do not overgrow due to increased apoptosis mediated by the Jnk pathway, again highlighting potentially divergent consequences of clonal versus tissue-wide gene deletion (Brumby and Richardson, 2003). Co-expression of oncogenic Ras in these clones can rescue the apoptosis and induce tissue neoplasia (Pagliarini and Xu, 2003). This supports a cooperative model of tumorigenesis in this system, where a clonal mutation

resulting in disruption of epithelial integrity acts in concert with an oncogenic mutation that confers proliferative advantage to that clone either by further increasing proliferation or inhibiting apoptosis.

My analyses demonstrated a measurable effect of RAS-MAPK-dependent cell proliferation and TRP53-dependent cell death on *Ctnna1* loss-of-function phenotypes during skin morphogenesis. Unlike the *Drosophila* system, I did not detect an increase in Jnk activation, suggesting that different organisms and tissue might activate varied mechanisms upon sensing disruption of epithelial integrity. It is possible that a low level of Jnk signaling may be responsible for part of the apoptosis observed in *Ctnna1* mutant clones, as the rescue of apoptosis rates and cellular growth was not complete upon *Trp53* knockdown. Alternatively, the incomplete rescue may be due to the fact that even the most efficient *Trp53*-targeting shRNA hairpins did not achieve complete knockdown *in vivo*, suggesting that the remaining apoptosis could be mediated by residual TRP53 protein.

It is tempting to speculate that the uncovered genetic interactions between the RAS-MAPK and TRP53 pathways allow the epidermis to suppress neoplastic growth and sustain homeostasis following loss of α1-catenin. A similar phenomenon has been observed following loss of TGF-β signaling in the skin (Guasch et al., 2007). In the epidermis of mice lacking the TGF-β receptor II, hyperproliferation is balanced by increased apoptosis, which maintains a net homeostasis throughout much of the tissue. However, the anogenital regions, which are inherently more proliferative than backskin, develop spontaneous squamous cell carcinomas. Squamous cell carcinoma formation can be induced in

backskin cells through expression of oncogenic Ras, as in the *Drosophila* study described above. Given these new findings, I posit that this may be a common feature of tumor suppressors in skin epithelium. In this scenario, tipping the balance towards cell survival, through pro-survival signals or alteration in TRP53 pro-apoptotic function, could subsequently lead to development of epidermal tumors, reinforcing why the frequent occurrence of *Trp53* null mutations upon chronic UVB exposure contributes so greatly to skin cancers.

Materials and Methods

Lentiviral vectors

Lentiviral vectors were based on the pLKO.1 shRNA plasmid from The RNAi Consortium library (Sigma). Lentiviral constructs containing the puromycin resistance cassette were screened for knockdown efficiency in cultured keratinocytes, and the most efficient sequences were selected for use *in vivo*. The target sequences for hairpins described in the Results section are as follows:

shScram: CCTAAGGTTAAGTCGCCCTCG

shCtnna1-186: CCTGGTAAACACCAATAGTAA

shCtnna1-921: CGCTCTCAACAACTTTGATAA

shCtnna1-1764: GCCAGGAGTTTACACAGAGAA

shHras1-267: CTTCGAGGACATCCATCAGTA

shMapk3-357: GCCATGAGAGATGTTTACATT

shTrp53-1223: CCACTACAAGTACATGTGTAA

shTrp53-9132: CACTACAAGTACATGTGTA

For *in vivo* use, the hairpins were cloned into LV-RFP, LV-GFP or LV-Cre (described in the Methods section for Chapter 2) using *SphI* and *SacII* restriction sites, and *AgeI*/*EcoRI* restriction sites, respectively. Lentivirus production, concentration, and *in utero* microinjection was performed as described in the Methods section of Chapter 2.

Mice

The following mouse strains were used: CD1 (Charles River Laboratories), *Gt(ROSA)26Sor*$^{tm1(EYFP)Cos/+}$ referred to in the text as *r26*^{Yfp} (Jackson Laboratories, donated by A. McMahon), or *Ctnna1*$^{lox/lox}$ (Vasioukhin et al., 2001). *Ctnna1*$^{lox/lox}$ mice were bred with *r26*^{Yfp} mice to produce males that were doubly homozygous for the two genotypes. These males were mated with *Ctnna1*$^{lox/lox}$ females for LV-Cre mediated excision of *Ctnna1.* Each embryo was injected with 1.5 μl of lentivirus, and up to eight embryos were injected per litter. Surgical procedures were limited to 30 min for high survival rates. The Rockefeller University Animal Care and Use Committee approved animal experimentation protocols used in the study.

Skin culture.

Mouse keratinocytes were isolated as described in the Methods section of Chapter 2. Keratinocytes were maintained in culture in E-media containing 0.05 mM Ca^{2+} and supplemented with 15% serum. For viral infections, keratinocytes were plated in 12-well dishes at 70,000 cells per well and infected with lentivirus in the presence of polybrene (100 μg ml^{-1}) by centrifugation at 1100g for 30

minutes at 37°C. After centrifugation, infection media was replaced with fresh keratinocyte culture media. After 2 days of growth, keratinocytes were subjected to selection with puromycin (2 μg ml^{-1}), and subsequently processed for mRNA and protein analyses. For analysis of explant outgrowth, 5 mm punch biopsies were harvested from E18.5 embryos and plated onto glass-bottom dishes coated with fibronectin (10μg/ml). Explants were maintained in high Ca^{2+} (1.5 mM) E-media to support intercellular adhesion and incubated 24–48 h.

mRNA and protein quantification.

Total RNA was isolated from FACS-sorted cells using the Absolutely RNA Microprep kit (Stratagene). cDNAs were generated from 1 μg of total RNA using oligo(dT) primers and SuperScript III First-Strand Synthesis System kit (Invitrogen). Real-Time PCR was performed using the LightCycler 480 System (Roche) and gene-specific and *Ppib* control primers. Data were analyzed and transcript levels established using LightCycler 480 Software (Roche). For immunoblotting, FACS sorted cells were lysed in NuPAGE LDS sample buffer (Invitrogen), electrophoresed on NuPage Novex 4-12% gradient Bis-Tris gels (Invitrogen), and subjected to blotting in Odyssey blocking buffer (Li-Cor).

The following primary antibodies were used: mouse GAPDH (6C5, 1:5,000; Abcam), rabbit α1-catenin (C8114, 1:12,000; Sigma), rabbit ERK1 (K-23, 1:1,000; Santa Cruz) and rabbit RAS (3965, 1:200; Cell Signaling). Secondary antibodies conjugated to IRDye 680 and 800 were used (1:10,000; Li-Cor). Protein levels were quantified using the Odyssey Infrared Imaging System (Li-Cor).

Immunostaining and β-galactosidase detection.

The following primary antibodies were used for immunostaining: chicken GFP (1:2,000; Abcam); rat Ecad (ECCD-1, 1:500; M. Takeichi), Nidogen (ELM1, 1:2,000; Santa Cruz), Mac1 (M1/70, 1:100; Pharmingen), CD117 (2B8, 1:100; Pharmingen), GR1 (RB6-8C5, 1:100; Pharmingen), CD3 (KT3, 1:200; Chemicon) and CD45 (30-F11, 1:100; Pharmingen); rabbit α1-catenin (C8114, 1:2,000; Sigma), Caspase 3 (AF835, 1:1,000; R&D), K6 (1:500; P. Coulombe), K5 (1:500; E. Fuchs), K1 (1:500; E. Fuchs) and Involucrin (1:500; Covance). Secondary antibodies were conjugated to Alexa-488 (Molecular Probes), Cy3, or Cy5 (Jackson Laboratories). F-actin was detected by Alexa-546 phalloidin (Molecular Probes). The senescence-associated β-galactosidase assay was performed as recommended (Cell Signaling). Cells and tissues were processed as described in the Methods section of Chapter 2. Confocal images were captured by a scanning laser confocal microscope (LSM510 Meta; Carl Zeiss, Inc.) using C-Apochromat 40×/1.2 water lens or a 63x oil objective (n.a. 1.4). Images were processed using Adobe Photoshop and panels were labeled in Adobe Illustrator CS5.

Flow cytometry

Isolation of keratinocytes, intraperitoneal BrdU injection FACS analysis were performed as described in the Methods section of Chapter 2. Cells were purified using BD FACSAria II (BD Biosciences) and FACS analysis was performed on BD LSR II (BD Biosciences).

Statistics

Data were collected from experiments performed in at least triplicate, and expressed as mean ± standard deviation. Differences between groups were assayed using Student t-test. In analyses of CGI data, slopes of data distribution were compared using analyses of covariance (ANOCOVA) in Matlab Statistics.

CHAPTER 4: FURTHER INSIGHTS INTO THE ROLE OF α-CATENIN IN EPIDERMAL MORPHOGENESIS

Cell behavior during tissue development and homeostasis is regulated by an array of signal cues from the extracellular milieu, adjacent cells and intracellular events that is integrated to achieve coordination of cell shape, proliferation and movement. Disruption of any of these signaling routes, or the controlled integration thereof, has the potential to result in deleterious consequences for tissue development by impinging upon the other pathways in the network.

Studies in a variety of organisms, tissues and cancers have illustrated that disruption of cell-cell adhesion can affect cell migration, proliferation and survival (Carmeliet et al., 1999; Hajra and Fearon, 2002; Noren et al., 2000). Depletion of α-catenin in the epidermis, whether by traditional mouse genetics or lentiviral targeting *in vivo* weakens the junctions between keratinocytes and results in a loss of intercellular adhesion and cytoskeletal organization (Vasioukhin et al., 2001). These effects are accompanied by increases in both Ras-MAPK-dependent proliferation as well as Trp53-dependent cell death (Chapter 3). However, whether these downstream consequences of *Ctnna1* deletion occur independently, or are interrelated through common signaling pathways remains unclear.

In order to further probe the mechanisms of epidermal dysregulation in the absence of α-catenin, I utilize the *in utero* lentiviral delivery system (Chapter 2) in conjunction with tissue analysis, explant and cell culture approaches. Analyzing the spatiotemporal consequences of α-catenin deletion on epidermal

organization throughout development, I find evidence of epithelial disruption during the onset of stratification. This disruption correlates with breaks between the basal and suprabasal cell layers and a predisposition for apoptotic cell death specifically in the suprabasal layer, while the basal layer appears to be protected.

Signaling from the extracellular matrix via integrins has the potential to provide an additional survival cue in the basal layer that is not present in suprabasal cells that lose contact with the basement membrane. As numerous signaling mediators, such as growth factor receptors, cytoskeletal regulators and adapter proteins can localize to both cell-cell and cell-matrix adhesions, disruption of cell-cell adhesion in the absence of α-catenin may result in changes in cell-matrix signaling. These changes could manifest as alterations in cell survival, differentiation or migration (Braren et al., 2006; Stachelscheid et al., 2008). I address these possibilities by depleting components of the integrin signaling pathway on the background of *Ctnna1* deletion, and analyze their role in regulating cell survival and migration *in vivo* and *ex vivo*. I find that depletion of Fak or Pak proteins reduces both the survival and migration of basal α-catenin depleted cells.

Results

Characterization of epithelial disorganization in the absence of α-catenin

Previous analyses of α-catenin deletion in the epidermis have primarily relied on immunofluorescence in sagittal sections to assess the extent of disruption of cell-cell adhesion and cytoskeletal organization (Vasioukhin et al., 2001). Using this approach, E-cadherin appears to be maintained at cell-cell

boundaries, suggesting that loss of α-catenin might not immediately disrupt adherens junction maintenance within existing epidermal sheets *in vivo*.

To determine whether this is the case, I performed whole-mount immunofluorescence on skin pieces from control and LV-Cre infected skins, and imaged the tissues in the plane of the epidermis (Figure 4.1). Imaging of tissues at E15.5, during the early phase of stratification revealed striking differences between control and *Ctnna1*-null tissues. In control tissue, both basal and suprabasal cells showed colocalization of E-cadherin with actin (as marked by phalloidin staining), consistent with the formation of a junction-associated actin belt during cell-cell adhesion (Figure 4.1a,b). In the basal cells of *Ctnna1* null tissue, E-cadherin staining was slightly less continuous and more irregular (as in sections), but was still colocalized with phalloidin staining (Figure 4.1c). Additionally, the cells had more irregular morphology compared to the control. In contrast, the suprabasal cells of *Ctnna1* tissue showed a loss of colocalization between E-cadherin and actin and aberrant cell-cell adhesion (Figure 4.1d). While phalloidin still encircled suprabasal cells, E-cadherin staining was localized primarily in intracellular or cell-surface clusters, or at individual punctate adhesions between cells (Figure 4.1d, arrowhead). These results suggest that the suprabasal cells might be more sensitive to α-catenin loss, perhaps because of the increased junctional remodeling required during the process of stratification.

At E18.5, after the completion of stratification, control epidermis had developed an organized intercellular network of E-cadherin and actin fibers (Figure 4.2a). In the *Ctnna1* null, while the cell had recovered some cell-cell adhesion and peripheral E-cadherin staining, its localization was disorganized

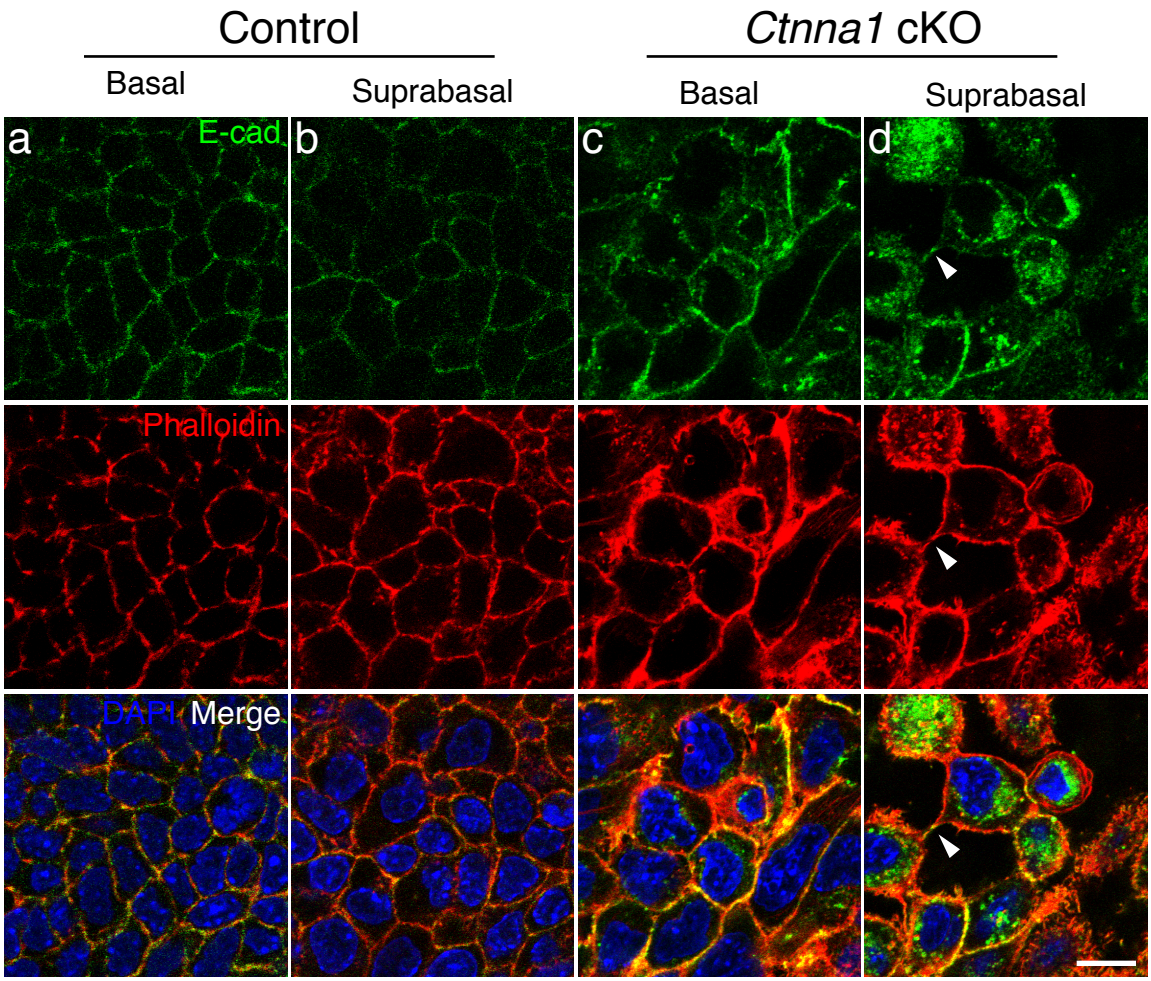

Figure 4.1 *Ctnna1* cKO tissue shows morphological, adhesive and cytoskeletal alterations by E15.5. Planar views of confocal sections from wild-type (a,b) and Ctnna1 cKO (c,d) skins at E15.5. (a) E-cadherin and F-actin (marked by Phalloidin) colocalize at borders between cells in the basal layer of wild type epidermal cells. (b) Colocalization is retained in the suprabasal layer (although E-cahderin immunofluorescence tends to be weaker in suprabasal layers under conditions of whole mount staining, possibly due to reduced antibody penetration into stratified epithelial layers). (c) Some colocalization between E-cadherin and F-actin is maintained in Ctnna1 cKO tissue, though E-cadherin staining is less sharply demarcated. Note less uniform cell morphologies. (d) Loss of E-cadherin and F-actin colocalization and formation of large breaks in cell-cell contact in cKO suprabasal layer. Punctate adhesions appear to join cells together (arrowhead) Scale bar, 10 μm.

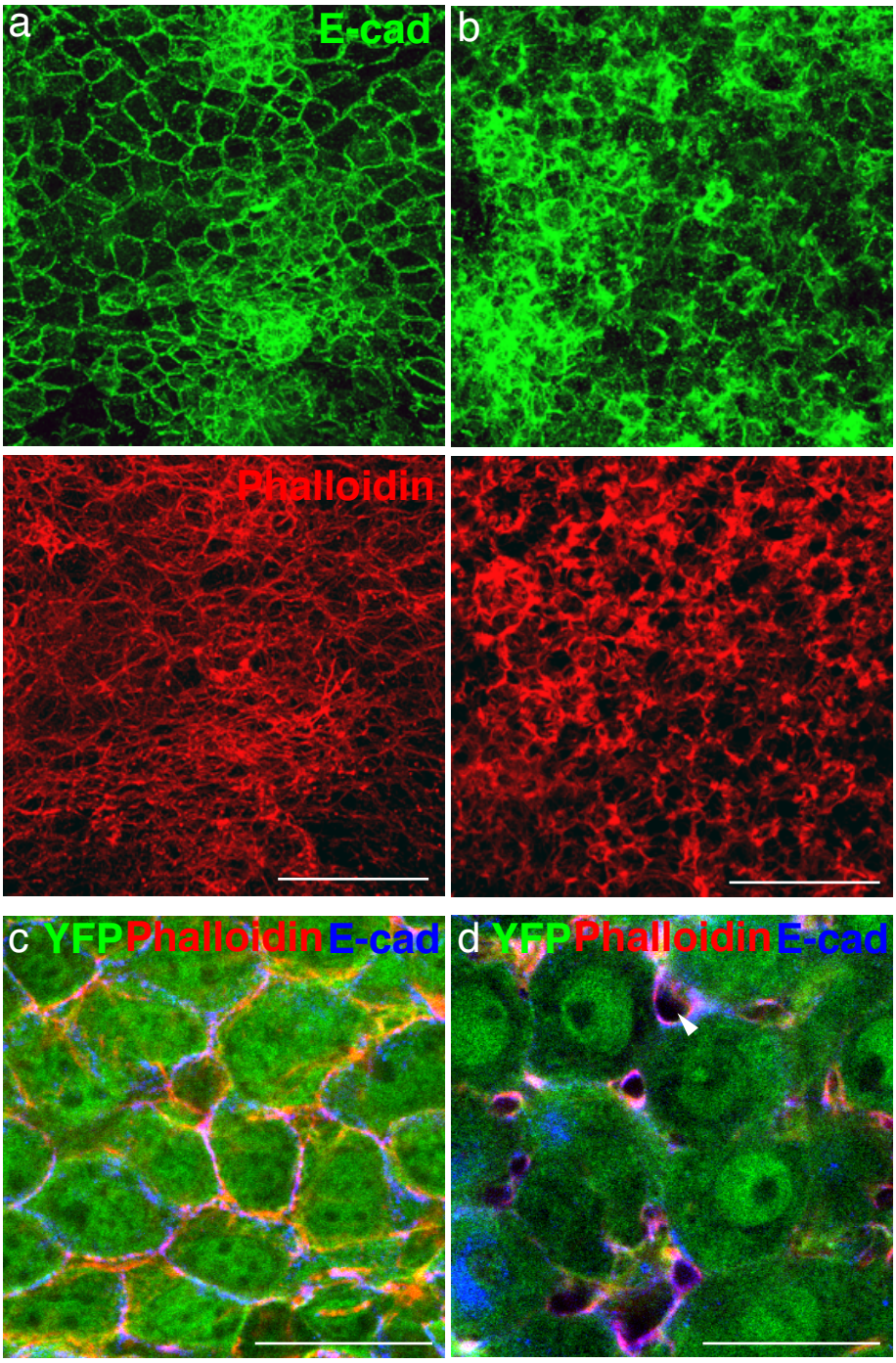

Figure 4.2 *Ctnna1* ablation results in disruption of epithelial networks *in vivo* (a,b) Planar view projection of a confocal stack of E18.5 epidermis. (a) Coordinated intercellular network of E-cadherin and actin (as marked by Phalloidin). (b) Lack of coordinated intercellular network in Ctnna1 KO tissue. (c,d) Single plane from confocal stack of E18.5 control (c) and Ctnna1 KO (d) epidermis. Note intercellular spaces in Ctnna1 KO, as shown by absence of cytoplasmic YFP staining (arrowhead). Scale bar, (a,b) 50 μm; (c,d) 20 μm.

and not coordinated across the epithelial sheet (Figure 4.2b). Similarly, the actin staining lacked coordination. Higher magnification of tissues expressing cytoplasmic YFP due to the $r26^{Yfp/+}$ Cre reporter enabled observation of intercellular gaps within the epithelial sheet in *Ctnna1* mutant tissue, which were absent in the control (Figure 4.2c,d). These gaps were encircled with phalloidin staining and resembled an intermediate stage of adherens junction formation.

The changes in epithelial morphology in *Ctnna1* mutant tissue correlated with the depletion of α-catenin protein (Figure 4.3a,b). Analysis of tissue sections also revealed the formation of breaks between the basal and first suprabasal layers at the onset of stratification at E14.5 and continued to be present at later developmental stages (Figure 4.3c,e). Apoptotic cells, as marked by active Caspase-3 staining were consistently associated with the inter-layer breaks (Figure 4.3d,f), suggesting that perhaps a loss of survival cues from adhesion to neighboring cells may contribute to apoptosis in the absence of α-catenin. Interestingly, these apoptotic cells were consistently localized in the suprabasal layer, despite the fact that both basal and suprabasal cells bordered the breaks (Figure 4.4ab). In contrast, in control tissue, the less frequent apoptotic cells were localized primarily in the basal layer (Figure 4.4b). In fact, the rate of apoptosis in the basal layer was lower for α-catenin mutant tissues than for control, suggesting that an additional mechanism might protect the basal layer cells from apoptosis in the absence of α-catenin.

Changes in integrin signaling in the absence of α-catenin

Integrin signaling at focal adhesions is an excellent candidate mechanism to afford specific protection to the basal layer. To assess whether signaling

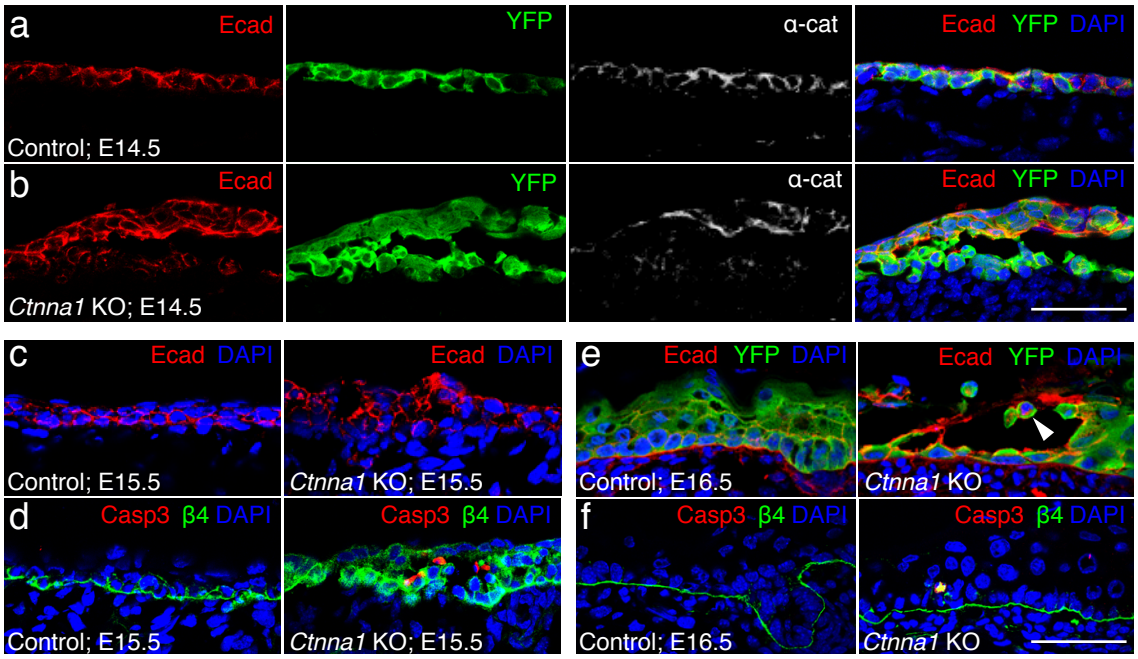

Figure 4.3 *Ctnna1* ablation rapidly induces breaks between the basal and spinous layers, which are associated with apoptotic cells. (a,b) Confocal sections of control and Ctnna1 KO tissues at E14.5. Control skins (a) exhibit an organized two-layered epithelium with E-cadherin and α-catenin colocalizing at cell-cell borders. (b) In Ctnna1 KO tissues, loss of α-catenin correlates with breaks between the basal and spinous layers. Note some residual α-catenin still present in suprabasal layer. (c) Control and Ctnna1 KO sections at E15.5 show continuation of intercellular breaks and disorganization of epithelium, as marked by E-cadherin staining. (d) Basal-spinous breaks are associated with apoptotic cells, as marked by active Caspase-3 staining. ß4 integrin is restricted to the basement membrane in control tissue, but loses polarization in the KO. (e) Sagittal sections at E16.5 show progression of stratification, accompanied by occasional complete loss of cell-cell adhesion (arrowhead) in Ctnna1 KO tissues. (f) Active Caspase-3 staining can be detected even in less morphologically aberrant tissues. Scale bar, 50 μm.

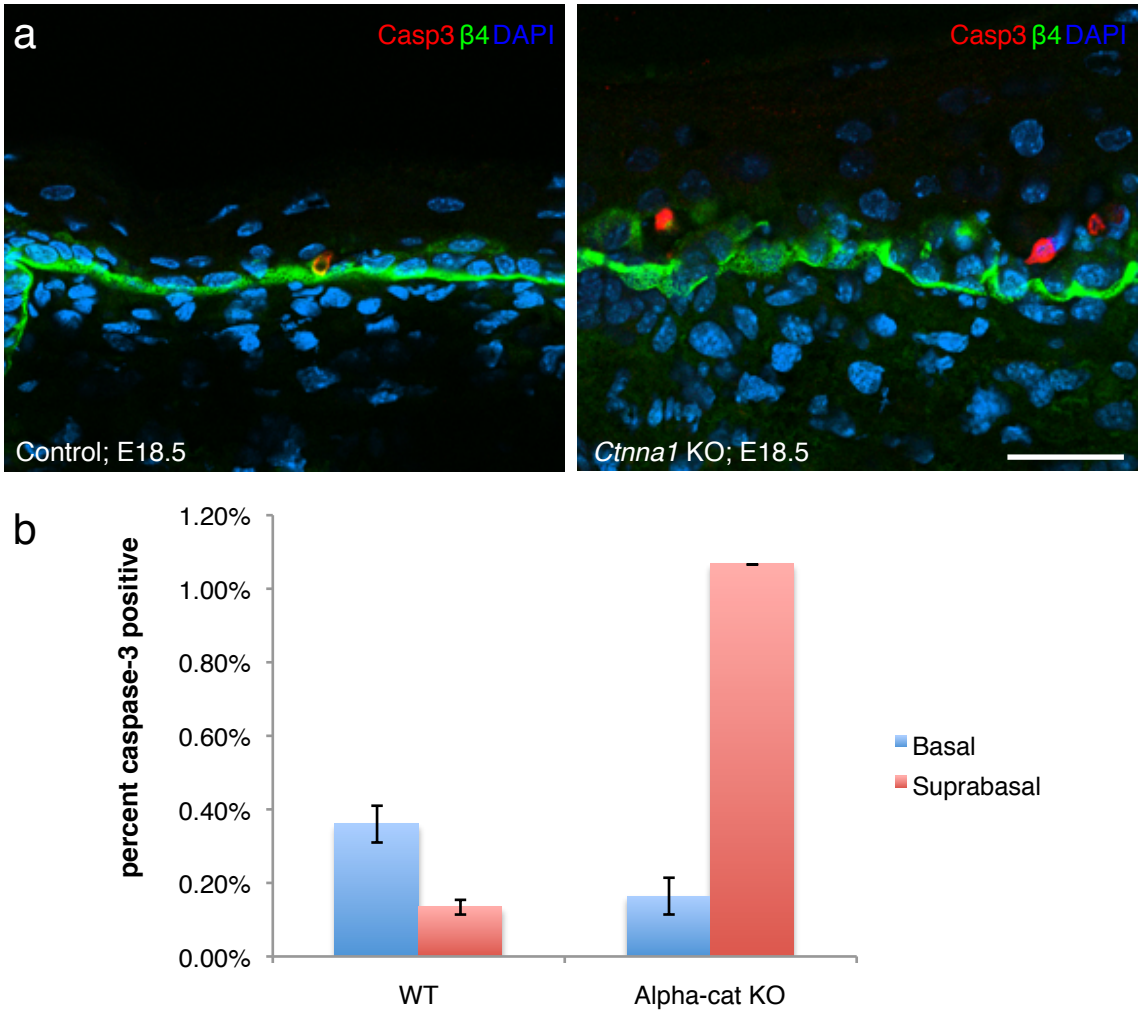

Figure 4.4 Suprabasal bias for apoptosis in *Ctnna1* KO tissues relative to wild-type. (a) Representative images of control and Ctnna1 KO skin sections stained with active Caspase-3 to detect apoptotic cells and integrin ß4 to label basal cells and the basement membrane. (b) Quantification of relative apoptosis frequencies between basal and suprabasal cells in control and Ctnna1 KO tissues. Scale bar, 30 μm.

through focal adhesions was altered in the absence of α-catenin, I performed immunoblots on lysates from control and α-catenin deficient epidermis and probed with antibodies against the active phosphorylated forms of Fak and Paxillin (Figure 4.5a). These proteins showed an increase in activation of 170% and 195%, respectively (Figure 4.5d). This modest but significant increase in activation was also observed for Rac1 (Figure 4.5b,d), which can become activated downstream of Paxillin and Pak signaling. Additionally, an increase in phospho-Fak immunofluorescence could be detected in the basal layer of *Ctnna1* null tissues, while under conditions of homeostasis in wild-type embryos, Fak activity is normally enriched specifically in the leading edge of the down-growing hair follicle (Figure 4.5c). These results suggest that in the absence of α-catenin, focal adhesion signaling is indeed enhanced *in vivo.*

Signaling activity at focal adhesions might be altered by changes in adherens junction stability as a variety of growth factor receptors and cytoskeletal regulators have been reported to localize to both structures (Canonici et al., 2008; Tomar and Schlaepfer, 2010). Thus, a change in composition of one adhesion type may shift the balance in localization of these proteins towards the other. To address this possibility, I analyzed the localization patterns of several proteins in the presence and absence of cell-cell adhesion in keratinocytes, using a calcium switch to induce adhesion formation. I found particularly striking changes in distribution of the insulin growth factor receptor (IGFR) in these studies. In wild-type cells under low Ca^{2+} conditions, the receptor localized to focal adhesions, as demonstrated by colocalization with Paxillin (Figure 4.6a). In *Ctnna1*-null cells, the receptor localized to focal adhesions under

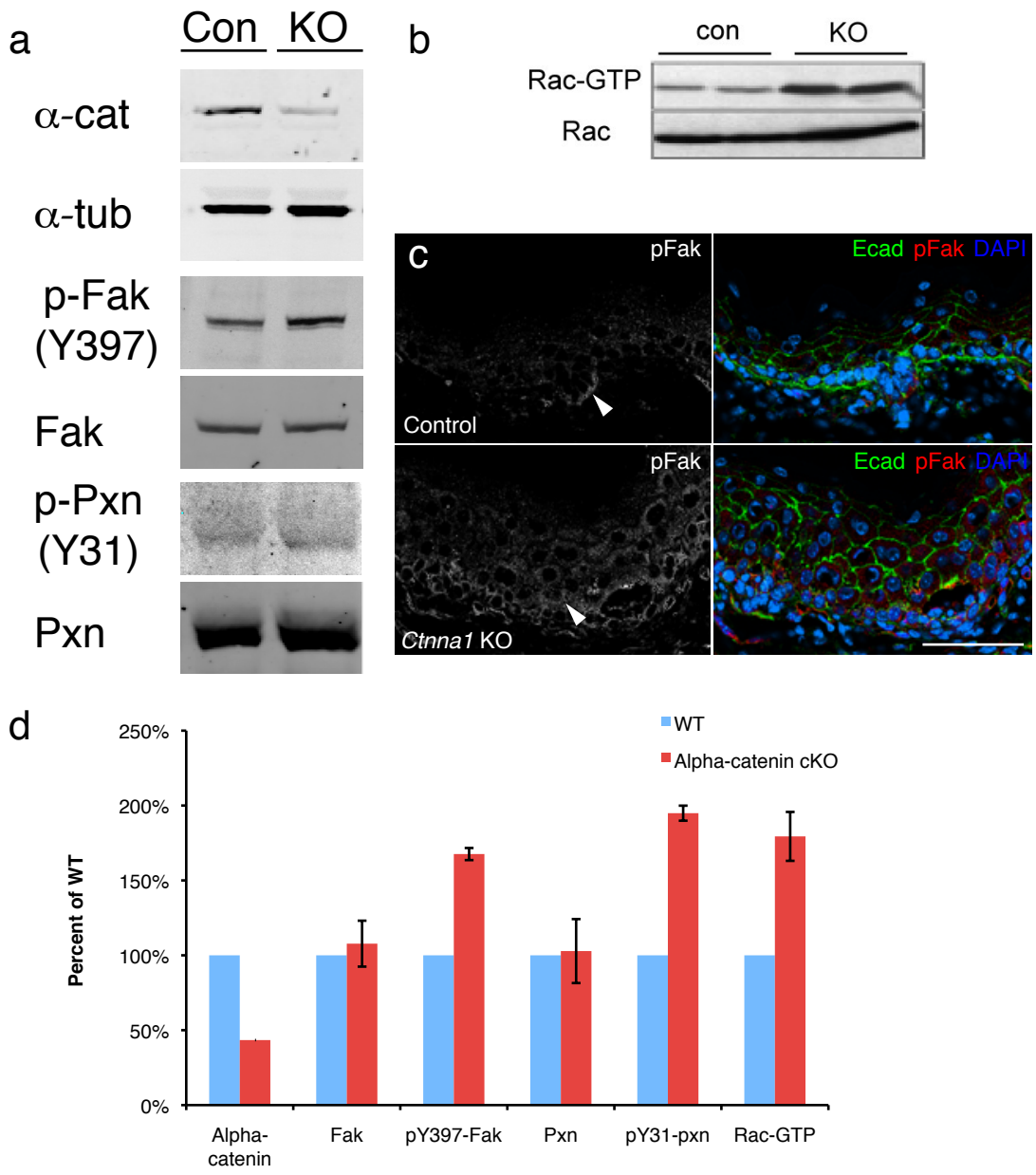

Figure 4.5 Slight but consistent activation of integrin signaling in the absence of *Ctnna1*. (a) Western blot of *in vivo* skin lysates for activation state of the focal adhesion proteins Fak and Paxillin, as determined by tyrosine phosphorylation of activating residues. (b) Activated GTP-bound Rac versus total Rac in control and KO skin. (c) Immunofluorescent staining for phosphorylated Fak in skin sections. Note Fak phosphorylation enrichment in hair placode of WT tissue, but distributed throughout basal layer in *Ctnna1* KO (arrowhead). (d) Quantification of activity change in integrin signaling components from panel (a). Error bars denote standard deviation. Scale bar, 50 μm.

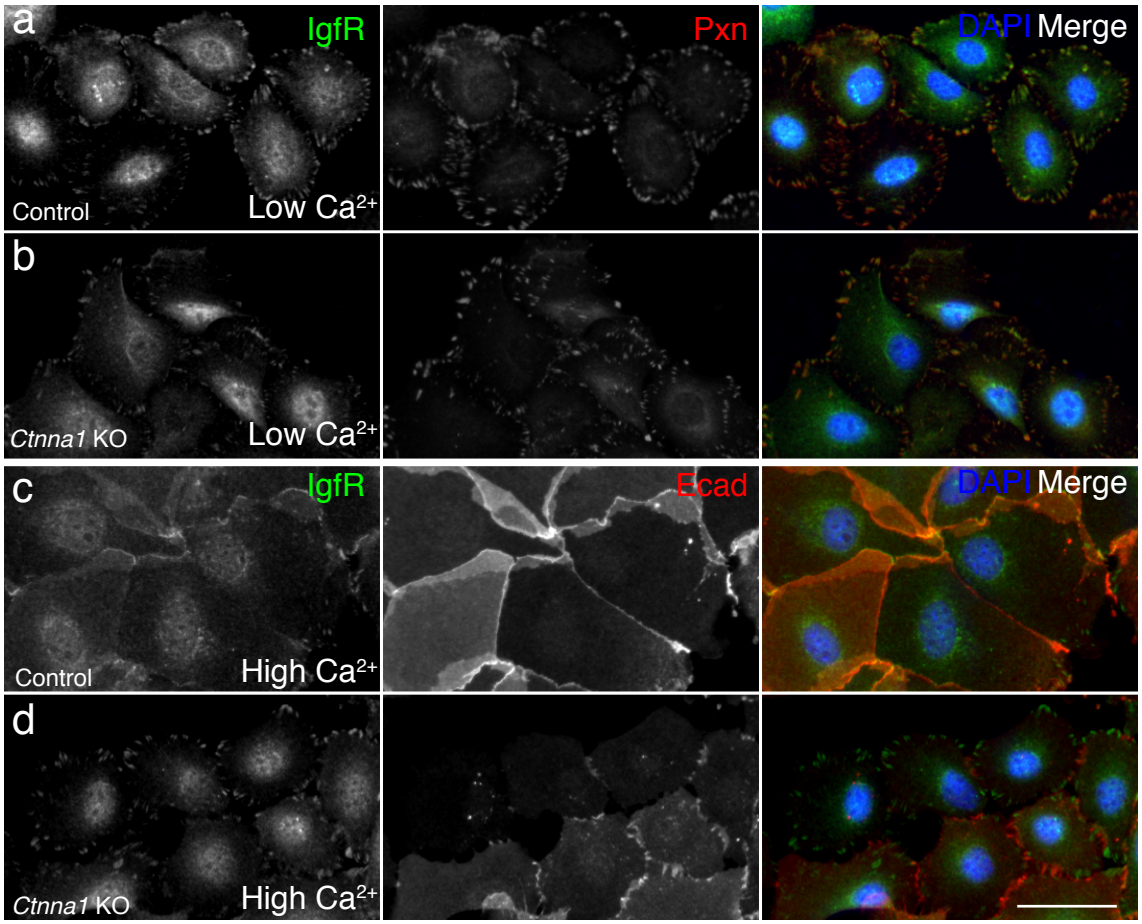

Figure 4.6 IGF-R localization shifts from focal adhesions to adherens junctions upon calcium switch in control but not *Ctnna1* cells. Wild-type (a) and Ctnna1 null (b) cells in low calcium stained for IGF-R and paxillin to mark focal adhesions. Wild-type (c) and Ctnna1 null (d) cells after 24 hours in high calcium stained for IGF-R and E-cadherin to mark adherens junctions. Note the colocalization of IGF-R and E-cadherin in control but not Ctnna1 null cells in the high calcium conditions. Scale bar, 50 μm.

these conditions as well (Figure 4.6b). Upon switching the control cells to high Ca^{2+} for 24 hours, the receptor distribution changed, and it now colocalized with E-cadherin at cell-cell contacts (Figure 4.6c). In contrast, in *Ctnna1*-null cells, the receptor remained at focal adhesions and did not colocalize with E-cadherin, even at the immature junctions that began to form in these cells.

A similar effect was observed in the case of the EGF receptor. While the EGFR did not localize specifically to focal adhesions in low Ca^{2+} in either control or *Ctnna1*-null cells (Figure 4.7a,b), shifting the cells to high Ca^{2+} induced its redistribution to cell-cell adhesions in control cells (Figure 4.7c). In the *Ctnna1*-null cells, some localization to cell-cell contacts could be observed, but this did not colocalize specifically with E-cadherin (Figure 4.7d). These results demonstrate that in keratinocytes, the localization of these critical growth factor receptors is regulated by cell-cell adhesion.

Interaction with components of focal adhesions has been shown to potentiate growth factor receptor signaling in a number of cell types, while associated with cadherin-based adhesions has been suggested to have an inhibitory effect (Fedor-Chaiken et al., 2003; Yamada and Even-Ram, 2002). To assess whether this might be the case in keratinocytes, I quantified fluorescence intensity of active (phosphorylated) IGFR to total IGFR in control (Figure 4.8ac) and *Ctnna1*-null (Figure 4.8b,c) cells under conditions of low and high Ca^{2+}. Interestingly, *Ctnna1*-null cells showed a mild increase in IGFR activity in low Ca^{2+} relative to control cells, but the difference was more pronounced upon switch to high Ca^{2+}. This suggested that IGFR activity in keratinocytes is at least

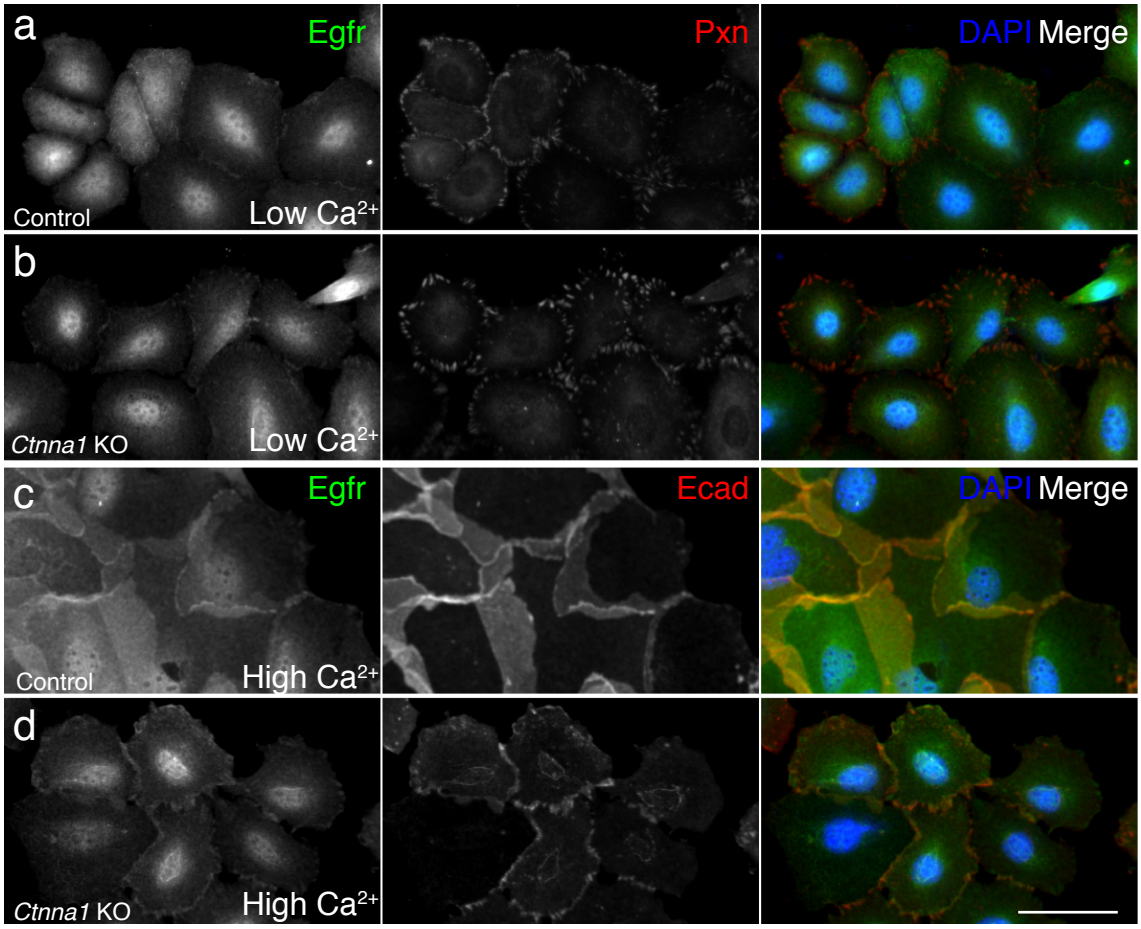

Figure 4.7 EGFR localization shifts to adherens junctions upon calcium switch in control but not *Ctnna1* cells. Wild-type (a) and Ctnna1 null (b) cells in low calcium stained for EGFR and paxillin to mark focal adhesions. Wild-type (c) and Ctnna1 null (d) cells after 24 hours in high calcium stained for EGFR and E-cadherin to mark adherens junctions. Note the colocalization of EGFR and E-cadherin in control but not Ctnna1 null cells in the high calcium conditions. Scale bar, 50 μm.

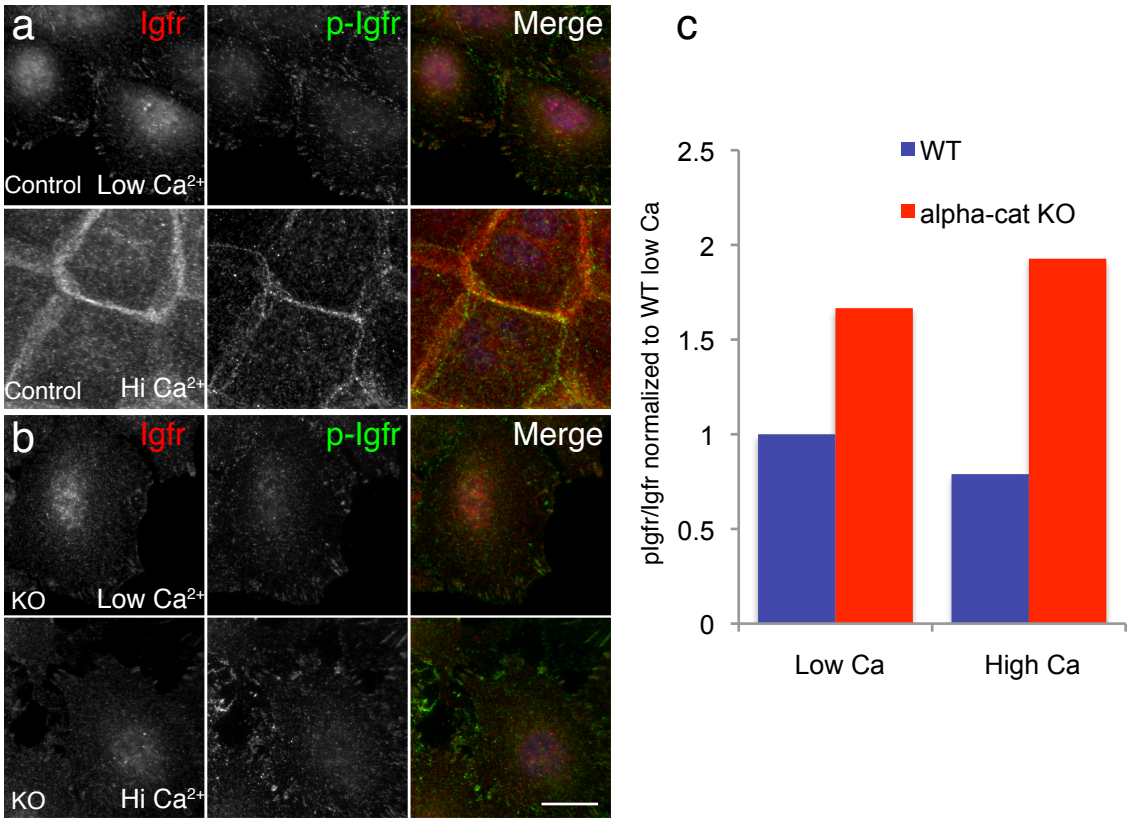

Figure 4.8 Calcium switch enhances the disparity in IGFR activation between control and *Ctnna1* null cells. (a) Representative image of wild-type cells in low and high calcium co-stained for phospho-IGFR and total IGFR. (b) Ctnna1 null cells in low and high calcium co-stained for phospho-IGFR and total IGFR. (c) Quantification of relative IGFR activity in both cell types in low and high calcium. Note the decrease in IGFR activity in wild-type but not Ctnna1 null cells upon calcium switch. Scale bar, 20 μm.

in part modulated by its localization and association with distinct adhesion types.

To test whether this difference in growth factor receptor localization was also observed *in vivo*, I performed whole mount immunofluorescence and microscopy on wild-type and *Ctnna1*-null E18.5 epidermis. In both control and *Ctnna1*-null cells, IGFR immunostaining could be detected in intracellular puncta (possibly endocytic vesicles) and at cell-cell borders. However, in control cells, the cell border staining colocalized with E-cadherin, while in the *Ctnna1*-null, IGFR staining was enriched at cell borders where E-cadherin staining was reduced (Figure 4.9a). The EGFR showed a similar pattern of colocalization with E-cadherin in control, but not *Ctnna1*-null tissues (Figure 4.9b). As the phospho-IGFR antibodies do not work in whole mount staining, I could not determine whether the altered localization corresponded with a change in activity *in vivo*, as was the case in cell culture. However, when taken together, these results suggest a possible mechanism for the enhancement of integrin signaling in the absence of α-catenin via the redistribution of growth factor receptors away from cell-cell junctions.

Effect of altered integrin signaling in the absence of α-catenin

Changes in integrin signaling have the potential to affect several downstream signaling pathways and cellular behaviors including cytoskeletal dynamics and survival signaling. To determine the effect on cytoskeletal dynamics, I analyzed membrane protrusion in cells growing out of control and *Ctnna1*-null explants by videomicroscopy. Membrane protrusion dynamics can

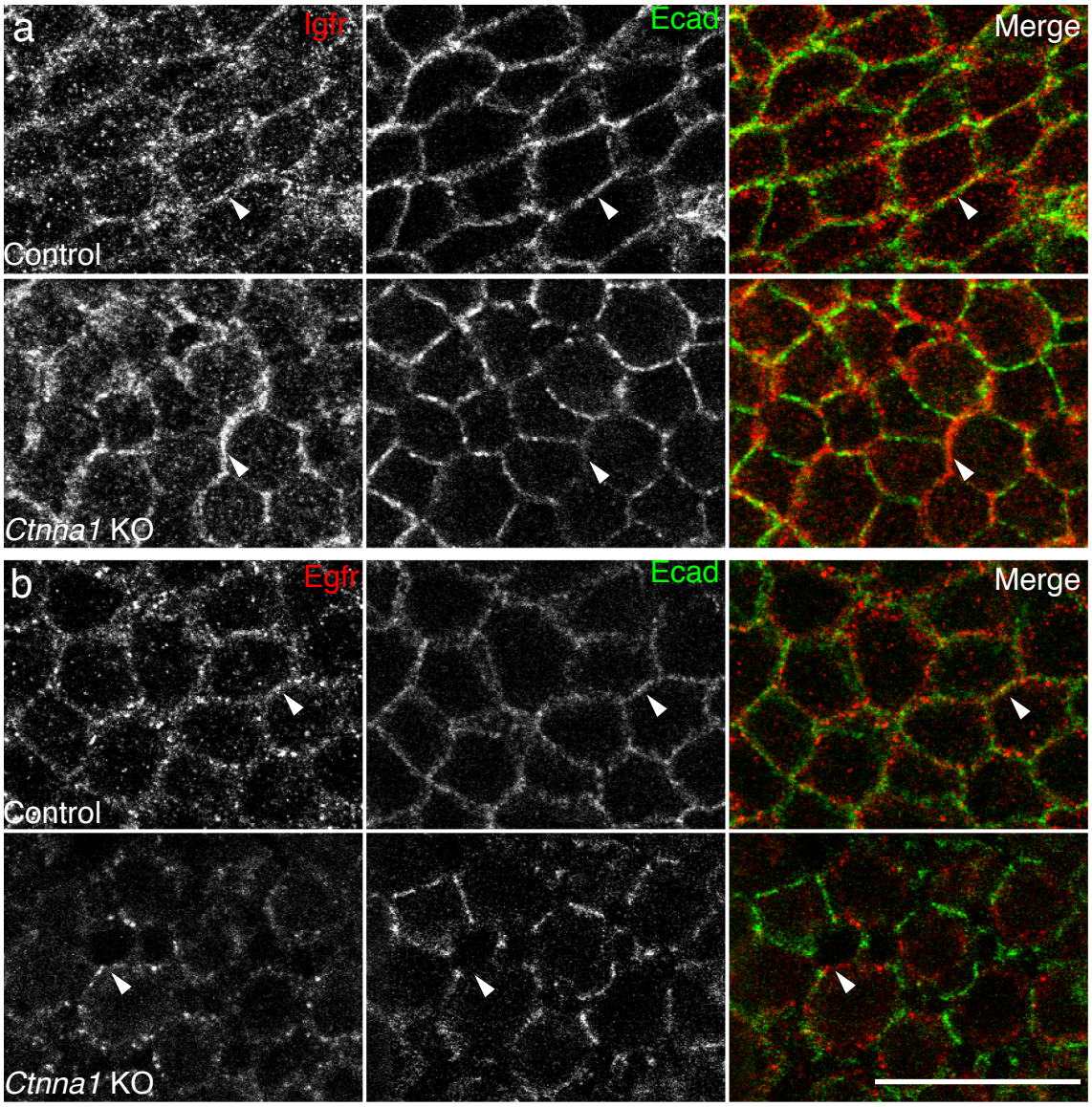

Figure 4.9 IGFR and EGFR localize near adherens junctions in control but not *Ctnna1* KO tissues in vivo. (a) Whole mount immunostaining of control and Ctnna1 epidermis at E18.5 with IGFR and E-cadherin. Confocal slice of basal layer cells is depicted. (b) Whole mount immunostaing of control and Ctnna1 epidermis at E18.5 with EGFR and E-cadherin. Scale bar, 20 μm.

act as a readout of actin cytoskeletal polymerization and Rac activity. Cells growing out of *Ctnna1*-null explants showed significant increases in both protrusion velocity (Figure 4.10a) and protrusion distance (Figure 4.10b), consistent with the increase in active Fak, Paxillin and Rac observed biochemically. A representative kymograph showing membrane protrusions over the course of 10-minute movies is shown in Figure 4.10c for wild-type and *Ctnna1*-null explants, illustrating the more dynamic nature of the membrane in the absence of α-catenin. This is also consistent with membrane dynamics in MDCK cells lacking α-catenin (Benjamin et al., 2010).

Signaling through Fak and Paxillin can also affect the MAPK signaling pathway by regulating Pak activity; Pak is an effector of Rac (as its phosphorylation activity is activated by association with active-Rac). It can become further activated via recruitment to phosphorylated Paxillin (Zhao et al., 2000). Activated Pak can also phosphorylate the MAP-kinase kinase Mek, leading to convergence with the MAPK signaling pathway (Slack-Davis et al., 2003). To test whether this might be taking place in the *Ctnna1*-null tissue, I performed immunoblots on lysates from control and *Ctnna1*-null tissue (Figure 4.10d). As expected, I observed an increase in Erk phosphorylation, as had previously been reported (Vasioukhin et al., 2001). Interestingly, I also observed an increase in Pak phosphorylation as well as an increase in Mek phosphorylation on the Pak target site (Figure 4.10e). Taken together, these results suggested that enhanced Pak signaling in the absence of α-catenin could result in both the increased membrane dynamics and MAPK signaling observed in the *Ctnna1* mutant tissue.

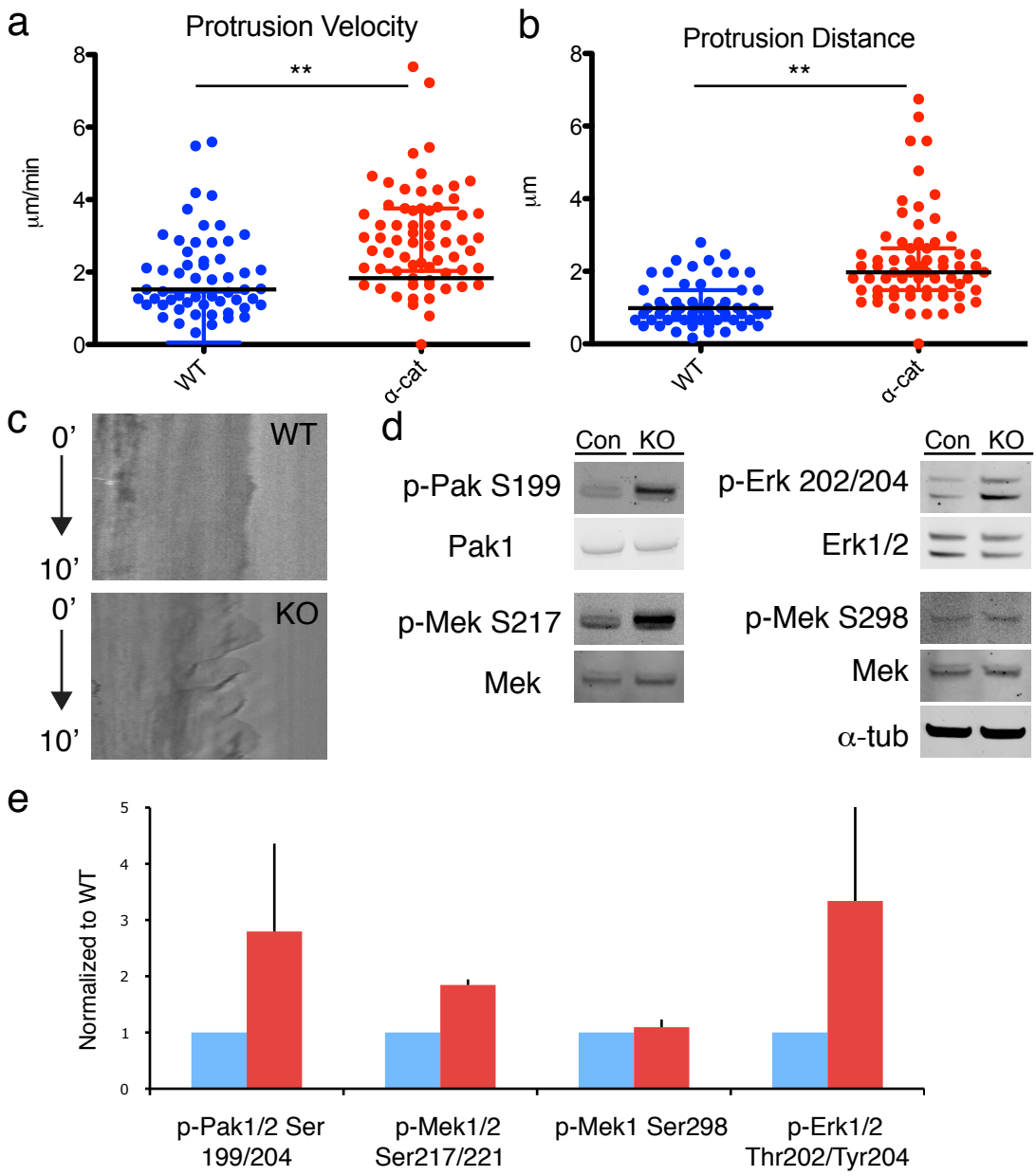

Figure 4.10 Increased membrane protrusion dynamics and Pak activation in Ctnna1 KO tissue relative to controls. Quantification of protrusion velocity (a) and protrusion distance (b) in cells growing out of control and Ctnna1 KO explants over 10 minutes. Black line marks median +/- interquartile range. Asterisks denote $p<0.01$. (c) Representative kymographs generated by drawing a line perpendicular to the membrane edge of control and Ctnna1 KO cells in 10 minute phase contrast recordings . Time is on Y axis and distance is on X axis. Protrusion kinetics were quantified by measuring the slope of the membrane edge. (d,e) Quantitative immunoblotting of lysates from control and KO skins.

To determine the importance of Pak signaling in these events, I took advantage of a recently developed chemical inhibitor of Pak activity, IPA-3 (Deacon et al., 2008) and cultured skin explants in its presence or absence. The explants were grown on fibronectin-coated glass-bottom dishes in an incubator-fluorescence microscope and were imaged over the course of 18 hours as keratinocytes grew out onto the dish surface. In wild-type explants treated with DMSO, as a control, the keratinocytes grew out as a cohesive sheet, whereas keratinocytes lacking α-catenin grew out as single cells (Figure 4.11a). Treatment of wild-type cells with 20μM IPA-3 slowed the migration of the epithelial sheet (quantified below), as would be expected due to the role of Pak in controlling cell migration and cytoskeletal dynamics. I was interested in assessing whether inhibition of Pak would reduce the migration of cells lacking α-catenin to a greater extent than control, due to their increased Pak activity and faster migration (quantified below). Surprisingly, treatment of *Ctnna1*-null explants with IPA-3 not only blocked keratinocyte outgrowth, but also induced the degeneration and death of the migrating keratinocytes. This suggested that in the absence of α-catenin, keratinocytes might be more sensitive to inhibition of the Pak signaling axis for their survival and migration.

To more carefully dissect these roles of focal adhesion signaling, I utilized keratinocyte culture, where loss of α-catenin also induces hyperactivation of Erk and Pak (Figure 4.11b,c). The mouse genome contains 3 Pak genes (Pak1-3); only Pak1 and 2 are expressed in the epidermis according to microarray data (Kobielak and Fuchs, 2006). These appear to have some common and some distinct functions, as Pak1 has been reported to mediate Erk activation through

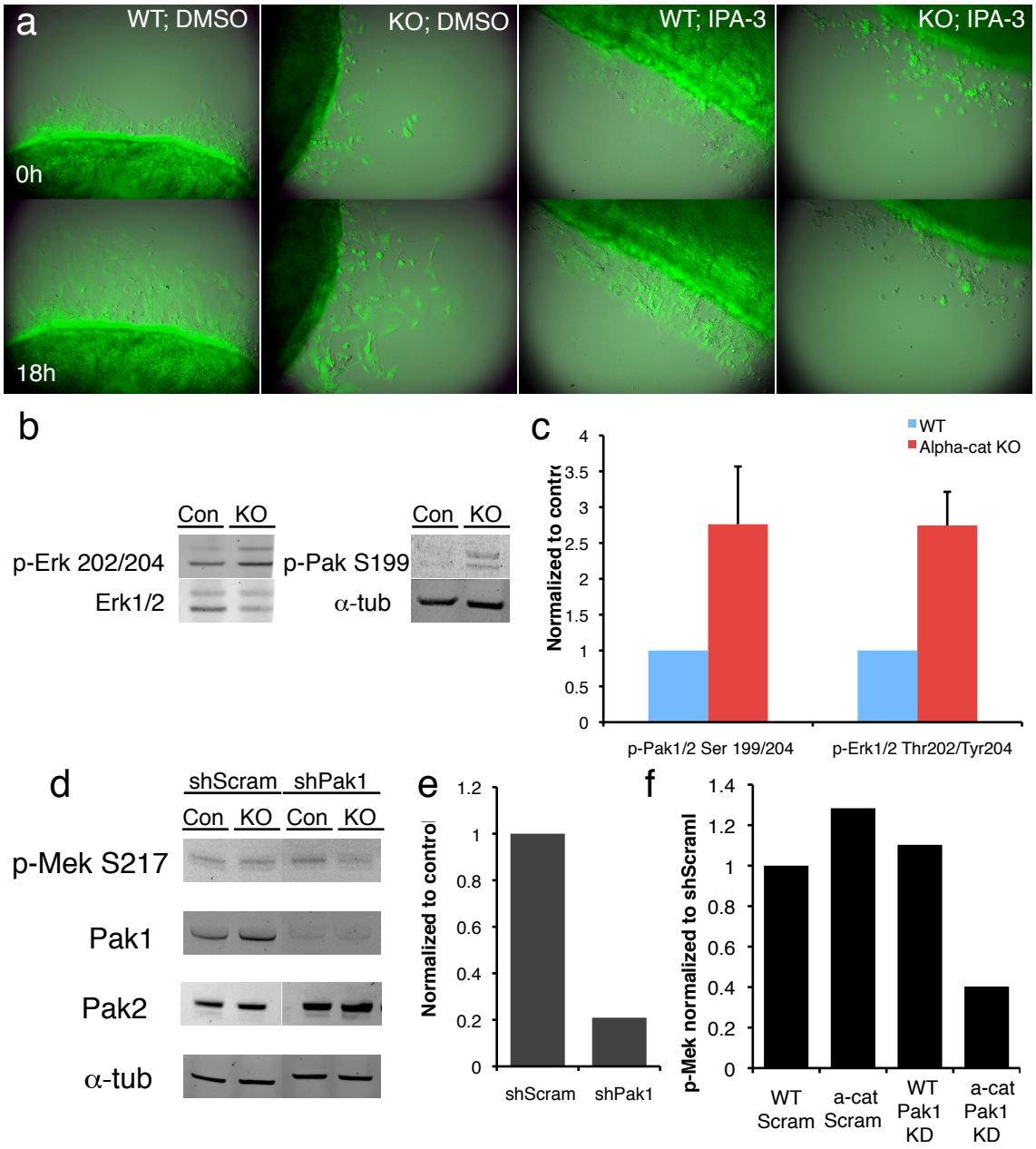

Figure 4.11 Ctnna1 KO cells are sensitized to inhibition of Pak signaling. (a) Frames from movies of control and Ctnna1 KO explant outgrowths treated with DMSO or 20 μM IPA-3. (b) Immunoblots of control and KO keratinocyte lysates probed for Erk and Pak activity. (c) Quantification of blots in (b). (d) Immunoblots showing Mek phosphorylation at S217 and Pak1 knockdown in keratinocytes. (e) Quantification of Pak1 knockdown in (d). (f) Quantification of Mek activity in (d).

phosphorylation of Mek on S217 (Wang et al., 2010). In contrast, Pak2 has been reported to act as a negative regulator of Myc and the actin depolymerizing factor Cofilin (Berta et al., 2010; Coniglio et al., 2008). Thus, Pak1 is a good candidate for mediating the increased Mek/Erk activation in the epidermis in the absence of α-catenin. Indeed, knockdown of Pak1 (Figure 4.11d,e) reduced Mek phosphorylation at S217 in *Ctnna1* keratinocytes by 60%, while Mek phosphorylation was not affected by Pak depletion in wild-type cells (Figure 4.11f).

Consistent with their divergent signaling targets, depletion of Pak1 and Pak2 produced different morphological consequences in cultured keratinocytes (Figure 4.12). While knockdown of Pak1 yielded thinner actin stress fibers in both wild-type and *Ctnna1*-null keratinocytes, knockdown of Pak2 increased stress fiber staining in both genotypes, consistent with its regulation of Cofilin. Fak depletion also resulted in an increase in stress fibers in both genotypes. This increase was consistent with previous analysis of Fak in keratinocytes (Schober et al., 2007). Importantly, none of these knockdowns rescued the defect in adherens junction formation in the absence of α-catenin, as it has been proposed that the defect in *Ctnna1-null* cells is due to increased actin dynamics that prevents the formation of stable adhesions between neighboring cells (Benjamin et al., 2010).

To directly assess the roles of Fak and Pak proteins in the context of a tissue, I again turned to the *in utero* lentiviral delivery system. After cloning the most efficient hairpins against Pak1 and Pak2 into the LV-Cre constructs and generating high-titer preparations (Chapter 2), I performed injections into the amniotic cavities of $r26^{Yfp/+}$ and $Ctnna1^{fl/fl}$; $r26^{Yfp/+}$ E9.5 embryos. I also took

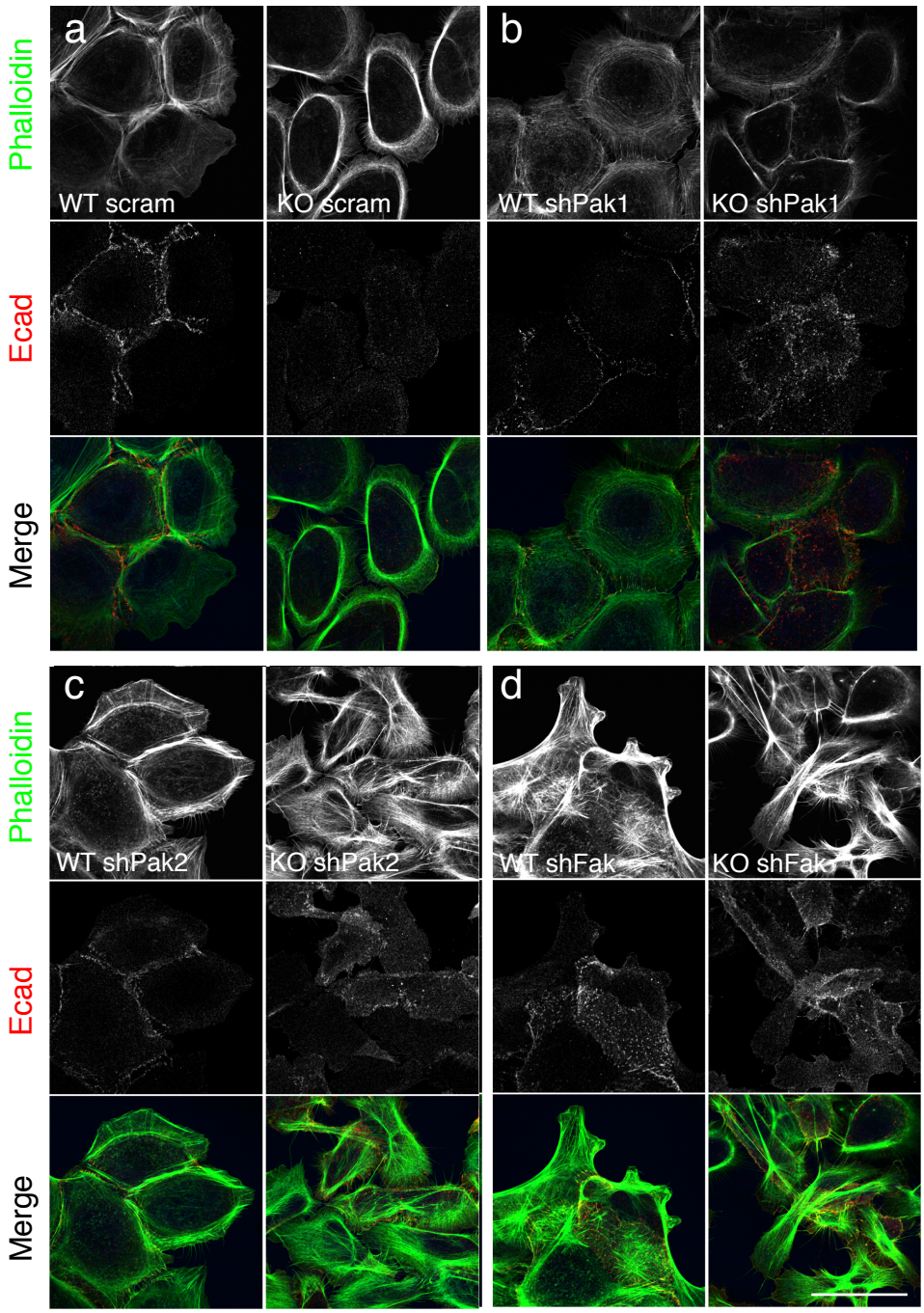

Figure 4.12 Morphological and cytoskeletal changes in keratinocytes upon depletion of Pak1, Pak2 or Fak. (a) Immunofluorescence of wild-type and Ctnna1-null keratinocytes infected with a scramble control hairpin after 3 hours in high calcium stained with phalloidin and E-cadherin to mark developing adherens junctions. (b) Cells as in (a), expressing a hairpin targeting Pak1. (c) Cells as in (a), expressing a hairpin targeting Pak2. (d) Cells as in (a) expressing a hairpin targeting Fak. Scale bar 50 μm.

advantage of the *Fak* $^{fl/fl}$ mice that are currently being studied in the laboratory, and crossed them to the *Ctnna1* ^{fl}; *r26* $^{Yfp/+}$ strain. As the use of lentiviral vectors eliminated the need crossing to K14-Cre transgenic lines, these mice could be produced in two rounds of mating, and can be maintained as triple homozygotes.

I first addressed the role of these focal adhesion signaling factors in the migration of keratinocytes out of a skin explant, as *Ctnna1*-null cells showed increased membrane dynamics and faster outgrowth than wild-type cells, and acute inhibition of Pak signaling with IPA-3 slowed wild-type migration. Depletion of neither Pak2 or Fak reduced the membrane protrusion distance of *Ctnna1*-expressing cells. While depletion on the *Ctnna1*-null background restored the elevated membrane protrusive activity of these cells back to control levels (Figure 4.13a). The experiment could not be performed with shPak1 explants due to technical difficulties.

To analyze the effect on explant outgrowth, tissue explants for each of the different genotypes and knockdown constructs were again monitored over an 18-hour growth period. During this time, wild-type and *Ctnna1*-null cells migrated an average of 164 μm and 270 μm respectively (Figure 4.13b, $p<0.001$). Depletion of Pak1 or Fak significantly reduced the migration of *r26* $^{Yfp/+}$ cells ($p<0.01$), while Pak2 also had a mild effect. This result was expected, based on the inhibitor experiment (Figure 4.11a) and the impaired explant outgrowth observed in the Fak mutant skin (Schober et al., 2007). Depletion of Pak1 or Fak on the *Ctnna1*-null background, however, had an even stronger effect and reduced their migration advantage; the outgrowth in these conditions did not

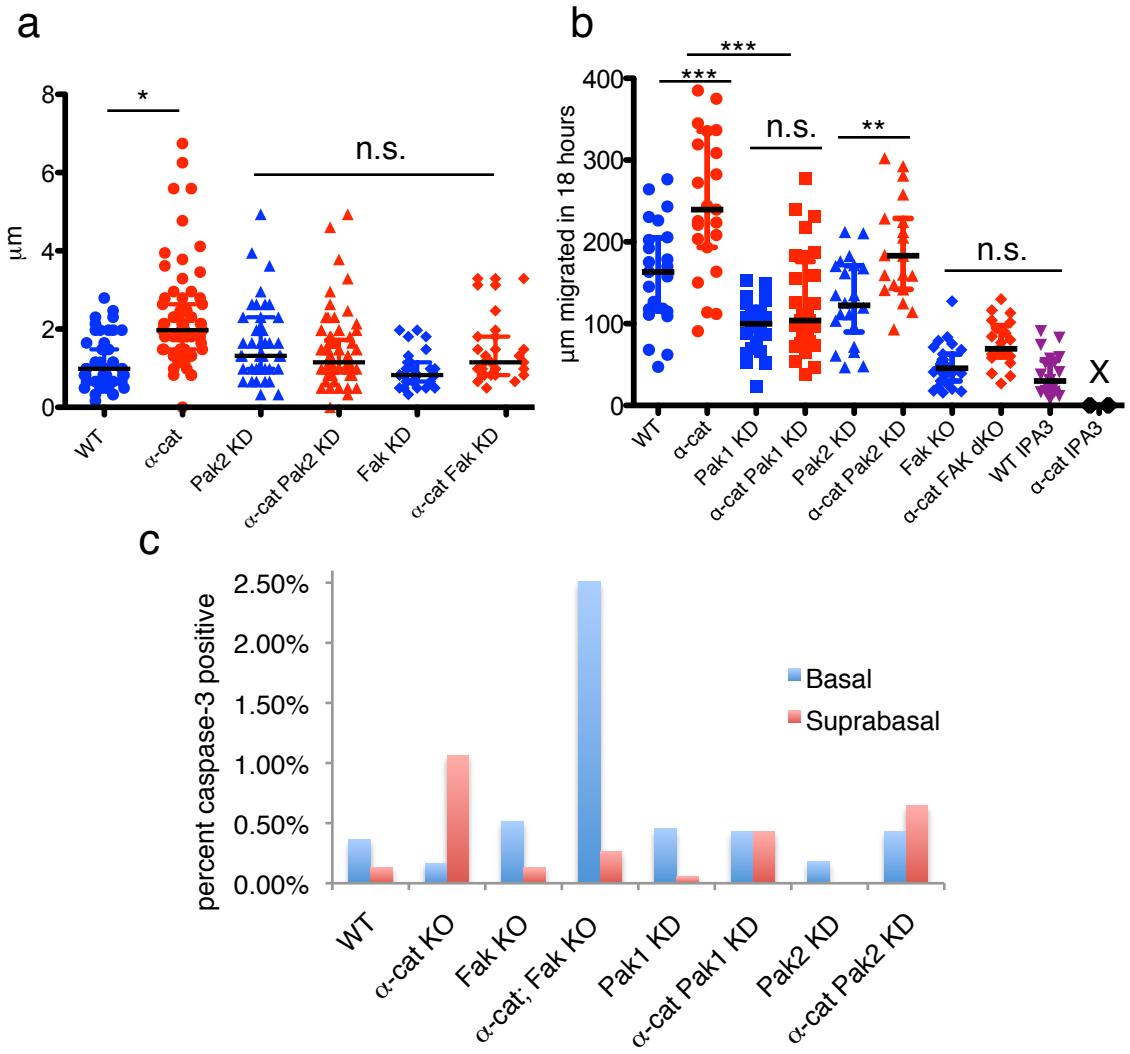

Figure 4.13 Concomitant depletion of focal adhesion signaling factors alters migration and apoptosis in the absence of α-catenin. (a) Quantification of membrane protrusion distance in growing explants in a 10-minute movie. (b) Quantification of explant outgrowth distance in explants over 18 hours under the listed conditions. IPA-3 denotes growth in the presence of 20 µM IPA-3 during imaging. There is no data for the Ctnna1 IPA-3 condition because treatment resulted in cell death. (a,b) Black line marks median +/- interquartile range. ***, p<0.001; **, p<0.01; *, p<0.05; ns, no significant difference. Significance between control and Ctnna1 null cells across knockdown conditions was quantified using two-way ANOVA and Tukey post-hoc tests. (c) Frequency of apoptotic cells, as marked by active caspase-3 in basal and suprabasal epidermal compartments. Note the reversal of apoptosis distribution upon deletion of Fak on the Ctnna1 null background.

significantly differ from then Pak1 or Fak ablation on the $r26^{Yfp/+}$ background alone. Taken together, these genetic interactions suggest that increased signaling through the Fak and Pak axis could account for the increased migration of *Ctnna1*-null cells out of an epithelial sheet.

Finally, in order to address the physiological effect of these genes on cell survival in the epidermis, I quantified the frequency of apoptotic cells in the basal and suprabasal layers of the epidermis across control and knockdown conditions. In wild-type epidermis, apoptotic cells were found primarily in the basal layer, and depletion of Fak, Pak1 or Pak2 did not alter this distribution. In the absence of α-catenin, the ratio was altered; apoptotic cells were more frequently observed in the suprabasal layer, and the basal layer exhibited less apoptosis than in wild-type. Ablation of Fak simultaneously with α-catenin resulted in a striking reversal of this pattern, with the majority of apoptotic cells localizing to the basal layer (Figure 4.13c). Depletion of Pak1 or Pak2 exerted a lesser effect, with an even proportion of basal and suprabasal apoptotic cells. Taken together, these results provide evidence for a role for focal adhesion signaling in maintaining the survival of basal layer cells in the absence of α-catenin.

Discussion

The ability to properly coordinate cell survival, adhesion and migration is of central importance for the development and maintenance of epithelial tissues while preventing cancerous overgrowth. My findings here suggest one possible mode for co-regulation of these pathways in the skin, depending on the presence of α-catenin at adherens junctions. I show that depletion of α-catenin from

embryonic epidermis rapidly induces alterations in tissue morphology, cytoskeletal organization and breaks between the basal and suprabasal layers. Additionally, I show that these breaks are associated with apoptotic cells in the suprabasal layer. I know that this cell death is at least in part dependent on TRP53 signaling (as discussed in Chapter 3), however, the exact mechanisms leading to induction of apoptosis remain to be determined. These cells may be undergoing "anoikis," defined as cell death due to loss of attachment (Desgrosellier and Cheresh, 2010).

However, the majority of the work on the subject has focused on death due to detachment from the extracellular matrix, and how apoptosis could be induced upon loss of cell-cell adhesion in stratified epithelia is not yet understood. For instance, reduction of PI3K and Akt signaling is commonly associated with anoikis. However, despite the fact that this pathway can be regulated by adherens junction assembly and disassembly, I did not detect changes in Akt phosphorylation in the *Ctnna1* mutant tissue. Other potential mechanisms for induction of cell death include changes in reactive oxygen species, Jun-kinase signaling and signaling through death receptor pathways (Frisch and Screaton, 2001). Future studies will be needed to determine how any of these pathways might contribute to the regulation of cell death upon loss of cell-cell adhesion.

The observation that the apoptosis in the *Ctnna1* mutant tissue is primarily found in suprabasal cells (as opposed to basal in wild-type tissue) correlated with the increased focal adhesion signaling also found in these mutants. If the death of *Ctnna1*-null cells occurs through common pathways to

anoikis, it would follow that elevated focal adhesion signaling could provide a strong protective, pro-survival signal that could override the pro-apoptotic signals from lost cell-cell adhesion.

One potential caveat of the experiment measuring Fak, Pak, Rac1 and Paxillin activity *in vivo* is that the analysis was performed on tissue lysates rather than FACS isolated keratinocytes based on YFP and integrin expression. This can allow for potential contamination by other cell types in the epidermis such as langerhans and merkel cells. Additionally, in the case of mosaic tissue, the effect may be dampened by the presence of wild-type cells. That said, the post-translational modifications I am measuring are quite unstable and hence could be rapidly lost by mechanical, enzymatic and FACS procedures. To minimize the confounding variables, I used tissue with equivalent levels of infection for protein analysis, such that any difference would likely be due to the absence of α-catenin. Thus, the measurements are likely to be an underestimate of the actual difference in signaling. This is also supported by the increased phospho-Fak immunofluorescence in the basal layer keratinocytes and by the increased migration and membrane protrusion of the mutant cells.

In searching for a mechanism for the increased focal adhesion signaling in the absence of α-catenin, I observed a change in the distribution of growth factor receptors in α-catenin null cells. Specifically, in wild-type cells, the IGF receptor colocalized with Paxillin at focal adhesion low under Ca^{2+} conditions, and was recruited to cell-cell junctions upon switching to high Ca^{2+}. The EGF receptor was similarly redistributed upon Ca^{2+} switch. However, in the absence of α-catenin, the redistribution did not occur and the IGFR was retained in focal adhesions.

Although focal adhesions cannot be seen in the epidermis *in vivo*, I observed colocalization between the growth factor receptors and E-cadherin in the wild-type but not *Ctnna1*-null tissue, suggesting evidence of a similar regulation. Growth factor receptors have previously been shown to interact with both focal adhesion and adherens junction components, but with different consequences: association with adherens junctions was shown to have an inhibitory effect on growth factor signaling, while interaction with focal adhesion proteins enhanced both growth factor and integrin signaling pathways (Qian et al., 2004; Slack-Davis et al., 2003). This is consistent with my observation of increased phospho-IGFR in *Ctnna1*-null cells relative to wild-type.

It remains to be seen whether inhibition of IGFR or EGFR signaling, whether by chemical inhibition in culture or *in vivo* lentiviral shRNA knockdown can restore the levels of focal adhesion signaling in *Ctnna1*-null cells back to wild-type levels. Interestingly, epidermal ablation of the insulin receptor and IGFR was recently shown to result in an 80% decrease in Rac1 activity and epidermal hypoplasia, thereby providing suggestive evidence for the interaction between these two pathways in the skin (Stachelscheid et al., 2008). Indeed, epidermal deletion of Rac1 results in reduced clonogenicity and migration, as well as an inhibition of tumor induction via oncogenic Ras (Benitah et al., 2005; Wang et al., 2010). These effects appear to be due to an impaired activation of Pak1 and subsequently Mek as measured by immunoblots, and inhibition or knockdown of these proteins impairs Ras-induced transformation. I observe an increased activation in all (Ras, Rac1, Pak, Mek, Erk) of these signaling proteins in the *Ctnna1* mutant tissue, corresponding with its increased tissue dysplasia

and progression to squamous cell carcinoma *in situ* (Kobielak and Fuchs, 2006). Additionally, I found that knockdown of Pak1 reduced Mek activation, suggesting that signaling through Pak1 may mediate the tumorigenicity and MAPK signaling of *Ctnna1*-null tissue as well.

To assess the role of the increased focal adhesion signaling in the absence of α-catenin, I depleted Fak, Pak1 or Pak2 on the control or *Ctnna1*-null background and assessed the tissues for changes in migration and cell survival. I found that depletion of any of these proteins significantly reduced the migratory outgrowth of keratinocytes from wild-type as well as *Ctnna1*-null skin explants. However, the effect of each knockdown was much stronger on the *Ctnna1*-null outgrowth, which had initially been significantly faster than control. Inhibition of Fak had the strongest effect, followed by Pak1 and then Pak2, which only yielded minor differences. The stronger effect of Fak ablation could be due to the fact that it is a complete knockout, rather than a knockdown as in the case of the Pak proteins. However, it is also possible that Fak deletion has a stronger effect due to some degree of functional redundancy between Pak1 and Pak2. Whether this is the case can be determined by simultaneous depletion of Pak1 and Pak2 using different color viral vectors to mark the doubly infected cells and assessing whether the migration rate is further reduced to the same extent as Fak deletion; these studies are currently underway. This possibility is supported by the fact that chemical inhibition of Pak1 and Pak2 by IPA-3 resulted in migration distances that were similar to Fak deletion on the *Ctnna1*-wild-type background.

The death of the *Ctnna1*-null keratinocytes upon treatment with IPA-3 also highlighted a role for Pak signaling in maintenance of cell survival. In agreement

with this, I found an equalization of basal and suprabasal apoptosis in the absence of -catenin upon knockdown of either Pak1 or Pak2. As was the case for migration, co-depletion of Fak had a more dramatic effect on apoptosis pattern, inducing a shift towards more basal cell death. Again, simultaneous depletion of Pak1 and Pak2 may reveal whether they function redundantly in this pathway, or whether Fak is a more potent regulator of cell survivor in the skin. Evidence in support of the latter comes from the recently described direct regulation of Trp53 by Fak: Fak can associate Trp53 and promote its ubiquitination and subsequent degradation (Lim et al., 2008). As Trp53 signaling is responsible for a significant portion of the apoptosis in the *Ctnna1* mutant, this mechanism may play a role in the protection of basal cells. In parallel with the control of cell survival, it will also be interesting to analyze the consequences of the Fak and Pak1/2 deletions on cell proliferation and relative tissue growth, using BrdU incorporation and the CGI assays (Chapter 2), respectively. The findings thus have implications for the treatment of the various epithelial cancers that show reduction of adherens junction signaling, as they may be more responsive to treatment with chemical inhibitors of Fak and Pak signaling due to their increased dependence on integrin signaling for survival.

Materials and Methods

Lentiviral vectors

Lentiviral vectors were based on the pLKO.1 shRNA plasmid from The RNAi Consortium library (Sigma). Lentiviral constructs containing the puromycin resistance cassette were screened for knockdown efficiency in cultured

keratinocytes, and the most efficient sequences were selected for use *in vivo*. The target sequences for hairpins described in the Results section are as follows:

shScram: CCTAAGGTTAAGTCGCCCTCG

shPak1-1003: CCGAAGAAAGAGCTGATTATT

shPak2-686: CGATGAAGAGATTATGGAGAA

For *in vivo* use, the hairpins were cloned into LV-Cre (described in the Methods section for Chapter 2) using *AgeI*/*EcoRI* restriction sites. Lentivirus production, concentration, and *in utero* microinjection was performed as described in the Methods section of Chapter 2.

Mice

The following mouse strains were used: CD1 (Charles River Laboratories), *Gt(ROSA)26Sor*$^{tm1(EYFP)Cos/+}$ referred to in the text as *r26*^{Yfp} (Jackson Laboratories, donated by A. McMahon); *Ctnna1*$^{lox/lox}$ and *Fak*$^{lox/lox}$(Beggs et al., 2003; Vasioukhin et al., 2001). *Ctnna1*$^{lox/lox}$ mice were bred with *r26*^{Yfp} and/or *Fak*$^{lox/lox}$ mice to produce males that were doubly or triply homozygous for the genotypes. These males were mated with *Ctnna1*$^{lox/lox}$ or *Fak*$^{lox/lox}$ females for LV-Cre mediated excision and/or shRNA knockdown. Each embryo was injected with 1.5 μl of lentivirus, and up to eight embryos were injected per litter. Surgical procedures were limited to 30 min for high survival rates. The Rockefeller University Animal Care and Use Committee approved animal experimentation protocols used in the study.

Tissue culture

Mouse keratinocytes were isolated as described in the Methods section of Chapter 2. Keratinocytes were maintained in culture in E-media containing 0.05 mM Ca^{2+} and supplemented with 15% serum. For viral infections, keratinocytes were plated in 12-well dishes at 70,000 cells per well and infected with lentivirus in the presence of polybrene (100 μg ml^{-1}) by centrifugation at 1100g for 30 minutes at 37°C. After centrifugation, infection media was replaced with fresh keratinocyte culture media. After 2 days of growth, keratinocytes were subjected to selection with puromycin (2 μg ml^{-1}), and subsequently processed for mRNA and protein analyses. For analysis of explant outgrowth, 3 mm punch biopsies were harvested from E18.5 embryos and plated onto glass-bottom dishes (MatTek) coated with fibronectin (10μg/ml). Explants were maintained in mixed Ca^{2+} (0.6mM) E-media to support intercellular adhesion and incubated 24–48 h. For IPA-3 experiments, explants were cultured in the presence of 20 μM IPA-3 (Sigma) dissolved in DMSO, or an equivalent volume of DMSO for control.

mRNA and protein quantification

Total RNA was isolated from FACS-sorted cells or cultured keratinocytes using the Absolutely RNA Microprep kit (Stratagene). cDNAs were generated from 1 μg of total RNA using oligo(dT) primers and SuperScript III First-Strand Synthesis System kit (Invitrogen). Real-Time PCR was performed using the LightCycler 480 System (Roche) and gene-specific and *Ppib* control primers. Data were analyzed and transcript levels established using LightCycler 480 Software (Roche). For immunoblotting, skins were snap-frozen in liquid nitrogen and

lysed in RIPA buffer (50 mM Tris-HCl, pH 7.4, 150 mM NaCl, 0.25% deoxycholic acid, 1% NP-40, 1 mM EDTA) supplemented with 2mM PMSF, Complete protease inhibitor tablets (Roche) and PhosStop phosphatase inhibitor tablets (Roche). Protein concentration was quantified using protein assay reagent (Bio-Rad Laboratories, Inc.) Equivalent amounts of protein were boiled in NuPage LDS sample buffer (Invitrogen), loaded onto NuPage Novex 4-12% gradient Bis-Tris gels (Invitrogen), transferred onto nitrocellulose membranes using the iBlot system (Invitrogen) and subjected to blotting in Odyssey blocking buffer (Li-Cor).

The following primary antibodies were used: rat α-tubulin (1:2000; Chemicon), mouse Fak (4.47, 1:1000; Millipore), Paxillin (5H11, 1:1000, Millipore), Mek1/2 (L38C12, 1:1000, Cell Signaling), phospho-Erk1/2 (Thr202/Tyr204) (1:1000, Santa Cruz); rabbit Erk1/2 (K-23, 1:1,000; Santa Cruz), Pak1 (N-20, 1:1000, Santa Cruz), pY397-Fak (1:1000, Cell Signaling), phospho-PAK1(Ser199/204)/PAK2(Ser192/197) (1:500, Cell Signaling), Pak2 (1:1000, Cell Signaling), pY31-Paxillin (1:1000, Invitrogen), phospho-Mek1 (Ser217)/Mek2(Ser221) (1:500, Cell Signaling), phospho-Mek1 (Ser298) (1:500, Cell Signaling). Secondary antibodies conjugated to IRDye 680 and 800 were used (1:10,000; Li-Cor). Protein levels were quantified using the Odyssey Infrared Imaging System (Li-Cor).

Immunofluorescence

Immunofluorescence and tissue processing was performed as described in the Methods section of Chapters 2 and 3. The following primary antibodies were used for immunostaining: chicken GFP (1:2,000; Abcam); rat Ecad (ECCD-1,

1:500; M. Takeichi), Nidogen (ELM1, 1:2,000; Santa Cruz), β4 integrin (1:300, BD), mouse Paxillin (5H11, 1:200 Millipore), phospho-Igf1R/InsR Tyr1131/Tyr1185 (JY202, 1:200, Upstate/Millipore), rabbit α1-catenin (C8114, 1:2,000; Sigma), Caspase 3 (AF835, 1:1,000; R&D), K5 (1:500; E. Fuchs), pY397-Fak (1:200, Cell Signaling), Igf1R (1:200, Santa Cruz), EgfR (1:200, Cell Signaling). Secondary antibodies were conjugated to Alexa-488 (Molecular Probes), Rhodamine Red-X, or Cy5 (Jackson Laboratories). F-actin was detected by Alexa-546 or Alexa-647 phalloidin (Molecular Probes) and nuclei were visualized using DAPI (1:2000, Sigma). Confocal images were captured by a scanning laser confocal microscope (LSM510 Meta; Carl Zeiss, Inc.) using C-Apochromat 40×/1.2 water lens or a 63x oil objective (n.a. 1.4). For quantification of Caspase-3 activation, epifluorescence images were acquired on a Zeiss Axioplan 2 microscope equipped with an OrcaER digital camera and using a 10x objective. Quantification of YFP and β4 integrin positive nuclei was performed using the Metamorph Multi-wavelength cell scoring module. Images were processed using Adobe Photoshop and panels were labeled in Adobe Illustrator CS5.

Videomicroscopy

For videomicroscopy of explant outgrowth, explants were visualized using an Olympus LCV110U Viva View incubator fluorescence microscope at set at 37°C and 5% CO_2. DIC and YFP fluorescence images were collected every 10 minutes for at least 18 hours. Outgrowth distance was quantified using Metamorph software by measuring the distance between the leading edge the keratinocyte sheet at the start of filming and after 18 hours (110 frames). At least 3 explants

were visualized for each condition, and multiple measurements were recorded for different sides of each explant.

For the measurement of membrane protrusion dynamics, explants were transferred into mixed Ca^{2+} (0.6mM) E-media containing 50 mM HEPES buffer, pH 7 and were imaged on an Olympus IX71 inverted microscope using phase contrast optics and a 40x air objective. Time-lapse images were acquired once every 3 seconds for 10 minutes, using a Hamamatsu Orca ER digital camera. A single YFP fluorescence image was also acquired for each movie to ascertain that the cells under analysis were infected. At least 6 movies, visualizing 3-6 cells were acquired for each condition. Kymographs were produced using Metamorph software by generating a montage of a 2-pixel line drawn perpendicular to the cell edge. The montage image represents membrane movement (x axis) over time (y axis). In these visualizations, membrane protrusions appear as peaks from left to right. Protrusion velocity, or rate of membrane extension, was calculated by the slope of peaks, and protrusion distance was defined as the maximum displacement of individual peaks.

Statistics

All quantitative data are expressed as mean ± standard deviation. Differences between two groups were assayed using Student t-test. Differences between multiple groups (for the explant migration experiments comparing control and *Ctnna1*-null +/- Fak or Pak1/2) were assessed with two-way ANOVA followed by Tukey post-hoc test, performed using Prism software (Graphpad). Migration data was plotted using Prism and represented as scatter plots showing median and interquartile range to illustrate population scatter.

CHAPTER 5: SUMMARY AND PERSPECTIVES

A key feature of epithelial tissues is their ability to coordinate cellular growth, survival, migration and differentiation to form and maintain three-dimensional epithelial structures. Central to this property is intercellular adhesion at adherens junctions, mediated by cadherin and catenin proteins. In addition to mechanically anchoring cells to their neighbors, adherens junctions also serve as signaling centers that intersect with diverse intracellular pathways that control the aforementioned cellular behaviors. While the adhesion functions of adherens junction proteins are better studied, their contribution to other signaling pathways is less well understood.

A variety of approaches have been utilized to probe the cellular mechanisms involved in coordinating these behaviors. These approaches include *in vitro* cell culture systems that enable rapid genetic manipulation, biochemistry and high throughput screening as well as *ex vivo* organ culture systems that allow for analysis and time-lapse imaging of cell behaviors in the context of a tissue. While these systems have significantly enriched our understanding of epithelial biology, they do not yet fully recapitulate all aspects of tissue morphogenesis, such as the impact of long range signaling from other organs in the body and the interaction with the vascular and immune systems. Conversely, the development of vertebrate and invertebrate animal models has enabled systematic analysis of the genetic underpinnings of organogenesis and tissue homeostasis. These *in vivo* systems come with their own set of advantages and disadvantages: while lower invertebrates such as *Drosophila* breed rapidly and are amenable to high throughput screening, their organ systems do not always

parallel human biology. Mammalian models such as mice are a closer representation of human biology, but are slow to breed, and thus can be costly and inefficient for exploratory studies.

In this work I have described a new methodology for rapid and non-invasive genetic manipulation of mouse epidermis *in vivo.* Additionally, I have used it to probe the cell autonomous downstream consequences of α-catenin deletion alone, and in combination with several signaling proteins that can regulate tissue growth. Both the methodology and the findings uncovered using the technique have numerous implications for our approaches to studying and understanding skin biology.

Applications and further development of the in utero epidermal targeting technology

Our proof of principle study focusing on α-catenin illustrated the utility of lentiviral vectors to target the epidermis *in utero*, as well as to alter expression of genes singly, in combination, and along with fluorescent reporter proteins such as GFP or YFP. I chose lentiviral vectors due to their ability to infect both dividing and non-dividing cells, in contrast to retroviral vectors, which require nuclear envelope breakdown to achieve stable integration into the host genome (Miller et al., 1990; Naldini et al., 1996). Genomic integration is an important feature for vectors used to target the epidermis, as the keratinocytes undergo many rounds of division, and genetic constructs that do not become integrated into, and replicate with, the host genome rapidly get diluted out (Ghazizadeh and Taichman, 2000). This is the case for adenoviral vectors and direct electroporation of DNA plasmids, both of which have successfully been used for *in utero* targeting in the central nervous system, where the cells divide less

frequently (Tabata and Nakajima, 2001). I was able to successfully infect $r26^{Yfp/+}$ and $r26^{LacZ/+}$ reporter mice with adenovirally expressed Cre, as the expression of the reporter genes in these mice can be permanently activated even with transient Cre expression. However, as the efficiency was lower as compared to the lentiviral constructs, and these vectors were not amenable to expression of shRNAs and other tagged proteins, I chose to focus on the lentiviral approach. It bears mentioning that adeno-associated viruses (AAV) are capable of integration into the host genome, but preferentially infect cells in S-phase of the cell cycle and have been reported to only poorly infect keratinocytes (Mühle et al., 2006). It is possible that this approach may eventually be optimized for keratinocyte infection, and could be used in addition to the lentiviral workflow.

A potential drawback of lentivirus, and other viral vectors that integrate into the host genome is potential disruption or activation of gene activity due to the random insertion of viral sequences. This issue was encountered in early gene therapy trials, where patients being treated for severe combined immunodeficiency developed leukemia due to viral integration near the LMO2 proto-oncogene (Hacein-Bey-Abina et al., 2003). I have looked for potential deleterious consequences in animals infected with control Scramble or LV-Cre viruses, by comparing them to uninjected littermates. However, over the 2 years that the technology has been widely adopted in our laboratory, no difference between these animals has yet been observed. It is possible that potential consequences of the insertional mutagenesis occur on a slower time scale than my mouse analysis. In the study mentioned above, the patients only developed symptoms 30-34 months after treatment, whereas the average mouse lifespan is

under two years and the majority of my research uses embryos or young mice. Thus, although future studies would be required to unequivocally address this issue, the consequences of random viral integration do not appear to have an observable effect in this system.

Another drawback of the lentiviral system in general is the relatively small packaging limit of lentiviral vectors compared to retrovirus or adenovirus (5kb vs. over 10kb, part of which contain viral packaging signals). (Kumar et al., 2001). For skin targeting, this severely limits the utility of an epidermis-specific promoter such as K14 due to its 2kb size, which leaves less than 1kb for expression of a protein of interest. Fortunately, analyses of periderm development and epidermal penetration of fluorospheres and virus revealed that epidermis-specific transduction could be achieved by intra-amniotic injection of embryos at E9.5. This alleviates the need for tissue specific promoters, and frees up space within the viral backbone for the inclusion of fluorescent reporters and, rescue constructs and other tagged proteins.

This combination of approaches has recently been used in our laboratory to probe the role of the protein LGN in asymmetric cell division in the epidermis by co-expressing an shRNA targeting endogenous LGN along with a full length or truncated LGN from the same viral construct (Williams et al., 2011). The rescue approach not only enabled the authors to eliminate the contribution of off-target effects, but also to gain insights into domain-specific contributions to the protein's function. This study also incorporated a GFP-expressing reporter of Notch transcriptional activity into the lentiviral H2B-RFP vector, further extending the utility of the system. Additionally, I have demonstrated that

epidermal cells can be co-transduced with up to four different viral constructs simultaneously, which can allow for the co-expression of genes that do not fit into a single viral vector.

In addition to the described uses of the *in utero* lentiviral transduction system, the viral vectors are easily amenable to further modification and customization for *in vivo* studies. For instance, the depletion of many genes, including α-catenin results in disruption of the epidermal barrier and epithelial morphology. Animals with high-level infection, and thus widespread depletion of these proteins, may die due to dehydration or an inability to eat, as occurs with the K14-Cre conditional mutants for similar genes. Using inducible shRNA expression could circumvent this lethality. This can be achieved by incorporating the tetracycline-inducible gene expression system into the lentiviral vector (Gossen and Bujard, 1992). Similarly, for studies using LV-Cre injection into a floxed or Cre reporter background, the use of tamoxifen-inducible Cre-ER can allow for regulation over the timing of Cre-mediated excision without the need for additional mating to the K14-CreER background (Vasioukhin et al., 1999).

Additionally, the Cre recombinase itself can also be tagged with a fluorescent protein, to eliminate the need for crossing floxed alleles onto a Cre reporter background. This approach, using a Cre-RFP fusion construct is currently being successfully used in our laboratory, and has demonstrated an excellent correlation between Cre-RFP expression and gene excision (Ezratty et al, submitted). Similarly, the same approach can be used to express miRNAs or fluorescently tagged markers of specific cellular compartments, such as primary cilia, focal adhesions etc.

An additional advantage of the lentiviral system is the development of several commercially available lentiviral libraries carrying shRNAs or shRNAmirs (shRNAs within a miRNA backbone) that target the majority of the mouse genome. A caveat of using shRNAs for gene depletion is the concern for off-target effects. I tried to control for this possibility in my studies by comparing to the complete knockout (as in the case of α-catenin), using multiple hairpins for each gene, or using previously characterized hairpins. I utilized the Mission shRNA library based on the pLKO.1 vector, which contains a puromycin resistance gene that I replaced with a variety of fluorescent proteins or Cre recombinase. However, other libraries are also currently available with a dual blasticidin/GFP cassette, which further simplifies the *in vivo* knockdown workflow by eliminating the need for cloning fluorescent proteins into the viral backbone for single gene analysis (OpenBiosystems). Furthermore, the use of commercially available lentiviral open reading frame (ORF) libraries (such as OpenBiosystems Lenti-ORF) can complement the loss-of-function shRNA or Cre approaches with ectopic expression or rescue studies. The availability of libraries also opens the door to increasing the throughput of *in vivo* gene analysis in the skin, whether systematic knockdown of single genes within a pathway, or by configuring pooled screens with a robust and appropriate readout. Efforts to test and develop these approaches are currently underway in our laboratory.

α-catenin in survival and cancer pathways

In addition to demonstrating the utility of *in utero* lentiviral transduction for studying the epidermis, my results have yielded new insights into the cell-autonomous consequences of α-catenin deletion in the context of a developing

tissue. I found that like the previously described K14-Cre conditional mutant, *Ctnna1*-null cells within a mosaic tissue displayed hyperproliferation and increased Ras-MAPK signaling. By simultaneously depleting both α-catenin and Hras or Erk1, I was able to demonstrate that the hyperproliferation is at least in part dependent upon the increased Ras-MAPK signaling, thereby identifying a functional genetic interaction between the genes *in vivo.* I also observed an increase in activation of the focal adhesion signaling pathway. As several components of this pathway (Fak, Pak1/2, Rac1) can synergize with signals downstream of growth factor receptors to potentiate Ras-MAPK signaling, it is possible that this mechanism can promote MAPK activation and cellular hyperproliferation in the absence of α-catenin. In preliminary support of this, I found an altered localization and apparent increase in activation of the IGF receptor at focal adhesions. This is consistent with the increased proliferation and MAPK activation of cultured *Ctnna1*-null keratinocytes in response insulin in the culture media (Vasioukhin et al., 2001). Depletion of Pak1 in *Ctnna1*-null keratinocytes cultured in insulin-rich media eliminated the hyperactivation of the MAPK kinase Mek, thereby placing Pak within this pathway. Whether this is also the case *in vivo*, and whether the other focal adhesion components are also required for the increased MAPK activation and hyperproliferation phenotype is currently under investigation.

During the last few months two new studies have reported additional links between α-catenin and growth signaling. The more recent study, from Fernando Camargo's group has identified α-catenin as a negative regulator of Yap1, a transcriptional effector of the Hippo growth control pathway

(Schlegelmilch et al., 2011). The authors demonstrate that α-catenin associates with phosphorylated (inactive) Yap1 via 14-3-3 and controls Yap1 activity by hindering its dephosphorylation by PP2A. They also find an increase in Yap1 activation in α-catenin deficient epidermis, and show that depletion of Yap1 in an α-catenin knockdown human keratinocyte cell line can reduce its hyperproliferation. Interestingly, they find that chemical inhibition of a variety of signaling pathways, including IGFR and MAPK did not alter the phosphorylation of Yap in keratinocytes, suggesting that these pathways may act in parallel downstream of α-catenin loss. It will be interesting to analyze the relative contributions of Yap1 and the IGFR-Pak-MAPK pathways to the growth of α-catenin deficient cells *in vivo.* Using the lentiviral knockdown system, this could be done by using the CGI assay to compare relative growth of Erk1, Pak1 and Yap1 depleted cells in control versus *Ctnna1*-null tissues. Alternatively, embryos simultaneously depleted of α-catenin and Yap1 could be analyzed for changes in BrdU incorporation by flow cytometry. Of course, caution must be taken in drawing conclusions from a comparison of shRNA knockdowns, as shRNA expression will likely not achieve a complete loss of the protein, and differences in knockdown efficiency may obscure the true contributions of the proteins to growth in the absence of α-catenin.

Interestingly, another recent study reported a direct association between α-catenin and NF2, a FERM domain tumor suppressor also known as Merlin that is mutated in the familial cancer syndrome neurofibromatosis type-2 (Gladden et al., 2010). α-catenin appears to recruit Merlin to cell-cell junctions, and depletion of Merlin results in a destabilization of cadherin-based adhesions and loss of

contact-inhibition of proliferation due to increased growth factor RTK and Rac1 activity (Curto et al., 2007; Okada et al., 2005). Additionally, Merlin can be regulated by and act as a negative regulator of Pak1/2 through a feedback loop. Active (non-phosphorylated) Merlin can bind Pak1 and inhibit its recruitment to focal adhesions, whereas this localization is enhanced in the absence of Merlin (Kissil et al., 2003). These facts are intriguing in light of my observation of the hyperactivation of these Pak and Rac1 in the α-catenin null cells.

It is possible that the absence of α-catenin in keratinocytes results in a retention of Merlin in its inactive state, which can thus contribute to the increased IGFR, Rac and Pak activity that I observe. As these proteins can then lead to MAPK activation through phosphorylation of Mek, it is possible inactivation of Merlin in the absence of α-catenin can reinforce the pro-proliferative signaling through convergence of these pathways. This notion can be tested by analyzing the phosphorylation status of Merlin in the absence of α-catenin, and by using the lentiviral targeting system to express a constitutively active, non-phophorylatable form of Merlin on the control and *Ctnna1*-null backgrounds.

Also intriguing is the fact that Merlin has been reported to act as a negative regulator of the Hippo signaling pathway, upstream of Yap (Zhang et al., 2010). This was first shown in *Drosophila*, and more recently in mammalian tissue (Hamaratoglu et al., 2006). This suggests the possibility of an additional mechanism of Yap regulation downstream of α-catenin via negative regulation of Merlin, in addition to the 14-3-3-mediated mechanism posited by Caramago's group (Schlegelmilch et al., 2011). These α-catenin specific mechanisms can

provide some explanation for the difference in phenotypes of E- and P-cadherins or α-catenin in the skin, where cadherin depletion also induces tissue dysplasia, but does not appear to lead to proliferation. Taken together, these studies suggest the notion of a complex signaling network, altered upon loss of α-catenin that impinges upon cytoskeletal regulators, and results in potentiation of growth factor and Ras-Mapk signaling. To what extent these pathways intersect or occur in parallel remains to be elucidated.

An additional feature of α-catenin depleted tissue is the increased propensity towards apoptotic cell death, which I find to be specific to the first suprabasal layer. Indeed, I found less apoptosis within the basal layer of *Ctnna1*-null tissues as compared to the control, where apoptotic cells localized primarily to the basal layer. Importantly, I found that depletion of Fak or Pak1 proteins eliminated this protection of basal layer cells from apoptosis, consistent with their roles in cell survival signaling and hyperactivation in the absence of α-catenin. Based on the studies described above, it would be interesting to test whether increased activation of Yap signaling might also play a role in maintaining basal cell survival, as it has previously been shown to negatively regulate apoptosis (Zhang et al., 2011). In light of my observations on the suprabasal bias of apoptosis upon α-catenin deletion, it is tempting to speculate that loss of α-catenin may produce a different effect on non-stratified tissues, where despite destabilization of cell-cell adhesion, all of the cells in the sheet would retain contact with the extracellular matrix and thus exposure to survival signals. In support of this notion, deletion of α-catenin in the cerebral cortex was shown to cause less apoptosis (Lien et al., 2006).

Using the CGI assay, I found that despite the observed hyperproliferation, the net effect of α-catenin loss is a significant growth disadvantage relative to control wild-type cells due to the increase in apoptosis. The measured increase in Trp53 transcriptional target expression as well as the partial rescue of apoptosis frequency and CGI upon concomitant depletion of Trp53 indicated that Trp53 activity was at least in part responsible for the increase in apoptosis. An increase in apoptosis was also observed upon ablation of epidermal E- and P-cadherins (Tinkle et al., 2008). This suggests that while the increased MAPK and hyperproliferation appear to be specific to α-catenin, the predisposition towards apoptosis may be a general consequence of disruption of cell-cell adhesion. It would be interesting to see whether the location of apoptotic cells is also overwhelmingly suprabasal in the E-cad/P-cad mutant epidermis as in the α-catenin mutants. Similarly, whether these animals show hyperactivation of focal adhesion signaling can serve as an indicator as to whether activation of that pathway results simply from loss of adherens junctions or via an α-catenin-specific mechanism. The dependence of apoptosis on Trp53 can also be compared in these animals. Studies in other tissues would suggest that some dependence on Trp53 is quite likely: conditional deletion of E-cadherin from the mammary gland induces apoptosis and degeneration, while inactivation of both E-cadherin and Trp53 induces metastatic lobular carcinoma (Boussadia et al., 2002; Derksen et al., 2006).

The proclivity towards apoptosis in the absence of genes commonly characterized as tumor suppressors appears to be a common theme in epithelial cancers. Like the α-catenin mutant tissue, epidermal-specific deletion of the TGF-

β receptor II (TβRII) induces an increase in both proliferation and apoptosis. These opposing alterations are able restore epidermal homeostasis and the mutant mice do not develop tumors in the backskin epidermis (Guasch et al., 2007). Only upon further changes, such as expression of constitutively active Ras or treatment with DNA-mutagenizing agents do epidermal tumors develop. In further parallel to the α-catenin mutant tissue, epidermis lacking TβRII shows elevated focal adhesion kinase signaling, which corresponds with the increased migration rate of the TβRII KO keratinocytes. Due to the high level of crosstalk between focal adhesion and growth signaling described above, this effect may be related to the elevated proliferation in these cells.

Indeed, increased expression or activation of Fak as well as Pak is commonly found in a variety of human carcinomas (Owens et al., 1995). Deletion of Fak in mouse models of breast, colon and other cancers have shown a requirement for Fak in tumorigenesis induced by Ras activation (Luo et al., 2009; Pylayeva et al., 2009). Deletion of Fak induced apoptotic cell death in mammary gland tissue transformed with the polyoma middle T oncoprotein (PyMT), whereas wild-type tissue was unaffected. Such studies highlight a potential increased dependence on Fak signaling for survival upon destabilization of epithelial homeostasis. I observed a similar effect in the epidermis, where removal of Fak drastically increased basal apoptosis in the *Ctnna1*-null epidermis but not the wild-type tissue. Tumorigenesis studies of the *Ctnna1*-null and *Ctnna1*/*Fak* double mutants can extend this functional interaction and determine whether deletion of Fak is also inhibitory to tumorigenesis induced by loss of α-catenin. As I have shown that focal deletion of α-catenin alone induces a net loss

of the mutant cells rather than tumor formation, tumorigenesis must be induced by an additional mechanism, such as treatment with tumor promoting agents or concomitant removal of Trp53. Using the *in utero* lentiviral targeting system, such an endeavor can be achieved within months, as the mice do not need to be mated onto a K14-Cre transgenic background, but can use LV-Cre or LV-Cre-ER instead. Additionally, it will be interesting to see whether there is a correlation between α-catenin loss and Fak or Pak activity in human tumors by analysis of human cancer tissue arrays. Perhaps if an increased dependency on focal adhesion signaling might be a common feature of tumors with reduced adherens junction components, these tumors might be more susceptible than other tumors to treatment with the chemical inhibitors of Fak and Pak currently under development to treat cancer metastasis. Thus, screening for α-catenin expression can be incorporated into the growing field of personalized medicine in cancer.

The work presented here has contributed a new methodology for research into both simple and complex genetic pathways in epidermal biology and yielded new insights into the roles of cell-cell and cell-matrix adhesion in epidermal development and homeostasis. It is hoped that these studies further add to our mammalian *in vivo* toolbox and open new avenues of research into the crosstalk between cell-cell adhesion, cell-matrix adhesion and cell survival in tissue growth and disease.

REFERENCES

Abe, K., and Takeichi, M. (2008). EPLIN mediates linkage of the cadherin catenin complex to F-actin and stabilizes the circumferential actin belt. Proc Natl Acad Sci USA *105*, 13-19.

Adams, C.L., Chen, Y.T., Smith, S.J., and Nelson, W.J. (1998). Mechanisms of epithelial cell-cell adhesion and cell compaction revealed by high-resolution tracking of E-cadherin-green fluorescent protein. J Cell Biol *142*, 1105-1119.

Adams, C.L., Nelson, W.J., and Smith, S.J. (1996). Quantitative analysis of cadherin-catenin-actin reorganization during development of cell-cell adhesion. J Cell Biol *135*, 1899-1911.

Alonso, L., and Fuchs, E. (2006). The hair cycle. J Cell Sci *119*, 391-393.

Anastasiadis, P.Z., Moon, S.Y., Thoreson, M.A., Mariner, D.J., Crawford, H.C., Zheng, Y., and Reynolds, A.B. (2000). Inhibition of RhoA by p120 catenin. Nat Cell Biol *2*, 637-644.

Andl, T., Reddy, S.T., Gaddapara, T., and Millar, S.E. (2002). WNT signals are required for the initiation of hair follicle development. Dev Cell *2*, 643-653.

Asselineau, D., Bernard, B.A., Bailly, C., and Darmon, M. (1989). Retinoic acid improves epidermal morphogenesis. Dev Biol *133*, 322-335.

Backman, M., Machon, O., Mygland, L., van den Bout, C.J., Zhong, W., Taketo, M.M., and Krauss, S. (2005). Effects of canonical Wnt signaling on dorso-ventral specification of the mouse telencephalon. Dev Biol *279*, 155-168.

Bajpai, S., Feng, Y., Krishnamurthy, R., Longmore, G.D., and Wirtz, D. (2009). Loss of alpha-catenin decreases the strength of single E-cadherin bonds between human cancer cells. J Biol Chem *284*, 18252-18259.

Beggs, H.E., Schahin-Reed, D., Zang, K., Goebbels, S., Nave, K.A., Gorski, J., Jones, K.R., Sretavan, D., and Reichardt, L.F. (2003). FAK deficiency in cells contributing to the basal lamina results in cortical abnormalities resembling congenital muscular dystrophies. Neuron *40*, 501-514.

Bello, B., Resendez-Perez, D., and Gehring, W.J. (1998). Spatial and temporal targeting of gene expression in Drosophila by means of a tetracycline-dependent transactivator system. Development *125*, 2193-2202.

Benitah, S.A., Frye, M., Glogauer, M., and Watt, F.M. (2005). Stem cell depletion through epidermal deletion of Rac1. Science *309*, 933-935.

Benjamin, J.M., Kwiatkowski, A.V., Yang, C., Korobova, F., Pokutta, S., Svitkina, T., Weis, W.I., and Nelson, W.J. (2010). AlphaE-catenin regulates actin dynamics independently of cadherin-mediated cell-cell adhesion. J Cell Biol *189*, 339-352.

Benjamin, J.M., and Nelson, W.J. (2008). Bench to bedside and back again: molecular mechanisms of alpha-catenin function and roles in tumorigenesis. Semin Cancer Biol *18*, 53-64.

Beronja, S., Livshits, G., Williams, S., and Fuchs, E. (2010). Rapid functional dissection of genetic networks via tissue-specific transduction and RNAi in mouse embryos. Nat Med *16*, 821-827.

Berrier, A.L., and Yamada, K.M. (2007). Cell-matrix adhesion. J Cell Physiol *213*, 565-573.

Berta, M.A., Baker, C.M., Cottle, D.L., and Watt, F.M. (2010). Dose and context dependent effects of Myc on epidermal stem cell proliferation and differentiation. EMBO Mol Med *2*, 16-25.

Bier, E. (2005). Drosophila, the golden bug, emerges as a tool for human genetics. Nat Rev Genet *6*, 9-23.

Bilder, D., Li, M., and Perrimon, N. (2000). Cooperative regulation of cell polarity and growth by Drosophila tumor suppressors. Science *289*, 113-116.

Bishop, A.L., and Hall, A. (2000). Rho GTPases and their effector proteins. Biochem J *348 Pt 2*, 241-255.

Blanpain, C., and Fuchs, E. (2006). Epidermal stem cells of the skin. Annu Rev Cell Dev Biol *22*, 339-373.

Blanpain, C., Lowry, W.E., Geoghegan, A., Polak, L., and Fuchs, E. (2004). Self-renewal, multipotency, and the existence of two cell populations within an epithelial stem cell niche. Cell *118*, 635-648.

Blanpain, C., Lowry, W.E., Pasolli, H.A., and Fuchs, E. (2006). Canonical notch signaling functions as a commitment switch in the epidermal lineage. Genes Dev *20*, 3022-3035.

Boller, K., Vestweber, D., and Kemler, R. (1985). Cell-adhesion molecule uvomorulin is localized in the intermediate junctions of adult intestinal epithelial cells. J Cell Biol *100*, 327-332.

Bonifas, J.M., Rothman, A.L., and Epstein, E.H. (1991). Epidermolysis bullosa simplex: evidence in two families for keratin gene abnormalities. Science *254*, 1202-1205.

Boudreau, N., Sympson, C.J., Werb, Z., and Bissell, M.J. (1995). Suppression of ICE and apoptosis in mammary epithelial cells by extracellular matrix. Science *267*, 891-893.

Boussadia, O., Kutsch, S., Hierholzer, A., Delmas, V., and Kemler, R. (2002). E-cadherin is a survival factor for the lactating mouse mammary gland. Mech Dev *115*, 53-62.

Braga, V.M., Betson, M., Li, X., and Lamarche-Vane, N. (2000). Activation of the small GTPase Rac is sufficient to disrupt cadherin-dependent cell-cell adhesion in normal human keratinocytes. Mol Biol Cell *11*, 3703-3721.

Braga, V.M., Machesky, L.M., Hall, A., and Hotchin, N.A. (1997). The small GTPases Rho and Rac are required for the establishment of cadherin-dependent cell-cell contacts. J Cell Biol *137*, 1421-1431.

Brand, A.H., and Perrimon, N. (1993). Targeted gene expression as a means of altering cell fates and generating dominant phenotypes. Development *118*, 401-415.

Braren, R., Hu, H., Kim, Y.H., Beggs, H.E., Reichardt, L.F., and Wang, R. (2006). Endothelial FAK is essential for vascular network stability, cell survival, and lamellipodial formation. J Cell Biol *172*, 151-162.

Brinster, R.L., Chen, H.Y., Warren, R., Sarthy, A., and Palmiter, R.D. (1982). Regulation of metallothionein--thymidine kinase fusion plasmids injected into mouse eggs. Nature *296*, 39-42.

Brown, M.C., and Turner, C.E. (2004). Paxillin: adapting to change. Physiol Rev *84*, 1315-1339.

Brumby, A.M., and Richardson, H.E. (2003). scribble mutants cooperate with oncogenic Ras or Notch to cause neoplastic overgrowth in Drosophila. EMBO J *22*, 5769-5779.

Bullions, L.C., Notterman, D.A., Chung, L.S., and Levine, A.J. (1997). Expression of wild-type alpha-catenin protein in cells with a mutant alpha-

catenin gene restores both growth regulation and tumor suppressor activities. Mol Cell Biol *17*, 4501-4508.

Byrne, C., Tainsky, M., and Fuchs, E. (1994). Programming gene expression in developing epidermis. Development *120*, 2369-2383.

Cance, W.G., Harris, J.E., Iacocca, M.V., Roche, E., Yang, X., Chang, J., Simkins, S., and Xu, L. (2000). Immunohistochemical analyses of focal adhesion kinase expression in benign and malignant human breast and colon tissues: correlation with preinvasive and invasive phenotypes. Clin Cancer Res *6*, 2417-2423.

Cano, A., Pérez-Moreno, M.A., Rodrigo, I., Locascio, A., Blanco, M.J., del Barrio, M.G., Portillo, F., and Nieto, M.A. (2000). The transcription factor snail controls epithelial-mesenchymal transitions by repressing E-cadherin expression. Nat Cell Biol *2*, 76-83.

Canonici, A., Steelant, W., Rigot, V., Khomitch-Baud, A., Boutaghou-Cherid, H., Bruyneel, E., Van Roy, F., Garrouste, F., Pommier, G., and André, F. (2008). Insulin-like growth factor-I receptor, E-cadherin and alpha v integrin form a dynamic complex under the control of alpha-catenin. Int J Cancer *122*, 572-582.

Carmeliet, P., Lampugnani, M.G., Moons, L., Breviario, F., Compernolle, V., Bono, F., Balconi, G., Spagnuolo, R., Oosthuyse, B., Dewerchin, M., *et al.* (1999). Targeted deficiency or cytosolic truncation of the VE-cadherin gene in mice impairs VEGF-mediated endothelial survival and angiogenesis. Cell *98*, 147-157.

Castilho, R.M., Squarize, C.H., Patel, V., Millar, S.E., Zheng, Y., Molinolo, A., and Gutkind, J.S. (2007). Requirement of Rac1 distinguishes follicular from interfollicular epithelial stem cells. Oncogene *26*, 5078-5085.

Cavallaro, U., and Christofori, G. (2004). Cell adhesion and signalling by cadherins and Ig-CAMs in cancer. Nat Rev Cancer *4*, 118-132.

Chen, Q., Lin, T.H., Der, C.J., and Juliano, R.L. (1996). Integrin-mediated activation of MEK and mitogen-activated protein kinase is independent of Ras [corrected]. J Biol Chem *271*, 18122-18127.

Chiang, C., Swan, R.Z., Grachtchouk, M., Bolinger, M., Litingtung, Y., Robertson, E.K., Cooper, M.K., Gaffield, W., Westphal, H., Beachy, P.A., *et al.* (1999). Essential role for Sonic hedgehog during hair follicle morphogenesis. Dev Biol *205*, 1-9.

Chrostek, A., Wu, X., Quondamatteo, F., Hu, R., Sanecka, A., Niemann, C., Langbein, L., Haase, I., and Brakebusch, C. (2006). Rac1 is crucial for hair follicle integrity but is not essential for maintenance of the epidermis. Mol Cell Biol *26*, 6957-6970.

Clayton, E., Doupé, D.P., Klein, A.M., Winton, D.J., Simons, B.D., and Jones, P.H. (2007). A single type of progenitor cell maintains normal epidermis. Nature *446*, 185-189.

Clevers, H. (2006). Wnt/beta-catenin signaling in development and disease. Cell *127*, 469-480.

Collado, M., Gil, J., Efeyan, A., Guerra, C., Schuhmacher, A.J., Barradas, M., Benguría, A., Zaballos, A., Flores, J.M., Barbacid, M., *et al.* (2005). Tumour biology: senescence in premalignant tumours. Nature *436*, 642.

Coniglio, S.J., Zavarella, S., and Symons, M.H. (2008). Pak1 and Pak2 mediate tumor cell invasion through distinct signaling mechanisms. Mol Cell Biol *28*, 4162-4172.

Copp, A.J., Greene, N.D.E., and Murdoch, J.N. (2003). The genetic basis of mammalian neurulation. Nat Rev Genet *4*, 784-793.

Cotsarelis, G., Sun, T.T., and Lavker, R.M. (1990). Label-retaining cells reside in the bulge area of pilosebaceous unit: implications for follicular stem cells, hair cycle, and skin carcinogenesis. Cell *61*, 1329-1337.

Coulombe, P.A., Hutton, M.E., Letai, A., Hebert, A., Paller, A.S., and Fuchs, E. (1991). Point mutations in human keratin 14 genes of epidermolysis bullosa simplex patients: genetic and functional analyses. Cell *66*, 1301-1311.

Cowin, P., Rowlands, T.M., and Hatsell, S.J. (2005). Cadherins and catenins in breast cancer. Curr Opin Cell Biol *17*, 499-508.

Cox, R.T., Kirkpatrick, C., and Peifer, M. (1996). Armadillo is required for adherens junction assembly, cell polarity, and morphogenesis during Drosophila embryogenesis. J Cell Biol *134*, 133-148.

Curto, M., Cole, B.K., Lallemand, D., Liu, C.-H., and McClatchey, A.I. (2007). Contact-dependent inhibition of EGFR signaling by Nf2/Merlin. J Cell Biol *177*, 893-903.

Damiano, L., Stefano, P.D., Leal, M.P.C., Barba, M., Mainiero, F., Cabodi, S., Tordella, L., Sapino, A., Castellano, I., Canel, M., *et al.* (2010). p140Cap dual regulation of E-cadherin|[sol]|EGFR cross-talk and Ras signalling in tumour cell scatter and proliferation. Oncogene *29*, 3677.

Danen, E.H.J., and Sonnenberg, A. (2003). Integrins in regulation of tissue development and function. J Pathol *201*, 632-641.

Davis, M.A., Ireton, R.C., and Reynolds, A.B. (2003). A core function for p120-catenin in cadherin turnover. J Cell Biol *163*, 525-534.

Davis, M.A., and Reynolds, A.B. (2006). Blocked acinar development, E-cadherin reduction, and intraepithelial neoplasia upon ablation of p120-catenin in the mouse salivary gland. Dev Cell *10*, 21-31.

Deacon, S.W., Beeser, A., Fukui, J.A., Rennefahrt, U.E.E., Myers, C., Chernoff, J., and Peterson, J.R. (2008). An isoform-selective, small-molecule inhibitor targets the autoregulatory mechanism of p21-activated kinase. Chem Biol *15*, 322-331.

Derksen, P.W.B., Liu, X., Saridin, F., van der Gulden, H., Zevenhoven, J., Evers, B., van Beijnum, J.R., Griffioen, A.W., Vink, J., Krimpenfort, P., *et al.* (2006). Somatic inactivation of E-cadherin and p53 in mice leads to metastatic lobular mammary carcinoma through induction of anoikis resistance and angiogenesis. Cancer Cell *10*, 437-449.

Desgrosellier, J.S., and Cheresh, D.A. (2010). Integrins in cancer: biological implications and therapeutic opportunities. Nat Rev Cancer *10*, 9-22.

Devenport, D., and Fuchs, E. (2008). Planar polarization in embryonic epidermis orchestrates global asymmetric morphogenesis of hair follicles. Nat Cell Biol *10*, 1257-1268.

Dickson, B.J., van der Straten, A., Dominguez, M., and Hafen, E. (1996). Mutations Modulating Raf signaling in Drosophila eye development. Genetics *142*, 163-171.

Dimri, G.P., Lee, X., Basile, G., Acosta, M., Scott, G., Roskelley, C., Medrano, E.E., Linskens, M., Rubelj, I., and Pereira-Smith, O. (1995). A biomarker that identifies senescent human cells in culture and in aging skin in vivo. Proc Natl Acad Sci USA *92*, 9363-9367.

Ding, L., Ellis, M.J., Li, S., Larson, D.E., Chen, K., Wallis, J.W., Harris, C.C., McLellan, M.D., Fulton, R.S., Fulton, L.L., *et al.* (2010). Genome remodelling in a basal-like breast cancer metastasis and xenograft. Nature *464*, 999-1005.

Drees, F., Pokutta, S., Yamada, S., Nelson, W.J., and Weis, W.I. (2005). Alpha-catenin is a molecular switch that binds E-cadherin-beta-catenin and regulates actin-filament assembly. Cell *123*, 903-915.

Ehrlich, J.S., Hansen, M.D.H., and Nelson, W.J. (2002). Spatio-temporal regulation of Rac1 localization and lamellipodia dynamics during epithelial cell-cell adhesion. Dev Cell *3*, 259-270.

Elia, L.P., Yamamoto, M., Zang, K., and Reichardt, L.F. (2006). p120 catenin regulates dendritic spine and synapse development through Rho-family GTPases and cadherins. Neuron *51*, 43-56.

Endo, M., Zoltick, P.W., Peranteau, W.H., Radu, A., Muvarak, N., Ito, M., Yang, Z., Cotsarelis, G., and Flake, A.W. (2008). Efficient in vivo targeting of epidermal stem cells by early gestational intraamniotic injection of lentiviral vector driven by the keratin 5 promoter. Mol Ther *16*, 131-137.

Espina, C., Céspedes, M.V., García-Cabezas, M.A., Gómez del Pulgar, M.T., Boluda, A., Oroz, L.G., Benitah, S.A., Cejas, P., Nistal, M., Mangues, R., *et al.* (2008). A critical role for Rac1 in tumor progression of human colorectal adenocarcinoma cells. The American Journal of Pathology *172*, 156-166.

Etienne-Manneville, S., and Hall, A. (2002). Rho GTPases in cell biology. Nature *420*, 629-635.

Fagotto, F., and Gumbiner, B.M. (1996). Cell contact-dependent signaling. Dev Biol *180*, 445-454.

Farquhar, M.G., and Palade, G.E. (1963). Junctional complexes in various epithelia. J Cell Biol *17*, 375-412.

Fata, J.E., Mori, H., Ewald, A.J., Zhang, H., Yao, E., Werb, Z., and Bissell, M.J. (2007). The MAPK(ERK-1,2) pathway integrates distinct and antagonistic signals from TGFalpha and FGF7 in morphogenesis of mouse mammary epithelium. Dev Biol *306*, 193-207.

Fedor-Chaiken, M., Hein, P.W., Stewart, J.C., Brackenbury, R., and Kinch, M.S. (2003). E-cadherin binding modulates EGF receptor activation. Cell Commun Adhes *10*, 105-118.

Feng, Q., Di, R., Tao, F., Chang, Z., Lu, S., Fan, W., Shan, C., Li, X., and Yang, Z. (2010). PDK1 regulates vascular remodeling and promotes epithelial-mesenchymal transition in cardiac development. Mol Cell Biol *30*, 3711-3721.

Follenzi, A., Santambrogio, L., and Annoni, A. (2007). Immune responses to lentiviral vectors. Curr Gene Ther *7*, 306-315.

Franke, W.W. (2009). Discovering the molecular components of intercellular junctions--a historical view. Cold Spring Harb Perspect Biol *1*, a003061.

Frisch, S.M., and Screaton, R.A. (2001). Anoikis mechanisms. Curr Opin Cell Biol *13*, 555-562.

Fuchs, E. (2007). Scratching the surface of skin development. Nature *445*, 834-842.

Fuchs, E., and Cleveland, D.W. (1998). A structural scaffolding of intermediate filaments in health and disease. Science *279*, 514-519.

Fuchs, E., and Green, H. (1980). Changes in keratin gene expression during terminal differentiation of the keratinocyte. Cell *19*, 1033-1042.

Fuchs, E., and Horsley, V. (2008). More than one way to skin. Genes Dev *22*, 976-985.

Furth, P.A., St Onge, L., Boger, H., Gruss, P., Gossen, M., Kistner, A., Bujard, H., and Hennighausen, L. (1994). Temporal control of gene expression in transgenic mice by a tetracycline-responsive promoter. Proc Natl Acad Sci U S A *91*, 9302-9306.

Gat, U., DasGupta, R., Degenstein, L., and Fuchs, E. (1998). De Novo hair follicle morphogenesis and hair tumors in mice expressing a truncated beta-catenin in skin. Cell *95*, 605-614.

Geiger, B., Bershadsky, A., Pankov, R., and Yamada, K.M. (2001). Transmembrane crosstalk between the extracellular matrix--cytoskeleton crosstalk. Nat Rev Mol Cell Biol *2*, 793-805.

Geiger, B., Spatz, J.P., and Bershadsky, A.D. (2009). Environmental sensing through focal adhesions. Nat Rev Mol Cell Biol *10*, 21-33.

Ghazizadeh, S., and Taichman, L.B. (2000). Virus-mediated gene transfer for cutaneous gene therapy. Hum Gene Ther *11*, 2247-2251.

Gladden, A.B., Hebert, A.M., Schneeberger, E.E., and McClatchey, A.I. (2010). The NF2 tumor suppressor, Merlin, regulates epidermal development through the establishment of a junctional polarity complex. Dev Cell *19*, 727-739.

Godt, D., and Tepass, U. (1998). Drosophila oocyte localization is mediated by differential cadherin-based adhesion. Nature *395*, 387-391.

Gossen, M., and Bujard, H. (1992). Tight control of gene expression in mammalian cells by tetracycline-responsive promoters. Proc Natl Acad Sci USA *89*, 5547-5551.

Gossen, M., Freundlieb, S., Bender, G., Müller, G., Hillen, W., and Bujard, H. (1995). Transcriptional activation by tetracyclines in mammalian cells. Science *268*, 1766-1769.

Greco, V., Chen, T., Rendl, M., Schober, M., Pasolli, H.A., Stokes, N., Dela Cruz-Racelis, J., and Fuchs, E. (2009). A two-step mechanism for stem cell activation during hair regeneration. Cell Stem Cell *4*, 155-169.

Guasch, G., Schober, M., Pasolli, H.A., Conn, E.B., Polak, L., and Fuchs, E. (2007). Loss of TGFbeta signaling destabilizes homeostasis and promotes squamous cell carcinomas in stratified epithelia. Cancer Cell *12*, 313-327.

Gumbiner, B.M. (2005). Regulation of cadherin-mediated adhesion in morphogenesis. Nat Rev Mol Cell Biol *6*, 622-634.

Guvakova, M.A., and Surmacz, E. (1997). Overexpressed IGF-I receptors reduce estrogen growth requirements, enhance survival, and promote E-cadherin-mediated cell-cell adhesion in human breast cancer cells. Exp Cell Res *231*, 149-162.

Haase, I., Evans, R., Pofahl, R., and Watt, F.M. (2003). Regulation of keratinocyte shape, migration and wound epithelialization by IGF-1- and EGF-dependent signalling pathways. J Cell Sci *116*, 3227-3238.

Hacein-Bey-Abina, S., Von Kalle, C., Schmidt, M., McCormack, M.P., Wulffraat, N., Leboulch, P., Lim, A., Osborne, C.S., Pawliuk, R., Morillon, E., *et al.* (2003). LMO2-associated clonal T cell proliferation in two patients after gene therapy for SCID-X1. Science *302*, 415-419.

Haegel, H., Larue, L., Ohsugi, M., Fedorov, L., Herrenknecht, K., and Kemler, R. (1995). Lack of beta-catenin affects mouse development at gastrulation. Development *121*, 3529-3537.

Hajra, K.M., and Fearon, E.R. (2002). Cadherin and catenin alterations in human cancer. Genes Chromosomes Cancer *34*, 255-268.

Halbleib, J.M., and Nelson, W.J. (2006). Cadherins in development: cell adhesion, sorting, and tissue morphogenesis. Genes Dev *20*, 3199-3214.

Hamaratoglu, F., Willecke, M., Kango-Singh, M., Nolo, R., Hyun, E., Tao, C., Jafar-Nejad, H., and Halder, G. (2006). The tumour-suppressor genes NF2/Merlin and Expanded act through Hippo signalling to regulate cell proliferation and apoptosis. Nat Cell Biol *8*, 27-36.

Hamelers, I.H.L., Olivo, C., Mertens, A.E.E., Pegtel, D.M., van der Kammen, R.A., Sonnenberg, A., and Collard, J.G. (2005). The Rac activator Tiam1 is required for (alpha)3(beta)1-mediated laminin-5 deposition, cell spreading, and cell migration. J Cell Biol *171*, 871-881.

Hanahan, D. (1985). Heritable formation of pancreatic beta-cell tumours in transgenic mice expressing recombinant insulin/simian virus 40 oncogenes. Nature *315*, 115-122.

Harris, T.J.C., and Tepass, U. (2010). Adherens junctions: from molecules to morphogenesis. Nat Rev Mol Cell Biol *11*, 502-514.

Hermiston, M.L., Wong, M.H., and Gordon, J.I. (1996). Forced expression of E-cadherin in the mouse intestinal epithelium slows cell migration and provides evidence for nonautonomous regulation of cell fate in a self-renewing system. Genes Dev *10*, 985-996.

Herrenknecht, K., Ozawa, M., Eckerskorn, C., Lottspeich, F., Lenter, M., and Kemler, R. (1991). The uvomorulin-anchorage protein alpha catenin is a vinculin homologue. Proc Natl Acad Sci USA *88*, 9156-9160.

Hirano, S., Kimoto, N., Shimoyama, Y., Hirohashi, S., and Takeichi, M. (1992). Identification of a neural alpha-catenin as a key regulator of cadherin function and multicellular organization. Cell *70*, 293-301.

Hodak, E., Gottlieb, A.B., Anzilotti, M., and Krueger, J.G. (1996). The insulin-like growth factor 1 receptor is expressed by epithelial cells with proliferative potential in human epidermis and skin appendages: correlation of increased expression with epidermal hyperplasia. J Invest Dermatol *106*, 564-570.

Hogan, B.L. (1999). Morphogenesis. Cell *96*, 225-233.

Holtfreter, J. (1939). Gewebeaffinitä t, ein Mittel der embryo- nalen Formbildung. Arch Exp Zellforsch *23*, 169–209.

Holzinger, A., Trapnell, B.C., Weaver, T.E., Whitsett, J.A., and Iwamoto, H.S. (1995). Intraamniotic administration of an adenoviral vector for gene transfer to fetal sheep and mouse tissues. Pediatr Res *38*, 844-850.

Hoshino, R., Chatani, Y., Yamori, T., Tsuruo, T., Oka, H., Yoshida, O., Shimada, Y., Ari-i, S., Wada, H., Fujimoto, J., *et al.* (1999). Constitutive activation of the 41-/43-kDa mitogen-activated protein kinase signaling pathway in human tumors. Oncogene *18*, 813-822.

Huelsken, J., Vogel, R., Erdmann, B., Cotsarelis, G., and Birchmeier, W. (2001). β-Catenin Controls Hair Follicle Morphogenesis and Stem Cell Differentiation in the Skin. Cell *105*, 533-545.

Hyafil, F., Babinet, C., and Jacob, F. (1981). Cell-cell interactions in early embryogenesis: a molecular approach to the role of calcium. Cell *26*, 447-454.

Ise, K., Nakamura, K., Nakao, K., Shimizu, S., Harada, H., Ichise, T., Miyoshi, J., Gondo, Y., Ishikawa, T., Aiba, A., *et al.* (2000). Targeted deletion of the H-ras

gene decreases tumor formation in mouse skin carcinogenesis. Oncogene *19*, 2951-2956.

Ito, M., Liu, Y., Yang, Z., Nguyen, J., Liang, F., Morris, R.J., and Cotsarelis, G. (2005). Stem cells in the hair follicle bulge contribute to wound repair but not to homeostasis of the epidermis. Nat Med *11*, 1351-1354.

Jamora, C., DasGupta, R., Kocieniewski, P., and Fuchs, E. (2003). Links between signal transduction, transcription and adhesion in epithelial bud development. Nature *422*, 317-322.

Janssens, B., Goossens, S., Staes, K., Gilbert, B., van Hengel, J., Colpaert, C., Bruyneel, E., Mareel, M., and van Roy, F. (2001). alphaT-catenin: a novel tissue-specific beta-catenin-binding protein mediating strong cell-cell adhesion. J Cell Sci *114*, 3177-3188.

Janssens, B., Staes, K., and van Roy, F. (1999). Human alpha-catulin, a novel alpha-catenin-like molecule with conserved genomic structure, but deviating alternative splicing. Biochim Biophys Acta *1447*, 341-347.

Jemal, A., Siegel, R., Xu, J., and Ward, E. (2010). Cancer statistics, 2010. CA: A Cancer Journal for Clinicians *60*, 277-300.

Kanda, T., Sullivan, K.F., and Wahl, G.M. (1998). Histone-GFP fusion protein enables sensitive analysis of chromosome dynamics in living mammalian cells. Curr Biol *8*, 377-385.

Kaufman, C.K., Zhou, P., Pasolli, H.A., Rendl, M., Bolotin, D., Lim, K.-C., Dai, X., Alegre, M.-L., and Fuchs, E. (2003). GATA-3: an unexpected regulator of cell lineage determination in skin. Genes Dev *17*, 2108-2122.

Khavari, T.A., and Rinn, J. (2007). Ras/Erk MAPK signaling in epidermal homeostasis and neoplasia. Cell Cycle *6*, 2928-2931.

Kissil, J.L., Walmsley, M.J., Hanlon, L., Haigis, K.M., Bender Kim, C.F., Sweet-Cordero, A., Eckman, M.S., Tuveson, D.A., Capobianco, A.J., Tybulewicz, V.L.J., *et al.* (2007). Requirement for Rac1 in a K-ras induced lung cancer in the mouse. Cancer Research *67*, 8089-8094.

Kissil, J.L., Wilker, E.W., Johnson, K.C., Eckman, M.S., Yaffe, M.B., and Jacks, T. (2003). Merlin, the product of the Nf2 tumor suppressor gene, is an inhibitor of the p21-activated kinase, Pak1. Mol Cell *12*, 841-849.

Klemke, R.L., Cai, S., Giannini, A.L., Gallagher, P.J., de Lanerolle, P., and Cheresh, D.A. (1997). Regulation of cell motility by mitogen-activated protein kinase. J Cell Biol *137*, 481-492.

Knox, S.M., Lombaert, I.M.A., Reed, X., Vitale-Cross, L., Gutkind, J.S., and Hoffman, M.P. (2010). Parasympathetic innervation maintains epithelial progenitor cells during salivary organogenesis. Science *329*, 1645-1647.

Kobielak, A., and Fuchs, E. (2006). Links between alpha-catenin, NF-kappaB, and squamous cell carcinoma in skin. Proc Natl Acad Sci USA *103*, 2322-2327.

Kobielak, A., Pasolli, H.A., and Fuchs, E. (2004). Mammalian formin-1 participates in adherens junctions and polymerization of linear actin cables. Nat Cell Biol *6*, 21-30.

Kopan, R., Traska, G., and Fuchs, E. (1987). Retinoids as important regulators of terminal differentiation: examining keratin expression in individual epidermal cells at various stages of keratinization. J Cell Biol *105*, 427-440.

Kovacs, E.M., Ali, R.G., McCormack, A.J., and Yap, A.S. (2002). E-cadherin homophilic ligation directly signals through Rac and phosphatidylinositol 3-kinase to regulate adhesive contacts. J Biol Chem *277*, 6708-6718.

Kraynov, V.S., Chamberlain, C., Bokoch, G.M., Schwartz, M.A., Slabaugh, S., and Hahn, K.M. (2000). Localized Rac activation dynamics visualized in living cells. Science *290*, 333-337.

Kumar, M., Keller, B., Makalou, N., and Sutton, R.E. (2001). Systematic determination of the packaging limit of lentiviral vectors. Hum Gene Ther *12*, 1893-1905.

Kuroda, S., Fukata, M., Nakagawa, M., Fujii, K., Nakamura, T., Ookubo, T., Izawa, I., Nagase, T., Nomura, N., Tani, H., *et al.* (1998). Role of IQGAP1, a target of the small GTPases Cdc42 and Rac1, in regulation of E-cadherin-mediated cell-cell adhesion. Science *281*, 832-835.

Lane, E.B., Rugg, E.L., Navsaria, H., Leigh, I.M., Heagerty, A.H., Ishida-Yamamoto, A., and Eady, R.A. (1992). A mutation in the conserved helix termination peptide of keratin 5 in hereditary skin blistering. Nature *356*, 244-246.

Lark, A.L., Livasy, C.A., Calvo, B., Caskey, L., Moore, D.T., Yang, X., and Cance, W.G. (2003). Overexpression of focal adhesion kinase in primary colorectal carcinomas and colorectal liver metastases: immunohistochemistry and real-time PCR analyses. Clin Cancer Res *9*, 215-222.

Larue, L., Ohsugi, M., Hirchenhain, J., and Kemler, R. (1994a). E-cadherin null mutant embryos fail to form a trophectoderm epithelium. Proc Natl Acad Sci U S A *91*, 8263-8267.

Larue, L., Ohsugi, M., Hirchenhain, J., and Kemler, R. (1994b). E-cadherin null mutant embryos fail to form a trophectoderm epithelium. Proc Natl Acad Sci USA *91*, 8263-8267.

le Duc, Q., Shi, Q., Blonk, I., Sonnenberg, A., Wang, N., Leckband, D., and de Rooij, J. (2010). Vinculin potentiates E-cadherin mechanosensing and is

recruited to actin-anchored sites within adherens junctions in a myosin II-dependent manner. J Cell Biol *189*, 1107-1115.

Lechler, T., and Fuchs, E. (2005). Asymmetric cell divisions promote stratification and differentiation of mammalian skin. Nature *437*, 275-280.

Lechler, T., and Fuchs, E. (2007). Desmoplakin: an unexpected regulator of microtubule organization in the epidermis. J Cell Biol *176*, 147-154.

Lemmon, M.A., and Schlessinger, J. (2010). Cell signaling by receptor tyrosine kinases. Cell *141*, 1117-1134.

Leon, J., Guerrero, I., and Pellicer, A. (1987). Differential expression of the ras gene family in mice. Mol Cell Biol *7*, 1535-1540.

Levy, V., Lindon, C., Harfe, B.D., and Morgan, B.A. (2005). Distinct stem cell populations regenerate the follicle and interfollicular epidermis. Dev Cell *9*, 855-861.

Lickert, H., Kutsch, S., Kanzler, B., Tamai, Y., Taketo, M.M., and Kemler, R. (2002). Formation of multiple hearts in mice following deletion of beta-catenin in the embryonic endoderm. Dev Cell *3*, 171-181.

Lien, W.-H., Klezovitch, O., Fernandez, T.E., Delrow, J., and Vasioukhin, V. (2006). alphaE-catenin controls cerebral cortical size by regulating the hedgehog signaling pathway. Science *311*, 1609-1612.

Lim, S.-T., Chen, X.L., Lim, Y., Hanson, D.A., Vo, T.-T., Howerton, K., Larocque, N., Fisher, S.J., Schlaepfer, D.D., and Ilic, D. (2008). Nuclear FAK promotes cell proliferation and survival through FERM-enhanced p53 degradation. Mol Cell *29*, 9-22.

Lis, J.T., Simon, J.A., and Sutton, C.A. (1983). New heat shock puffs and beta-galactosidase activity resulting from transformation of Drosophila with an hsp70-lacZ hybrid gene. Cell *35*, 403-410.

Liu, A., Joyner, A.L., and Turnbull, D.H. (1998). Alteration of limb and brain patterning in early mouse embryos by ultrasound-guided injection of Shh-expressing cells. Mech Dev *75*, 107-115.

Liu, F., Jia, L., Thompson-Baine, A.-M., Puglise, J.M., ter Beest, M.B.A., and Zegers, M.M.P. (2010). Cadherins and Pak1 control contact inhibition of proliferation by Pak1-betaPIX-GIT complex-dependent regulation of cell-matrix signaling. Mol Cell Biol *30*, 1971-1983.

Liu, J., Nethery, D., and Kern, J.A. (2004). Neuregulin-1 induces branching morphogenesis in the developing lung through a P13K signal pathway. Exp Lung Res *30*, 465-478.

Long, W., Yi, P., Amazit, L., LaMarca, H.L., Ashcroft, F., Kumar, R., Mancini, M.A., Tsai, S.Y., Tsai, M.-J., and O'Malley, B.W. (2010). SRC-3Delta4 mediates the interaction of EGFR with FAK to promote cell migration. Mol Cell *37*, 321-332.

Lozano, E., Betson, M., and Braga, V.M.M. (2003). Tumor progression: Small GTPases and loss of cell-cell adhesion. Bioessays *25*, 452-463.

Lozano, E., Frasa, M.A.M., Smolarczyk, K., Knaus, U.G., and Braga, V.M.M. (2008). PAK is required for the disruption of E-cadherin adhesion by the small GTPase Rac. J Cell Sci *121*, 933-938.

Lu, B., Federoff, H.J., Wang, Y., Goldsmith, L.A., and Scott, G. (1997). Topical application of viral vectors for epidermal gene transfer. J Invest Dermatol *108*, 803-808.

Luo, M., Fan, H., Nagy, T., Wei, H., Wang, C., Liu, S., Wicha, M.S., and Guan, J.-L. (2009). Mammary epithelial-specific ablation of the focal adhesion kinase suppresses mammary tumorigenesis by affecting mammary cancer stem/progenitor cells. Cancer Research *69*, 466-474.

M'Boneko, V., and Merker, H.J. (1988). Development and morphology of the periderm of mouse embryos (days 9-12 of gestation). Acta Anat (Basel) *133*, 325-336.

Mackenzie, I.C. (1970). Relationship between mitosis and the ordered structure of the stratum corneum in mouse epidermis. Nature *226*, 653-655.

Malliri, A., van der Kammen, R.A., Clark, K., van der Valk, M., Michiels, F., and Collard, J.G. (2002). Mice deficient in the Rac activator Tiam1 are resistant to Ras-induced skin tumours. Nature *417*, 867-871.

Malliri, A., van Es, S., Huveneers, S., and Collard, J.G. (2004). The Rac exchange factor Tiam1 is required for the establishment and maintenance of cadherin-based adhesions. J Biol Chem *279*, 30092-30098.

Mansbridge, J.N., and Knapp, A.M. (1987). Changes in keratinocyte maturation during wound healing. J Invest Dermatol *89*, 253-263.

Margolis, B., and Skolnik, E.Y. (1994). Activation of Ras by receptor tyrosine kinases. J Am Soc Nephrol *5*, 1288-1299.

Matsumoto, H., Kimura, T., Haga, K., Kasahara, N., Anton, P., and McGowan, I. (2010). Effective in vivo and ex vivo gene transfer to intestinal mucosa by VSV-G-pseudotyped lentiviral vectors. BMC Gastroenterol *10*, 44.

McGuire, S.E., Roman, G., and Davis, R.L. (2004). Gene expression systems in Drosophila: a synthesis of time and space. Trends Genet *20*, 384-391.

McLean, G.W., Komiyama, N.H., Serrels, B., Asano, H., Reynolds, L., Conti, F., Hodivala-Dilke, K., Metzger, D., Chambon, P., Grant, S.G.N., *et al.* (2004). Specific deletion of focal adhesion kinase suppresses tumor formation and blocks malignant progression. Genes Dev *18*, 2998-3003.

Merdek, K.D., Nguyen, N.T., and Toksoz, D. (2004). Distinct activities of the alpha-catenin family, alpha-catulin and alpha-catenin, on beta-catenin-mediated signaling. Mol Cell Biol *24*, 2410-2422.

Miller, D.G., Adam, M.A., and Miller, A.D. (1990). Gene transfer by retrovirus vectors occurs only in cells that are actively replicating at the time of infection. Mol Cell Biol *10*, 4239-4242.

Miranti, C.K., and Brugge, J.S. (2002). Sensing the environment: a historical perspective on integrin signal transduction. Nat Cell Biol *4*, E83-90.

Miyamoto, S., Teramoto, H., Gutkind, J.S., and Yamada, K.M. (1996). Integrins can collaborate with growth factors for phosphorylation of receptor tyrosine kinases and MAP kinase activation: roles of integrin aggregation and occupancy of receptors. J Cell Biol *135*, 1633-1642.

Moffat, J., Grueneberg, D.A., Yang, X., Kim, S.Y., Kloepfer, A.M., Hinkle, G., Piqani, B., Eisenhaure, T.M., Luo, B., Grenier, J.K., *et al.* (2006). A lentiviral RNAi library for human and mouse genes applied to an arrayed viral high-content screen. Cell *124*, 1283-1298.

Moscona, A.A. (1962). Cellular interactions in experimental histogenesis. Int Rev Exp Pathol *1*, 371-428.

Mühle, C., Neuner, A., Park, J., Pacho, F., Jiang, Q., Waddington, S.N., and Schneider, H. (2006). Evaluation of prenatal intra-amniotic LAMB3 gene delivery in a mouse model of Herlitz disease. Gene Therapy *13*, 1665-1676.

Müller-Röver, S., Handjiski, B., van der Veen, C., Eichmüller, S., Foitzik, K., McKay, I.A., Stenn, K.S., and Paus, R. (2001). A comprehensive guide for the accurate classification of murine hair follicles in distinct hair cycle stages. J Invest Dermatol *117*, 3-15.

Myster, S.H., Cavallo, R., Anderson, C.T., Fox, D.T., and Peifer, M. (2003). Drosophila p120catenin plays a supporting role in cell adhesion but is not an essential adherens junction component. J Cell Biol *160*, 433-449.

Nagafuchi, A., and Takeichi, M. (1988). Cell binding function of E-cadherin is regulated by the cytoplasmic domain. EMBO J *7*, 3679-3684.

Nagafuchi, A., Takeichi, M., and Tsukita, S. (1991). The 102 kd cadherin-associated protein: similarity to vinculin and posttranscriptional regulation of expression. Cell *65*, 849-857.

Nakagawa, M., Fukata, M., Yamaga, M., Itoh, N., and Kaibuchi, K. (2001). Recruitment and activation of Rac1 by the formation of E-cadherin-mediated cell-cell adhesion sites. J Cell Sci *114*, 1829-1838.

Naldini, L., Blömer, U., Gallay, P., Ory, D., Mulligan, R., Gage, F.H., Verma, I.M., and Trono, D. (1996). In vivo gene delivery and stable transduction of nondividing cells by a lentiviral vector. Science *272*, 263-267.

Nanney, L.B., Sundberg, J.P., and King, L.E. (1996). Increased epidermal growth factor receptor in fsn/fsn mice. J Invest Dermatol *106*, 1169-1174.

Nayal, A., Webb, D.J., Brown, C.M., Schaefer, E.M., Vicente-Manzanares, M., and Horwitz, A.R. (2006). Paxillin phosphorylation at Ser273 localizes a GIT1-PIX-PAK complex and regulates adhesion and protrusion dynamics. J Cell Biol *173*, 587-589.

Nellen, D., Burke, R., Struhl, G., and Basler, K. (1996). Direct and long-range action of a DPP morphogen gradient. Cell *85*, 357-368.

Nemade, R.V., Bierie, B., Nozawa, M., Bry, C., Smith, G.H., Vasioukhin, V., Fuchs, E., and Hennighausen, L. (2004). Biogenesis and function of mouse mammary epithelium depends on the presence of functional alpha-catenin. Mech Dev *121*, 91-99.

Nguyen, D.X., Bos, P.D., and Massagué, J. (2009). Metastasis: from dissemination to organ-specific colonization. Nat Rev Cancer *9*, 274-284.

Nguyen, H., Rendl, M., and Fuchs, E. (2006). Tcf3 governs stem cell features and represses cell fate determination in skin. Cell *127*, 171-183.

Noramly, S., Freeman, A., and Morgan, B.A. (1999). beta-catenin signaling can initiate feather bud development. Development *126*, 3509-3521.

Noren, N.K., Liu, B.P., Burridge, K., and Kreft, B. (2000). p120 catenin regulates the actin cytoskeleton via Rho family GTPases. J Cell Biol *150*, 567-580.

Noren, N.K., Niessen, C.M., Gumbiner, B.M., and Burridge, K. (2001). Cadherin engagement regulates Rho family GTPases. J Biol Chem *276*, 33305-33308.

Nose, A., and Takeichi, M. (1986). A novel cadherin cell adhesion molecule: its expression patterns associated with implantation and organogenesis of mouse embryos. J Cell Biol *103*, 2649-2658.

Nozawa, N., Hashimoto, S., Nakashima, Y., Matsuo, Y., Koga, T., Sugio, K., Niho, Y., Harada, M., and Sueishi, K. (2006). Immunohistochemical alpha- and beta-catenin and E-cadherin expression and their clinicopathological significance in human lung adenocarcinoma. Pathol Res Pract *202*, 639-650.

O'brien, L.E., Zegers, M.M.P., and Mostov, K.E. (2002). Opinion: Building epithelial architecture: insights from three-dimensional culture models. Nat Rev Mol Cell Biol *3*, 531-537.

Ochiai, A., Akimoto, S., Shimoyama, Y., Nagafuchi, A., Tsukita, S., and Hirohashi, S. (1994). Frequent loss of alpha catenin expression in scirrhous carcinomas with scattered cell growth. Jpn J Cancer Res *85*, 266-273.

Ohsugi, M., Larue, L., Schwarz, H., and Kemler, R. (1997). Cell-junctional and cytoskeletal organization in mouse blastocysts lacking E-cadherin. Dev Biol *185*, 261-271.

Okada, T., Lopez-Lago, M., and Giancotti, F.G. (2005). Merlin/NF-2 mediates contact inhibition of growth by suppressing recruitment of Rac to the plasma membrane. J Cell Biol *171*, 361-371.

Oren, M., and Rotter, V. (2010). Mutant p53 gain-of-function in cancer. Cold Spring Harb Perspect Biol *2*, a001107.

Overduin, M., Harvey, T.S., Bagby, S., Tong, K.I., Yau, P., Takeichi, M., and Ikura, M. (1995). Solution structure of the epithelial cadherin domain responsible for selective cell adhesion. Science *267*, 386-389.

Owens, L.V., Xu, L., Craven, R.J., Dent, G.A., Weiner, T.M., Kornberg, L., Liu, E.T., and Cance, W.G. (1995). Overexpression of the focal adhesion kinase (p125FAK) in invasive human tumors. Cancer Research *55*, 2752-2755.

Ozawa, M., Baribault, H., and Kemler, R. (1989). The cytoplasmic domain of the cell adhesion molecule uvomorulin associates with three independent proteins structurally related in different species. EMBO J *8*, 1711-1717.

Ozawa, M., Ringwald, M., and Kemler, R. (1990). Uvomorulin-catenin complex formation is regulated by a specific domain in the cytoplasmic region of the cell adhesion molecule. Proc Natl Acad Sci U S A *87*, 4246-4250.

Pagès, G., Guérin, S., Grall, D., Bonino, F., Smith, A., Anjuere, F., Auberger, P., and Pouysségur, J. (1999). Defective thymocyte maturation in p44 MAP kinase (Erk 1) knockout mice. Science *286*, 1374-1377.

Pagliarini, R.A., and Xu, T. (2003). A genetic screen in Drosophila for metastatic behavior. Science *302*, 1227-1231.

Parkin, D.M., Bray, F., Ferlay, J., and Pisani, P. (2005). Global cancer statistics, 2002. CA: A Cancer Journal for Clinicians *55*, 74-108.

Perez-Moreno, M., Davis, M.A., Wong, E., Pasolli, H.A., Reynolds, A.B., and Fuchs, E. (2006). p120-catenin mediates inflammatory responses in the skin. Cell *124*, 631-644.

Perez-Moreno, M., and Fuchs, E. (2006). Catenins: keeping cells from getting their signals crossed. Dev Cell *11*, 601-612.

Perez-Moreno, M., Song, W., Pasolli, H.A., Williams, S.E., and Fuchs, E. (2008). Loss of p120 catenin and links to mitotic alterations, inflammation, and skin cancer. Proc Natl Acad Sci USA *105*, 15399-15404.

Perl, A.K., Wilgenbus, P., Dahl, U., Semb, H., and Christofori, G. (1998). A causal role for E-cadherin in the transition from adenoma to carcinoma. Nature *392*, 190-193.

Peterson, L.L., Zettergren, J.G., and Wuepper, K.D. (1983). Biochemistry of transglutaminases and cross-linking in the skin. J Invest Dermatol *81*, 95s-100s.

Petit, V., Boyer, B., Lentz, D., Turner, C.E., Thiery, J.P., and Vallés, A.M. (2000). Phosphorylation of tyrosine residues 31 and 118 on paxillin regulates cell migration through an association with CRK in NBT-II cells. J Cell Biol *148*, 957-970.

Pirraglia, C., Jattani, R., and Myat, M.M. (2006). Rac function in epithelial tube morphogenesis. Dev Biol *290*, 435-446.

Potten, C.S. (1974). The epidermal proliferative unit: the possible role of the central basal cell. Cell Tissue Kinet *7*, 77-88.

Poulson, N.D., and Lechler, T. (2010). Robust control of mitotic spindle orientation in the developing epidermis. J Cell Biol *191*, 915-922.

Punzo, C., and Cepko, C.L. (2008). Ultrasound-guided in utero injections allow studies of the development and function of the eye. Dev Dyn *237*, 1034-1042.

Pylayeva, Y., Gillen, K.M., Gerald, W., Beggs, H.E., Reichardt, L.F., and Giancotti, F.G. (2009). Ras- and PI3K-dependent breast tumorigenesis in mice and humans requires focal adhesion kinase signaling. J Clin Invest *119*, 252-266.

Qian, X., Karpova, T., Sheppard, A.M., McNally, J., and Lowy, D.R. (2004). E-cadherin-mediated adhesion inhibits ligand-dependent activation of diverse receptor tyrosine kinases. EMBO J *23*, 1739-1748.

Quintanilla, M., Brown, K., Ramsden, M., and Balmain, A. (1986). Carcinogen-specific mutation and amplification of Ha-ras during mouse skin carcinogenesis. Nature *322*, 78-80.

Rajewsky, K., Gu, H., Kühn, R., Betz, U.A., Müller, W., Roes, J., and Schwenk, F. (1996). Conditional gene targeting. J Clin Invest *98*, 600-603.

Renshaw, M.W., Ren, X.D., and Schwartz, M.A. (1997). Growth factor activation of MAP kinase requires cell adhesion. EMBO J *16*, 5592-5599.

Reuter, J.A., Ortiz-Urda, S., Kretz, M., Garcia, J., Scholl, F.A., Pasmooij, A.M.G., Cassarino, D., Chang, H.Y., and Khavari, P.A. (2009). Modeling inducible human tissue neoplasia identifies an extracellular matrix interaction network involved in cancer progression. Cancer Cell *15*, 477-488.

Reynolds, A.B., and Carnahan, R.H. (2004). Regulation of cadherin stability and turnover by p120ctn: implications in disease and cancer. Semin Cell Dev Biol *15*, 657-663.

Reynolds, A.B., Daniel, J., McCrea, P.D., Wheelock, M.J., Wu, J., and Zhang, Z. (1994). Identification of a new catenin: the tyrosine kinase substrate p120cas associates with E-cadherin complexes. Mol Cell Biol *14*, 8333-8342.

Ridky, T.W., Chow, J.M., Wong, D.J., and Khavari, P.A. (2010). Invasive three-dimensional organotypic neoplasia from multiple normal human epithelia. Nat Med *16*, 1450-1455.

Ridley, A.J., and Hall, A. (1992). The small GTP-binding protein rho regulates the assembly of focal adhesions and actin stress fibers in response to growth factors. Cell *70*, 389-399.

Ridley, A.J., Paterson, H.F., Johnston, C.L., Diekmann, D., and Hall, A. (1992). The small GTP-binding protein rac regulates growth factor-induced membrane ruffling. Cell *70*, 401-410.

Ridley, A.J., Schwartz, M.A., Burridge, K., Firtel, R.A., Ginsberg, M.H., Borisy, G., Parsons, J.T., and Horwitz, A.R. (2003). Cell migration: integrating signals from front to back. Science *302*, 1704-1709.

Rimm, D.L., Koslov, E.R., Kebriaei, P., Cianci, C.D., and Morrow, J.S. (1995). Alpha 1(E)-catenin is an actin-binding and -bundling protein mediating the attachment of F-actin to the membrane adhesion complex. Proc Natl Acad Sci USA *92*, 8813-8817.

Root, D.E., Hacohen, N., Hahn, W.C., Lander, E.S., and Sabatini, D.M. (2006). Genome-scale loss-of-function screening with a lentiviral RNAi library. Nat Methods *3*, 715-719.

Sadagurski, M., Yakar, S., Weingarten, G., Holzenberger, M., Rhodes, C.J., Breitkreutz, D., Leroith, D., and Wertheimer, E. (2006). Insulin-like growth factor 1 receptor signaling regulates skin development and inhibits skin keratinocyte differentiation. Mol Cell Biol *26*, 2675-2687.

Sato, T., Vries, R.G., Snippert, H.J., van de Wetering, M., Barker, N., Stange, D.E., van Es, J.H., Abo, A., Kujala, P., Peters, P.J., *et al.* (2009). Single Lgr5 stem cells build crypt-villus structures in vitro without a mesenchymal niche. Nature *459*, 262-265.

Schlegelmilch, K., Mohseni, M., Kirak, O., Pruszak, J., Rodriguez, J.R., Zhou, D., Kreger, B.T., Vasioukhin, V., Avruch, J., Brummelkamp, T.R., *et al.* (2011). Yap1 Acts Downstream of α-Catenin to Control Epidermal Proliferation. Cell *144*, 782-795.

Schmidt-Ullrich, R., and Paus, R. (2005). Molecular principles of hair follicle induction and morphogenesis. Bioessays *27*, 247-261.

Schober, M., Raghavan, S., Nikolova, M., Polak, L., Pasolli, H.A., Beggs, H.E., Reichardt, L.F., and Fuchs, E. (2007). Focal adhesion kinase modulates tension signaling to control actin and focal adhesion dynamics. J Cell Biol *176*, 667-680.

Sears, C.L. (2005). A dynamic partnership: celebrating our gut flora. Anaerobe *11*, 247-251.

Segre, J. (2003). Complex redundancy to build a simple epidermal permeability barrier. Curr Opin Cell Biol *15*, 776-782.

Shen, T.-L., Park, A.Y.-J., Alcaraz, A., Peng, X., Jang, I., Koni, P., Flavell, R.A., Gu, H., and Guan, J.-L. (2005). Conditional knockout of focal adhesion kinase in endothelial cells reveals its role in angiogenesis and vascular development in late embryogenesis. J Cell Biol *169*, 941-952.

Shiozaki, H., Iihara, K., Oka, H., Kadowaki, T., Matsui, S., Gofuku, J., Inoue, M., Nagafuchi, A., Tsukita, S., and Mori, T. (1994). Immunohistochemical detection of alpha-catenin expression in human cancers. The American Journal of Pathology *144*, 667-674.

Silva, J.M., Li, M.Z., Chang, K., Ge, W., Golding, M.C., Rickles, R.J., Siolas, D., Hu, G., Paddison, P.J., Schlabach, M.R., *et al.* (2005). Second-generation shRNA libraries covering the mouse and human genomes. Nat Genet *37*, 1281-1288.

Simon, M.A., Bowtell, D.D., Dodson, G.S., Laverty, T.R., and Rubin, G.M. (1991). Ras1 and a putative guanine nucleotide exchange factor perform crucial steps in signaling by the sevenless protein tyrosine kinase. Cell *67*, 701-716.

Slack-Davis, J.K., Eblen, S.T., Zecevic, M., Boerner, S.A., Tarcsafalvi, A., Diaz, H.B., Marshall, M.S., Weber, M.J., Parsons, J.T., and Catling, A.D. (2003). PAK1 phosphorylation of MEK1 regulates fibronectin-stimulated MAPK activation. J Cell Biol *162*, 281-291.

Slevin, J.C., Byers, L., Gertsenstein, M., Qu, D., Mu, J., Sunn, N., Kingdom, J.C.P., Rossant, J., and Adamson, S.L. (2006). High resolution ultrasound-guided microinjection for interventional studies of early embryonic and placental development in vivo in mice. BMC Dev Biol *6*, 10.

Soriano, P. (1999). Generalized lacZ expression with the ROSA26 Cre reporter strain. Nat Genet *21*, 70-71.

Soussi, T., Ishioka, C., Claustres, M., and Béroud, C. (2006). Locus-specific mutation databases: pitfalls and good practice based on the p53 experience. Nat Rev Cancer *6*, 83-90.

Srinivas, S., Watanabe, T., Lin, C.S., William, C.M., Tanabe, Y., Jessell, T.M., and Costantini, F. (2001). Cre reporter strains produced by targeted insertion of EYFP and ECFP into the ROSA26 locus. BMC Dev Biol *1*, 4.

St-Jacques, B., Dassule, H.R., Karavanova, I., Botchkarev, V.A., Li, J., Danielian, P.S., McMahon, J.A., Lewis, P.M., Paus, R., and McMahon, A.P. (1998). Sonic hedgehog signaling is essential for hair development. Curr Biol *8*, 1058-1068.

Stachelscheid, H., Ibrahim, H., Koch, L., Schmitz, A., Tscharntke, M., Wunderlich, F.T., Scott, J., Michels, C., Wickenhauser, C., Haase, I., *et al.* (2008). Epidermal insulin/IGF-1 signalling control interfollicular morphogenesis and proliferative potential through Rac activation. EMBO J *27*, 2091-2101.

Stepniak, E., Radice, G.L., and Vasioukhin, V. (2009). Adhesive and signaling functions of cadherins and catenins in vertebrate development. Cold Spring Harb Perspect Biol *1*, a002949.

Stocker, A.M., and Chenn, A. (2009). Focal reduction of alphaE-catenin causes premature differentiation and reduction of beta-catenin signaling during cortical development. Dev Biol *328*, 66-77.

Struhl, G., and Basler, K. (1993). Organizing activity of wingless protein in Drosophila. Cell *72*, 527-540.

Swartzendruber, D.C., Wertz, P.W., Kitko, D.J., Madison, K.C., and Downing, D.T. (1989). Molecular models of the intercellular lipid lamellae in mammalian stratum corneum. J Invest Dermatol *92*, 251-257.

Tabata, H., and Nakajima, K. (2001). Efficient in utero gene transfer system to the developing mouse brain using electroporation: visualization of neuronal migration in the developing cortex. Neuroscience *103*, 865-872.

Takahashi, K., and Suzuki, K. (1996). Density-dependent inhibition of growth involves prevention of EGF receptor activation by E-cadherin-mediated cell-cell adhesion. Exp Cell Res *226*, 214-222.

Takeichi, M. (1977). Functional correlation between cell adhesive properties and some cell surface proteins. J Cell Biol *75*, 464-474.

Tepass, U., Gruszynski-DeFeo, E., Haag, T.A., Omatyar, L., Török, T., and Hartenstein, V. (1996). shotgun encodes Drosophila E-cadherin and is preferentially required during cell rearrangement in the neurectoderm and other morphogenetically active epithelia. Genes Dev *10*, 672-685.

Tepass, U., Tanentzapf, G., Ward, R., and Fehon, R. (2001). Epithelial cell polarity and cell junctions in Drosophila. Annu Rev Genet *35*, 747-784.

Thiery, J.P., Acloque, H., Huang, R.Y.J., and Nieto, M.A. (2009). Epithelial-mesenchymal transitions in development and disease. Cell *139*, 871-890.

Thomas, K.R., and Capecchi, M.R. (1987). Site-directed mutagenesis by gene targeting in mouse embryo-derived stem cells. Cell *51*, 503-512.

Tinkle, C.L., Lechler, T., Pasolli, H.A., and Fuchs, E. (2004). Conditional targeting of E-cadherin in skin: insights into hyperproliferative and degenerative responses. Proc Natl Acad Sci USA *101*, 552-557.

Tinkle, C.L., Pasolli, H.A., Stokes, N., and Fuchs, E. (2008). New insights into cadherin function in epidermal sheet formation and maintenance of tissue integrity. Proc Natl Acad Sci USA *105*, 15405-15410.

To, K.C.W., Loh, K.T., Roskelley, C.D., Andersen, R.J., and O'Connor, T.P. (2006). The anti-invasive compound motuporamine C is a robust stimulator of neuronal growth cone collapse. Neuroscience *139*, 1263-1274.

Tomar, A., and Schlaepfer, D.D. (2010). A PAK-activated linker for EGFR and FAK. Dev Cell *18*, 170-172.

Torres, M., Stoykova, A., Huber, O., Chowdhury, K., Bonaldo, P., Mansouri, A., Butz, S., Kemler, R., and Gruss, P. (1997). An alpha-E-catenin gene trap mutation defines its function in preimplantation development. Proc Natl Acad Sci USA *94*, 901-906.

Tscharntke, M., Pofahl, R., Chrostek-Grashoff, A., Smyth, N., Niessen, C., Niemann, C., Hartwig, B., Herzog, V., Klein, H.W., Krieg, T., *et al.* (2007). Impaired epidermal wound healing in vivo upon inhibition or deletion of Rac1. J Cell Sci *120*, 1480-1490.

Tumbar, T., Guasch, G., Greco, V., Blanpain, C., Lowry, W.E., Rendl, M., and Fuchs, E. (2004). Defining the epithelial stem cell niche in skin. Science *303*, 359-363.

Tunggal, J.A., Helfrich, I., Schmitz, A., Schwarz, H., Gunzel, D., Fromm, M., Kemler, R., Krieg, T., and Niessen, C.M. (2005). E-cadherin is essential for in vivo epidermal barrier function by regulating tight junctions. EMBO J *24*, 1146-1156.

Vaezi, A., Bauer, C., Vasioukhin, V., and Fuchs, E. (2002). Actin cable dynamics and Rho/Rock orchestrate a polarized cytoskeletal architecture in the early steps of assembling a stratified epithelium. Dev Cell *3*, 367-381.

van de Wetering, M., Cavallo, R., Dooijes, D., van Beest, M., van Es, J., Loureiro, J., Ypma, A., Hursh, D., Jones, T., Bejsovec, A., *et al.* (1997). Armadillo coactivates transcription driven by the product of the Drosophila segment polarity gene dTCF. Cell *88*, 789-799.

van Genderen, C., Okamura, R.M., Fariñas, I., Quo, R.G., Parslow, T.G., Bruhn, L., and Grosschedl, R. (1994). Development of several organs that require inductive epithelial-mesenchymal interactions is impaired in LEF-1-deficient mice. Genes Dev *8*, 2691-2703.

Vasioukhin, V., Bauer, C., Degenstein, L., Wise, B., and Fuchs, E. (2001). Hyperproliferation and defects in epithelial polarity upon conditional ablation of alpha-catenin in skin. Cell *104*, 605-617.

Vasioukhin, V., Bauer, C., Yin, M., and Fuchs, E. (2000). Directed actin polymerization is the driving force for epithelial cell-cell adhesion. Cell *100*, 209-219.

Vasioukhin, V., Degenstein, L., Wise, B., and Fuchs, E. (1999). The magical touch: genome targeting in epidermal stem cells induced by tamoxifen application to mouse skin. Proc Natl Acad Sci USA *96*, 8551-8556.

Vassar, R., Coulombe, P.A., Degenstein, L., Albers, K., and Fuchs, E. (1991). Mutant keratin expression in transgenic mice causes marked abnormalities resembling a human genetic skin disease. Cell *64*, 365-380.

Vassar, R., and Fuchs, E. (1991). Transgenic mice provide new insights into the role of TGF-alpha during epidermal development and differentiation. Genes Dev *5*, 714-727.

Vassar, R., Rosenberg, M., Ross, S., Tyner, A., and Fuchs, E. (1989). Tissue-specific and differentiation-specific expression of a human K14 keratin gene in transgenic mice. Proc Natl Acad Sci USA *86*, 1563-1567.

Villunger, A., Michalak, E.M., Coultas, L., Müllauer, F., Böck, G., Ausserlechner, M.J., Adams, J.M., and Strasser, A. (2003). p53- and drug-induced apoptotic responses mediated by BH3-only proteins puma and noxa. Science *302*, 1036-1038.

Wang, W., Chen, J.X., Liao, R., Deng, Q., Zhou, J.J., Huang, S., and Sun, P. (2002). Sequential activation of the MEK-extracellular signal-regulated kinase and MKK3/6-p38 mitogen-activated protein kinase pathways mediates oncogenic ras-induced premature senescence. Mol Cell Biol *22*, 3389-3403.

Wang, Z., Pedersen, E., Basse, A., Lefever, T., Peyrollier, K., Kapoor, S., Mei, Q., Karlsson, R., Chrostek-Grashoff, A., and Brakebusch, C. (2010). Rac1 is crucial for Ras-dependent skin tumor formation by controlling Pak1-Mek-Erk hyperactivation and hyperproliferation in vivo. Oncogene *29*, 3362-3373.

Wary, K.K., Mainiero, F., Isakoff, S.J., Marcantonio, E.E., and Giancotti, F.G. (1996). The adaptor protein Shc couples a class of integrins to the control of cell cycle progression. Cell *87*, 733-743.

Wary, K.K., Mariotti, A., Zurzolo, C., and Giancotti, F.G. (1998). A requirement for caveolin-1 and associated kinase Fyn in integrin signaling and anchorage-dependent cell growth. Cell *94*, 625-634.

Watabe, M., Nagafuchi, A., Tsukita, S., and Takeichi, M. (1994). Induction of polarized cell-cell association and retardation of growth by activation of the E-cadherin-catenin adhesion system in a dispersed carcinoma line. J Cell Biol *127*, 247-256.

Watabe-Uchida, M., Uchida, N., Imamura, Y., Nagafuchi, A., Fujimoto, K., Uemura, T., Vermeulen, S., van Roy, F., Adamson, E.D., and Takeichi, M. (1998). alpha-Catenin-vinculin interaction functions to organize the apical junctional complex in epithelial cells. J Cell Biol *142*, 847-857.

Webb, D.J., Donais, K., Whitmore, L.A., Thomas, S.M., Turner, C.E., Parsons, J.T., and Horwitz, A.F. (2004). FAK-Src signalling through paxillin, ERK and MLCK regulates adhesion disassembly. Nat Cell Biol *6*, 154-161.

Welm, B.E., Dijkgraaf, G.J.P., Bledau, A.S., Welm, A.L., and Werb, Z. (2008). Lentiviral transduction of mammary stem cells for analysis of gene function during development and cancer. Cell Stem Cell *2*, 90-102.

Wilder, E.L. (2000). Ectopic expression in Drosophila. Methods Mol Biol *137*, 9-14.

Williams, S.E., Beronja, S., Pasolli, H.A., and Fuchs, E. (2011). Asymmetric cell divisions promote Notch-dependent epidermal differentiation. Nature *470*, 353-358.

Wilson, H.V. (1907). On some phenomena of coalescence and regeneration in sponges. J Exp Zool *5*, 245-258.

Wiseman, B.S., Sternlicht, M.D., Lund, L.R., Alexander, C.M., Mott, J., Bissell, M.J., Soloway, P., Itohara, S., and Werb, Z. (2003). Site-specific inductive and inhibitory activities of MMP-2 and MMP-3 orchestrate mammary gland branching morphogenesis. J Cell Biol *162*, 1123-1133.

Xiangming, C., Hokita, S., Natsugoe, S., Tanabe, G., Baba, M., Takao, S., Kuroshima, K., and Aikou, T. (1999). Cooccurrence of reduced expression of alpha-catenin and overexpression of p53 is a predictor of lymph node metastasis in early gastric cancer. Oncology *57*, 131-137.

Yamada, K.M., and Even-Ram, S. (2002). Integrin regulation of growth factor receptors. Nat Cell Biol *4*, E75-76.

Yamada, S., and Nelson, W.J. (2007). Localized zones of Rho and Rac activities drive initiation and expansion of epithelial cell-cell adhesion. J Cell Biol *178*, 517-527.

Yamada, S., Pokutta, S., Drees, F., Weis, W.I., and Nelson, W.J. (2005). Deconstructing the cadherin-catenin-actin complex. Cell *123*, 889-901.

Yao, K.M., and White, K. (1994). Neural specificity of elav expression: defining a Drosophila promoter for directing expression to the nervous system. J Neurochem *63*, 41-51.

Yap, A.S., Niessen, C.M., and Gumbiner, B.M. (1998). The juxtamembrane region of the cadherin cytoplasmic tail supports lateral clustering, adhesive strengthening, and interaction with p120ctn. J Cell Biol *141*, 779-789.

Yonemura, S., Itoh, M., Nagafuchi, A., and Tsukita, S. (1995). Cell-to-cell adherens junction formation and actin filament organization: similarities and differences between non-polarized fibroblasts and polarized epithelial cells. J Cell Sci *108 (Pt 1)*, 127-142.

Yonemura, S., Wada, Y., Watanabe, T., Nagafuchi, A., and Shibata, M. (2010). alpha-Catenin as a tension transducer that induces adherens junction development. Nat Cell Biol *12*, 533-542.

Yoshida, C., and Takeichi, M. (1982). Teratocarcinoma cell adhesion: identification of a cell-surface protein involved in calcium-dependent cell aggregation. Cell *28*, 217-224.

Yoshida, R., Kimura, N., Harada, Y., and Ohuchi, N. (2001). The loss of E-cadherin, alpha- and beta-catenin expression is associated with metastasis and poor prognosis in invasive breast cancer. Int J Oncol *18*, 513-520.

Yoshida-Noro, C., Suzuki, N., and Takeichi, M. (1984). Molecular nature of the calcium-dependent cell-cell adhesion system in mouse teratocarcinoma and embryonic cells studied with a monoclonal antibody. Dev Biol *101*, 19-27.

Young, P., Boussadia, O., Halfter, H., Grose, R., Berger, P., Leone, D.P., Robenek, H., Charnay, P., Kemler, R., and Suter, U. (2003). E-cadherin controls adherens junctions in the epidermis and the renewal of hair follicles. EMBO J *22*, 5723-5733.

Zegers, M.M.P., Forget, M.-A., Chernoff, J., Mostov, K.E., ter Beest, M.B.A., and Hansen, S.H. (2003). Pak1 and PIX regulate contact inhibition during epithelial wound healing. EMBO J *22*, 4155-4165.

Zhang, H., Pasolli, H.A., and Fuchs, E. (2011). Yes-associated protein (YAP) transcriptional coactivator functions in balancing growth and differentiation in skin. Proc Natl Acad Sci USA *108*, 2270-2275.

Zhang, N., Bai, H., David, K.K., Dong, J., Zheng, Y., Cai, J., Giovannini, M., Liu, P., Anders, R.A., and Pan, D. (2010). The Merlin/NF2 tumor suppressor functions through the YAP oncoprotein to regulate tissue homeostasis in mammals. Dev Cell *19*, 27-38.

Zhao, Z.S., Manser, E., Loo, T.H., and Lim, L. (2000). Coupling of PAK-interacting exchange factor PIX to GIT1 promotes focal complex disassembly. Mol Cell Biol *20*, 6354-6363.

Zhou, P., Byrne, C., Jacobs, J., and Fuchs, E. (1995). Lymphoid enhancer factor 1 directs hair follicle patterning and epithelial cell fate. Genes Dev *9*, 700-713.